5th Bishop Lecture

Several challenges in advanced laboratory testing of geomaterials with emphasis on unconventional types of liquefaction tests

Junichi KOSEKI

(*University of Tokyo, Japan*)

Acknowledgements

Without contributions by the current/past laboratory members, these challenges could not be made.

In particular, technical supports by Mr. Takeshi SATO in developing/improving the test apparatuses and sensors are sincerely acknowledged.

Outline

1. Introduction
2. Local measurements
    - 2.1 LDTs for cylindrical/prismatic specimens (triaxial)
    - 2.2 LDTs for hollow cylindrical specimen (torsional shear/triaxial)
    - 2.3 Local dynamic measurements
3. Unconventional liquefaction tests
    - 3.1 Liquefaction tests using motor-driven loading devices
    - 3.2 Cylindrical/prismatic specimens with thin sandy layer
    - 3.3 Segregated hollow cylindrical specimen
    - 3.4 Direct/indirect evaluation of local deformation during liquefaction
4. Other special tests
    - 4.1 Large deformation tests
    - 4.2 Direct tension tests
    - 4.3 Long-term tests
5. Concluding remarks

1950s

Bishop and Eldin (1950)

Undrained triaxial tests on sand

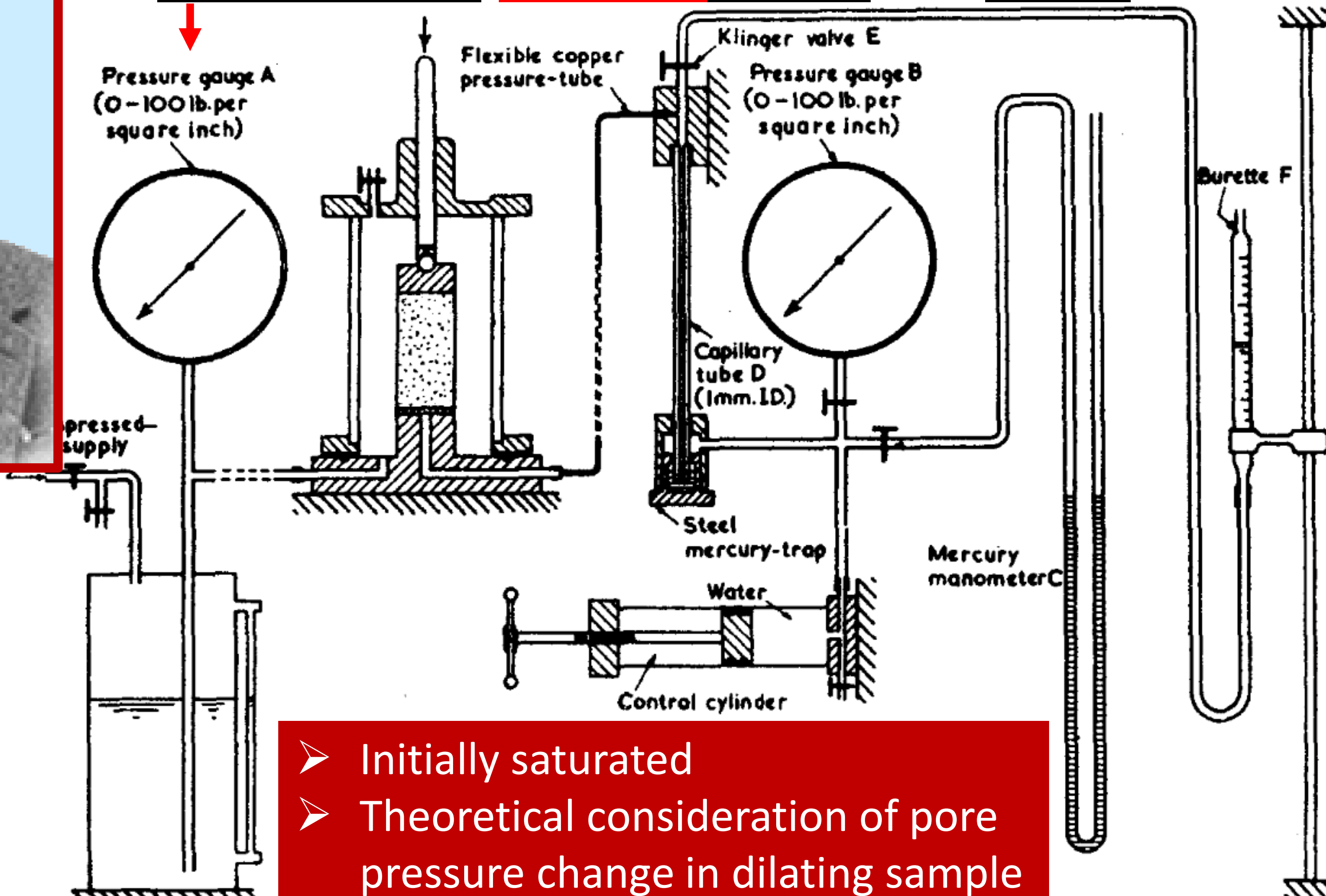

- Initially saturated
- Theoretical consideration of pore pressure change in dilating sample

1960s

Lee and Seed (1967)

Undrained cyclic triaxial tests on sand

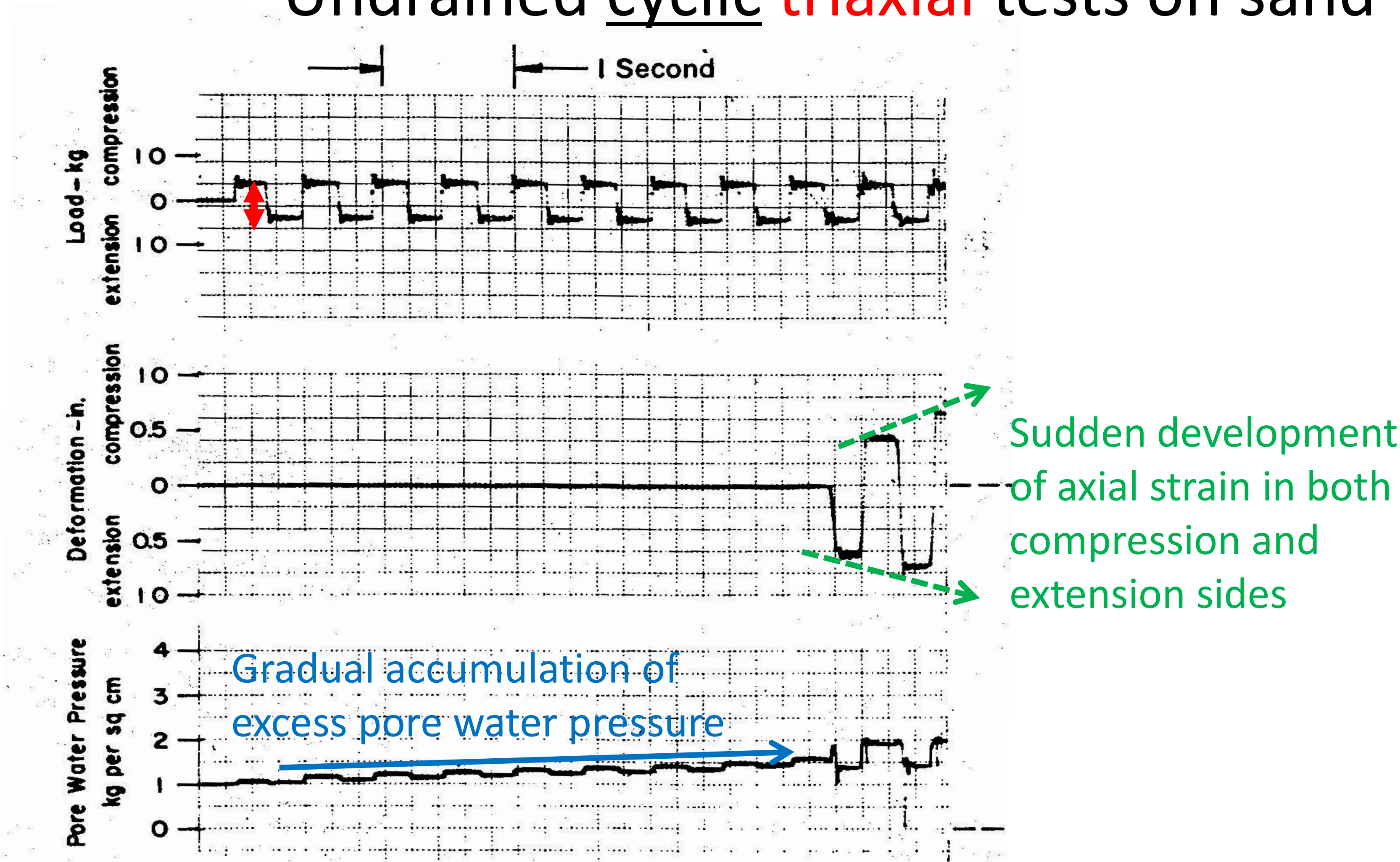

Ishihara and Yasuda (1972)

Undrained cyclic torsional shear tests on sand

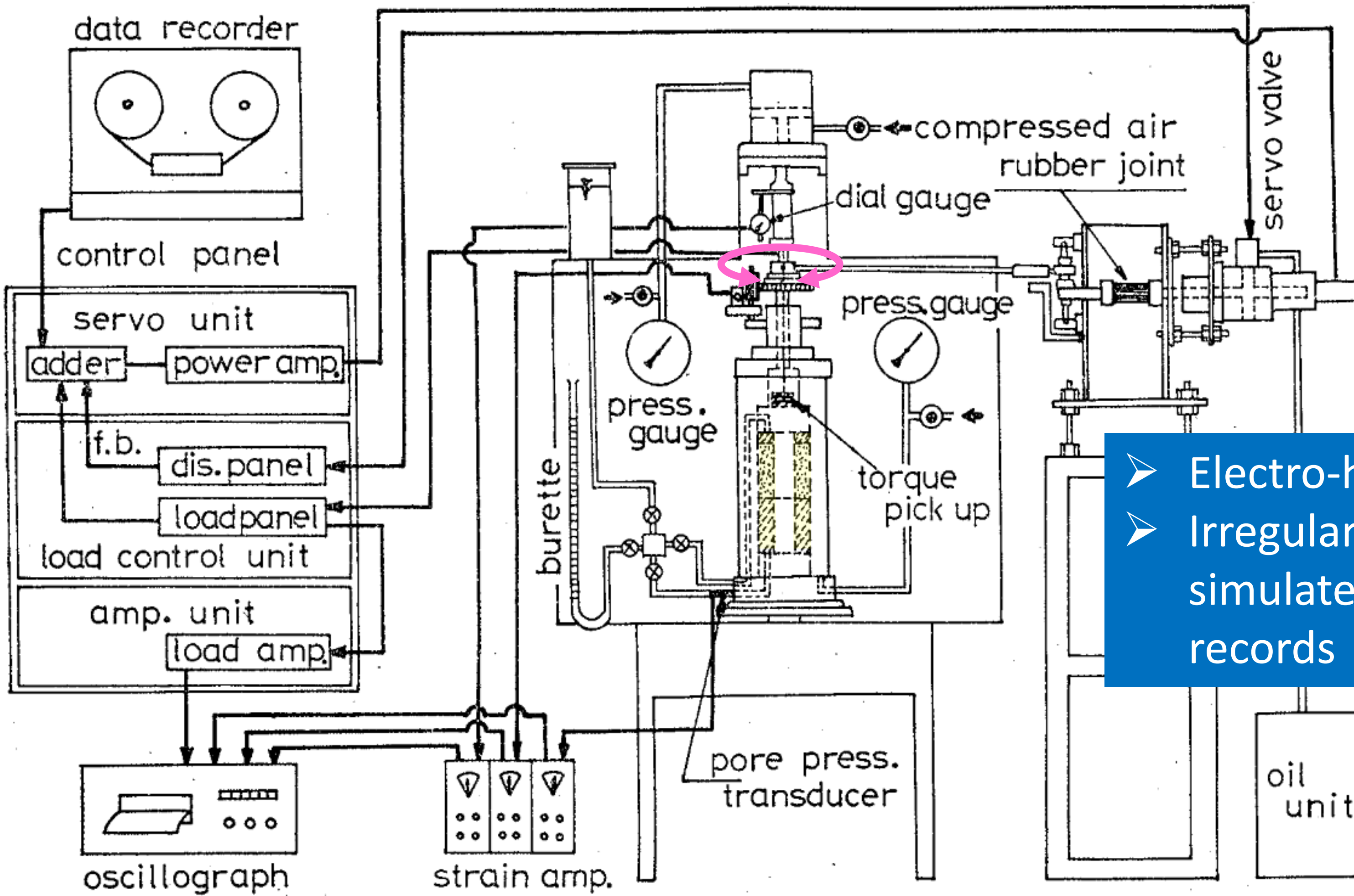

- Electro-hydraulic loading
- Irregular excitations to simulate strong motion records

1980s

Towhata and Ishihara (1985)

Undrained cyclic torsional shear/triaxial tests

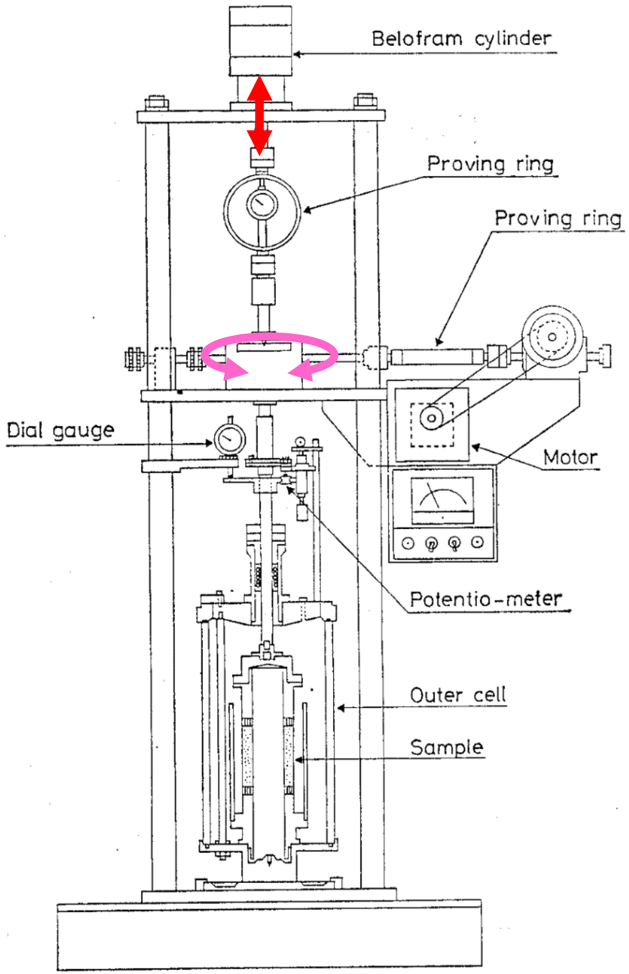

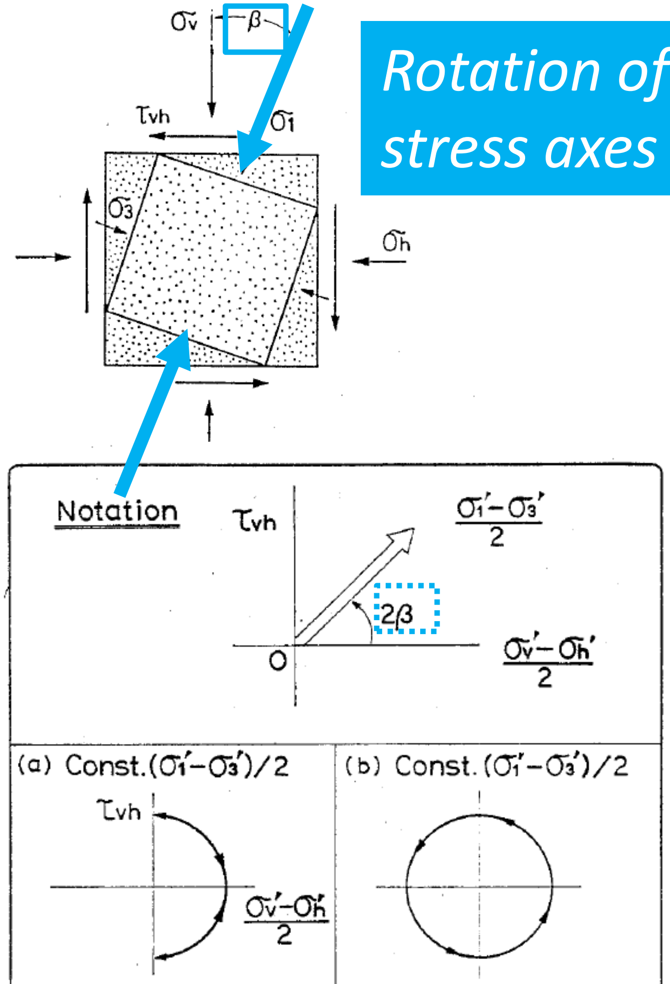

Rotation of principal stress axes

Conventional stress-controlled loading device

Koseki (1987, Master thesis)

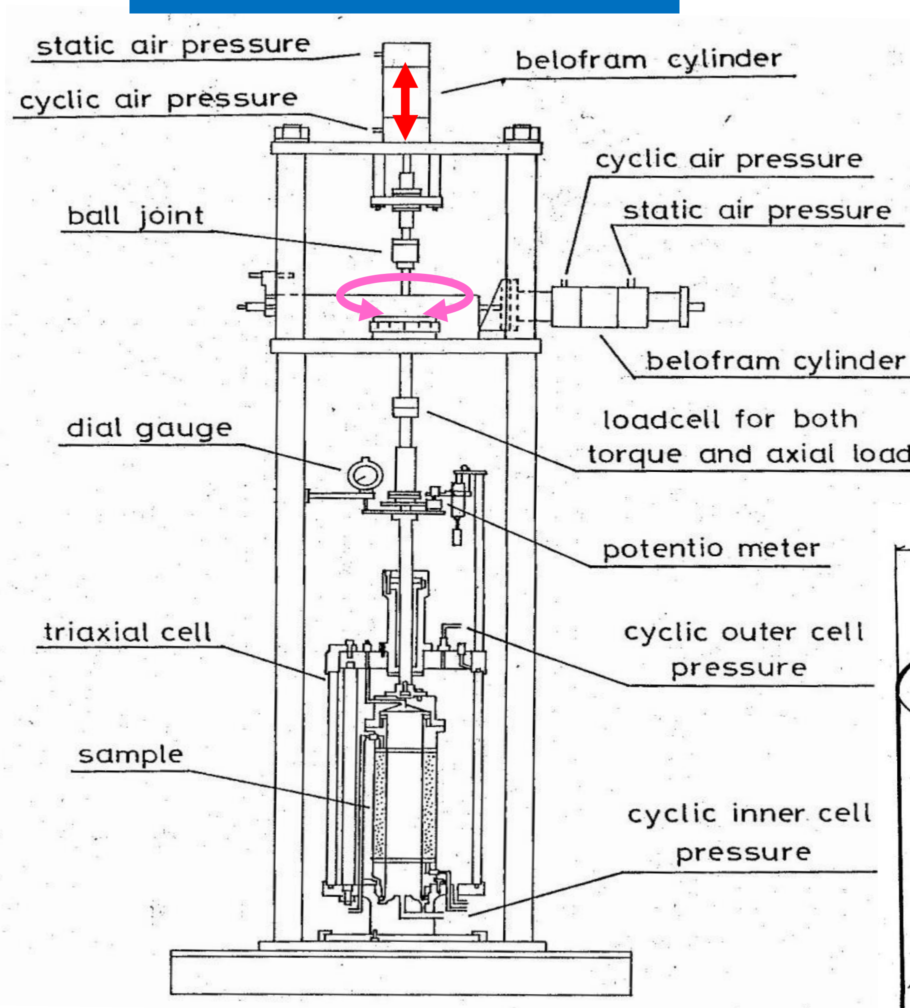

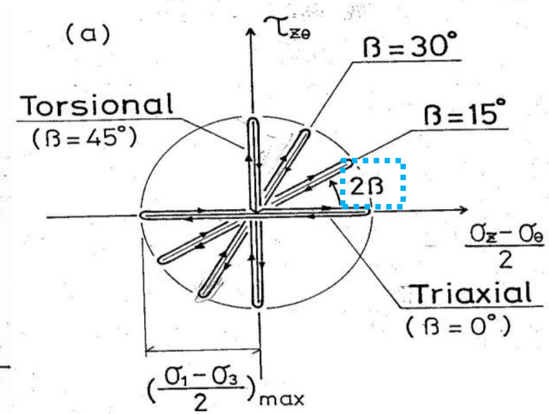

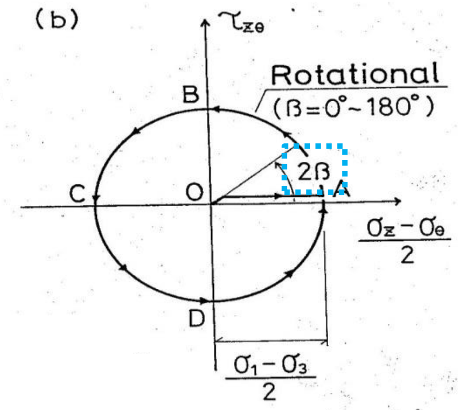

$$b = \frac{\sigma_2 - \sigma_3}{\sigma_1 - \sigma_3}$$

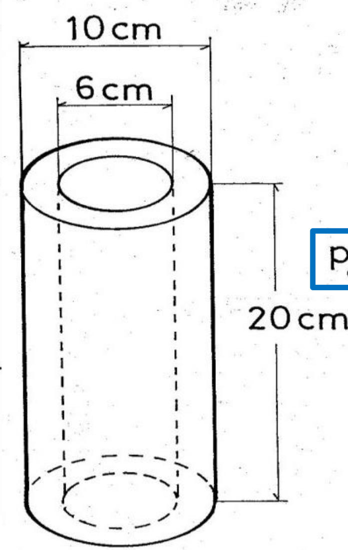

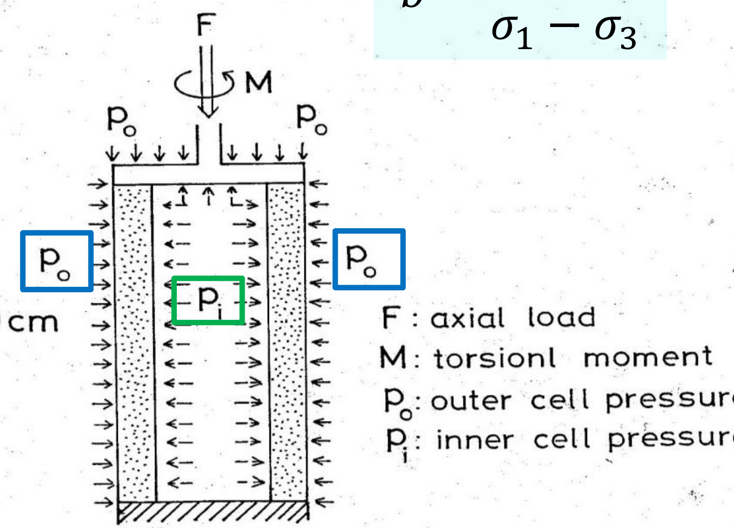

Koseki (1987, Master thesis)

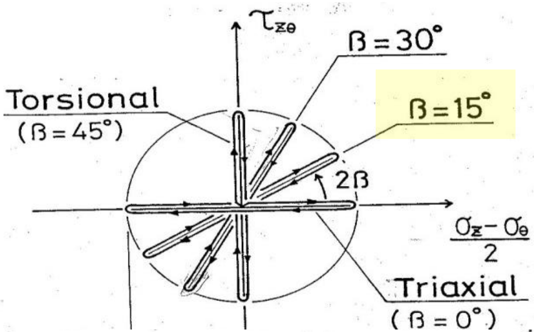

$$b = \frac{\sigma_2 - \sigma_3}{\sigma_1 - \sigma_3} = 0.5$$

Torque

Axial Load

Rotational Angle

Axial Displacement

Outer Cell Pressure

Inner Cell Pressure

Excess Pore Water Pressure

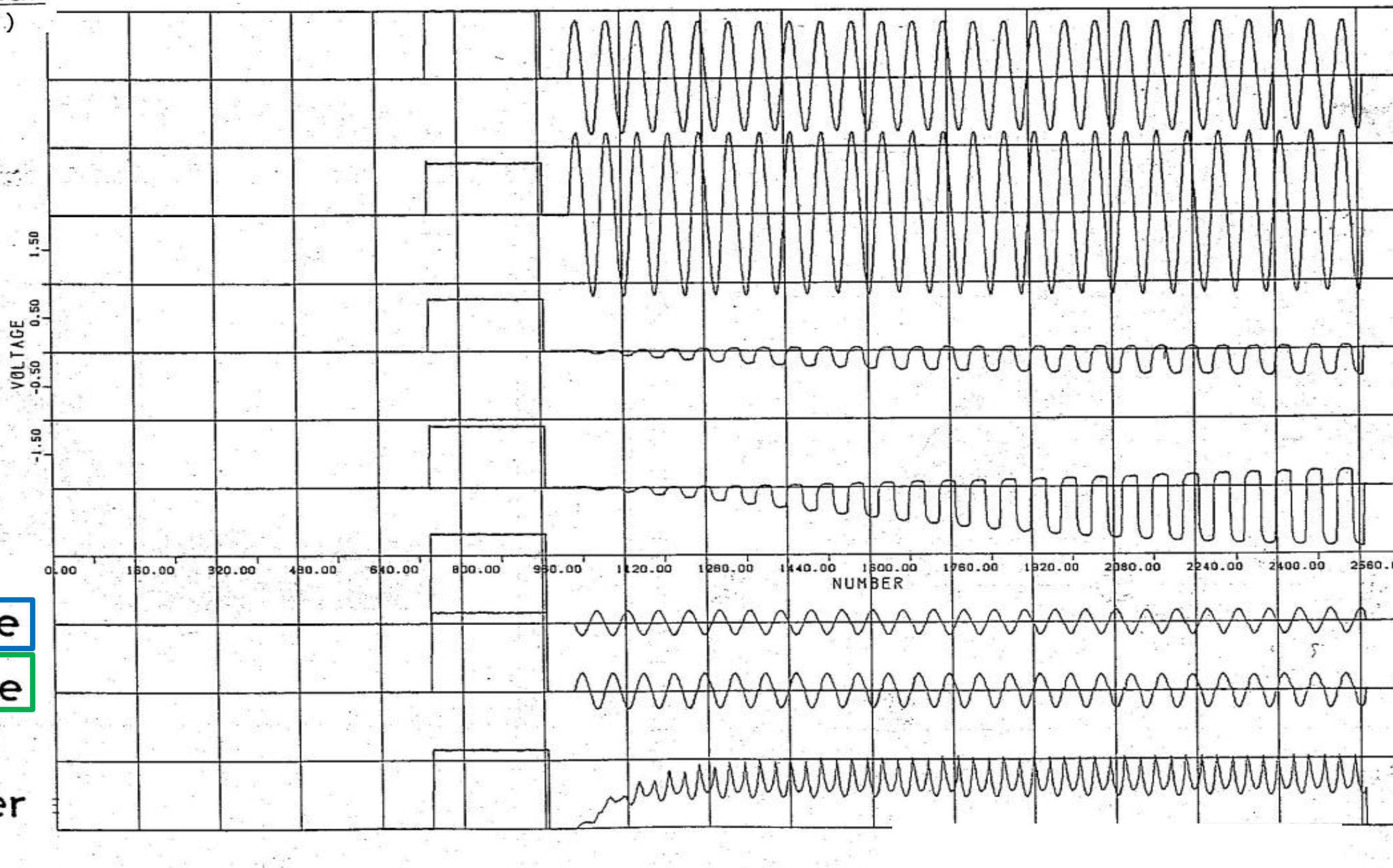

1990s till now

A variety of laboratory stress-strain tests have been conducted to reveal liquefaction properties of sandy soils and applicability of countermeasures such as densification, chemical stabilization & desaturation.

For example, developing/improving apparatuses & relevant control/measurement techniques have been made on the following issues:

- Multi-directional loadings
- Effects of sample disturbance
- Effects of partial drainage (and/or membrane penetration)
- Effects of specimen preparation methods
- Effects of consolidation time
- Possible link with small strain modulus

In this lecture, it is attempted to report some of relevant recent challenges, *including unsuccessful experiences,* in such development/improvement.

For example, developing/improving apparatuses & relevant control/measurement techniques have been made on the following issues:

- ☐ Multi-directional loadings
- ☐ Effects of sample disturbance
- ☐ Effects of partial drainage (and/or membrane penetration)
- ☐ Effects of specimen preparation methods
- ☐ Effects of consolidation time
- ☐ Possible link with small strain modulus

Keywords* in Bishop Lectures

(*excluding "*lab. testing*")

1st by Tatsuoka, F., 2011

Compaction, Design shear strength, Elastic/Viscous properties

2nd by Jardine, R., 2013

Sand, Non-linearity, Anisotropy, Breakage, Time-dependence, Driven piles, Field and model tests

3rd by Di Benedetto, H., 2015

Unbound granular materials, Bituminous mixtures, Rheological modelling, Linearity/Non-linearity, Viscous behaviour

4th by Muir Wood, D., 2017

Constitutive modelling, Inhomogeneity, Yield criterion

5th Lecture

Liquefaction, while touching on the colored keywords listed above

Outline

1. Introduction

2. Local measurements

    2.1 LDTs for cylindrical/prismatic specimens (triaxial)

    2.2 LDTs for hollow cylindrical specimen (torsional shear/triaxial)

    2.3 Local dynamic measurements

3. Unconventional liquefaction tests

    3.1 Liquefaction tests using motor-driven loading devices

    3.2 Cylindrical/prismatic specimens with thin sandy layer

    3.3 Segregated hollow cylindrical specimen

    3.4 Direct/indirect evaluation of local deformation during liquefaction

4. Other special tests

    4.1 Large deformation tests

    4.2 Direct tension tests

    4.3 Long-term tests

5. Concluding remarks

Local deformation transducers (LDTs)

Sensitivity of 0.001%

Affected by bedding error & end restraint

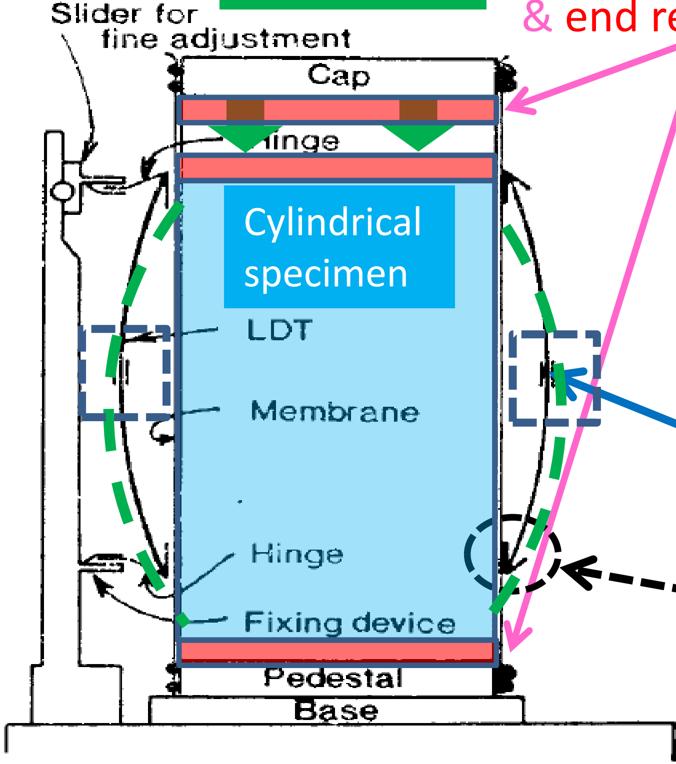

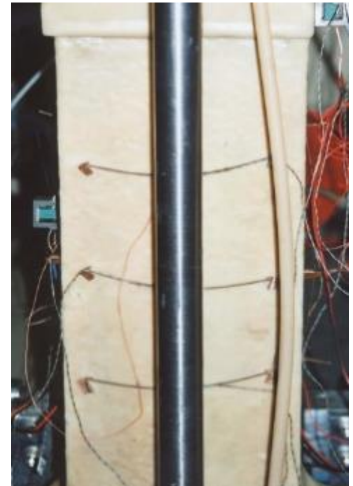

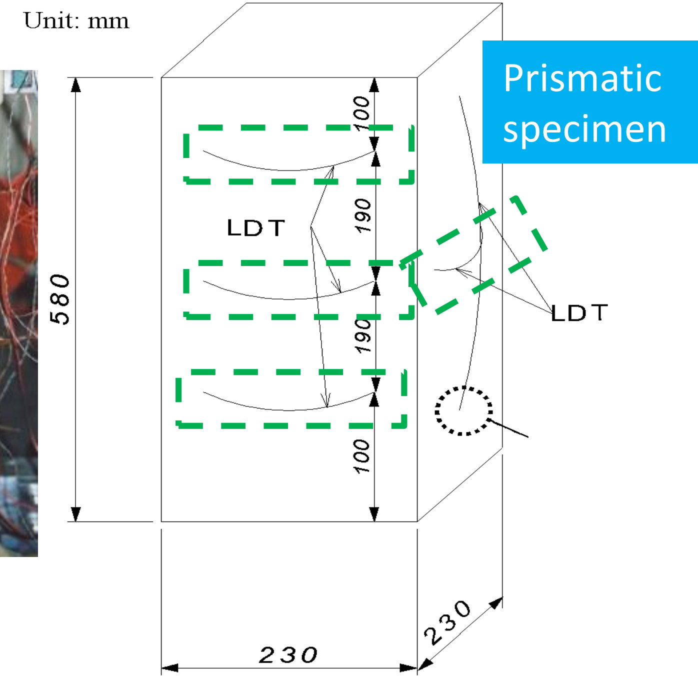

Strain gauges to measure bending deflection of phosphor bronze strip

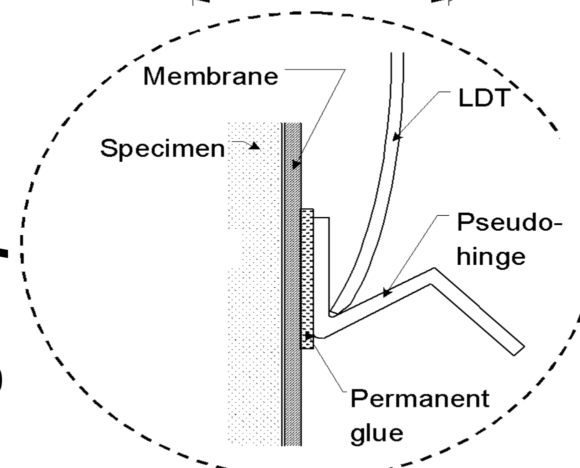

LDTs *(Goto et al., 1991)* with a strip length of 90 mm for 100 mm-high specimen and 500 mm for 600 mm-high specimen

Heterogeneous specimen retrieved from tunnel excavation site *(Koseki et al., 2011)*

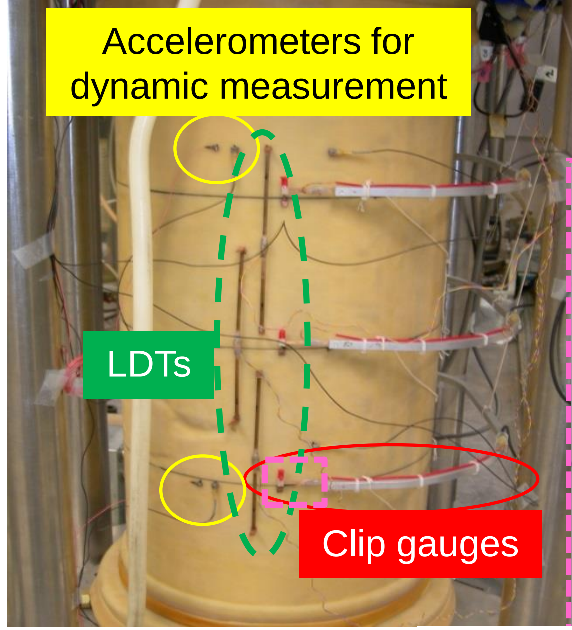

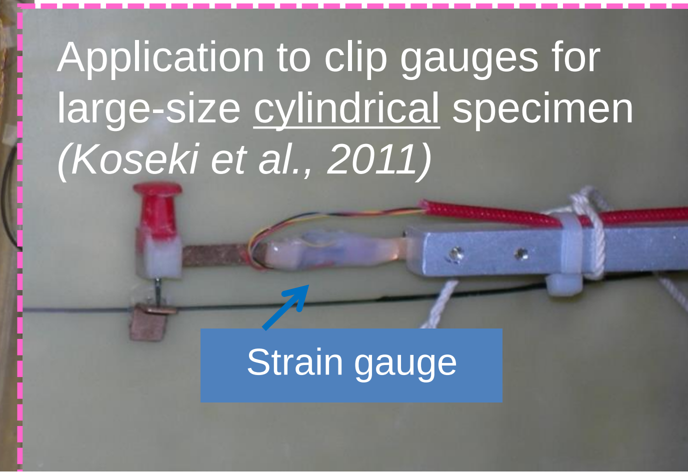

Attempts to improve the LDT performance under low confining stress *(Lenart et al., 2014)*

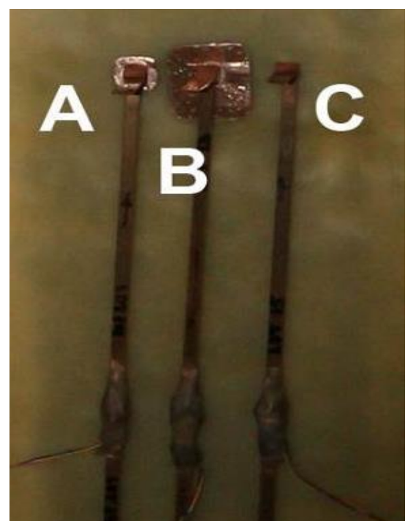

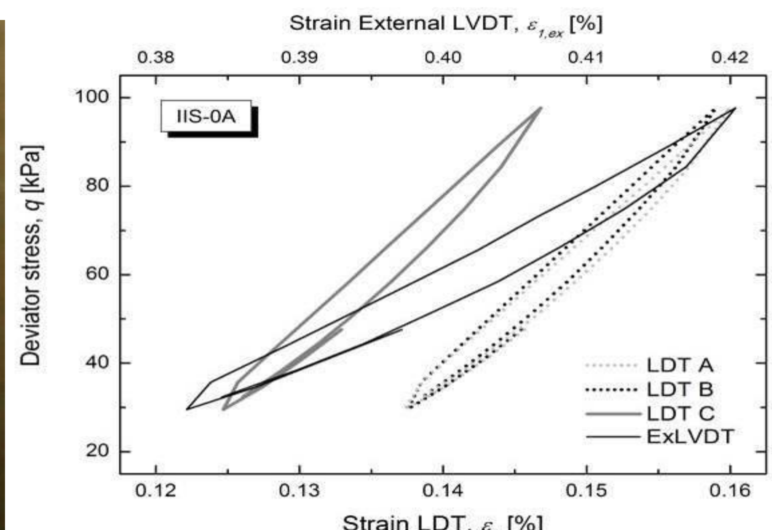

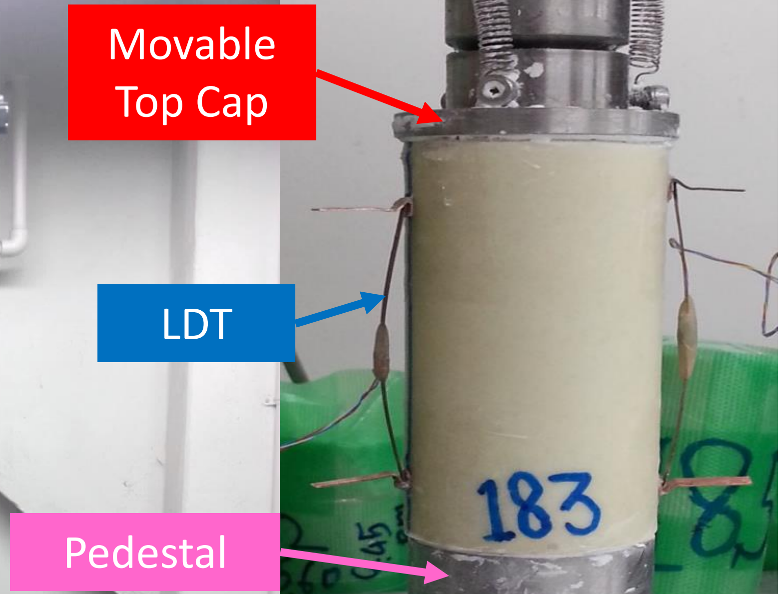

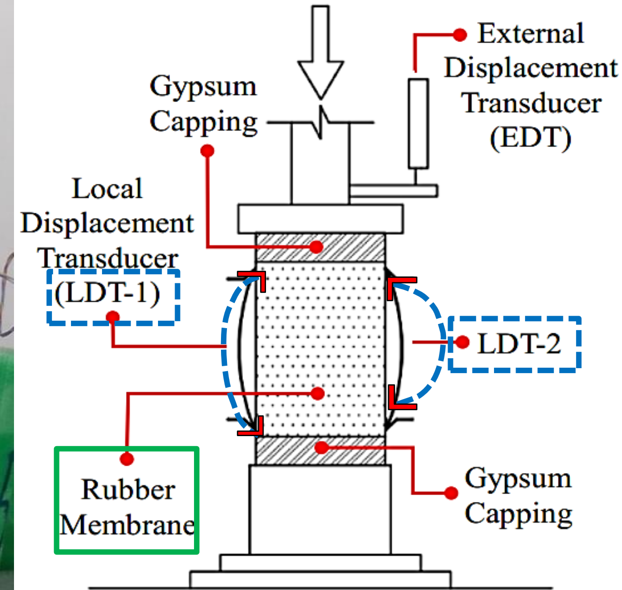

For long-term tests, rubber membrane is used.

LDTs in <u>unconfined compression</u> tests on gypsum-mixed sand
(Maqsood et al., 2019, this symposium)

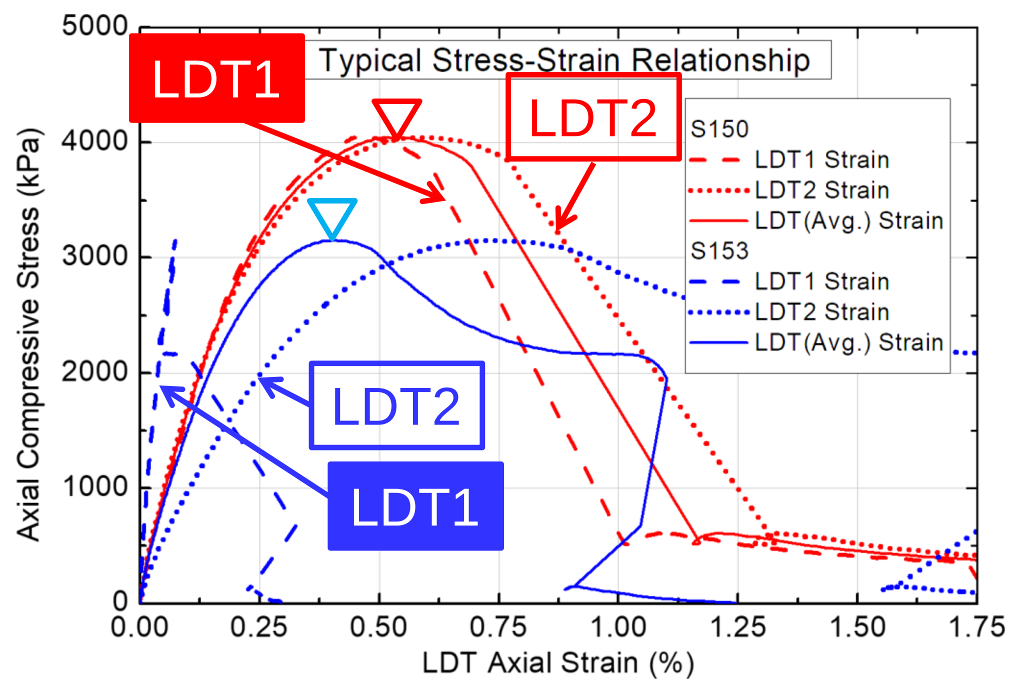

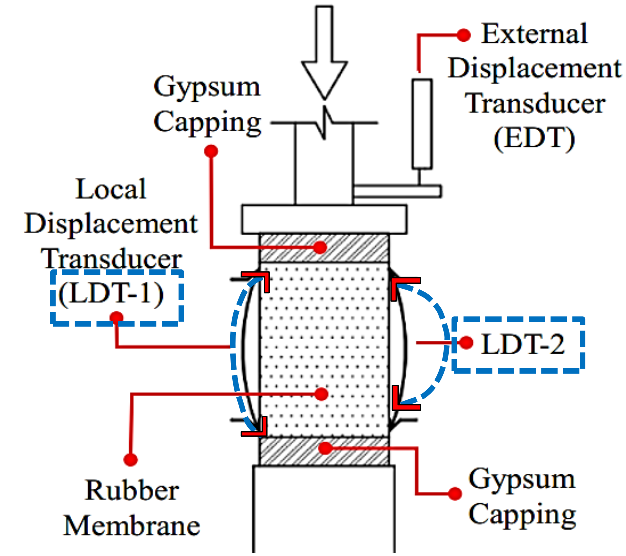

Absolute Average Difference of LDT strains *(Maqsood et al., 2018)* :

$$AAD = \left|\frac{\text{LDT1} - \text{LDT2}}{\text{LDT1} + \text{LDT2}}\right| \times 100\,(\%)$$

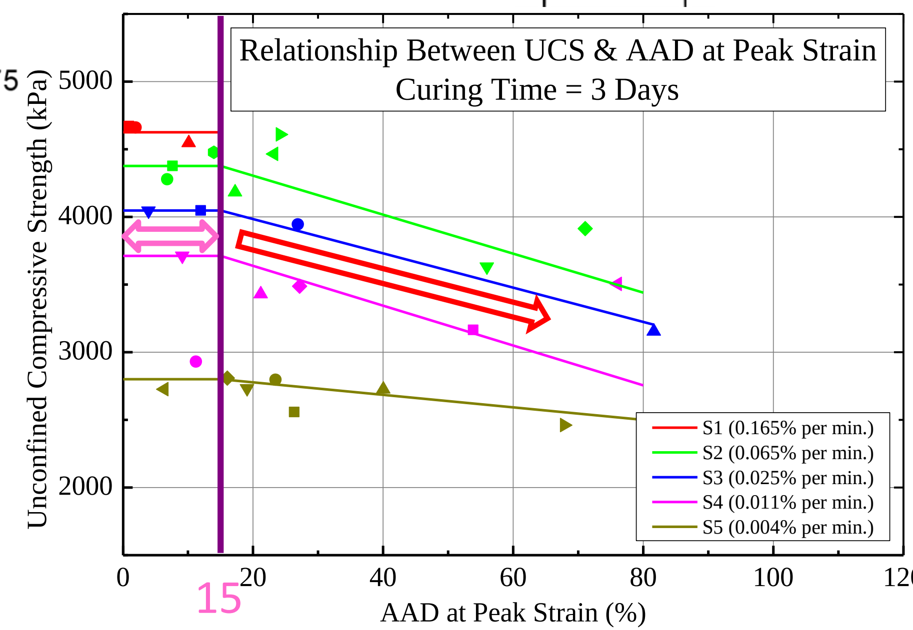

- ✓ *Peak strength decreases with increase in AAD*
- ✓ *Peak strength remains unaffected for AAD<15%*
- ✓ *AAD is used to assess reliability of test results*

Large scale plain strain compression tests on compacted gravel

(Maqbool & Koseki, 2007)

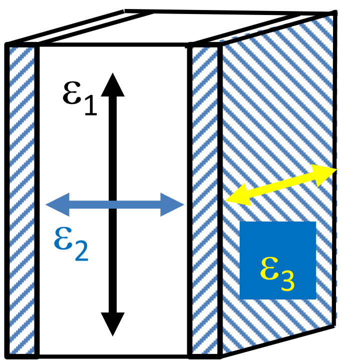

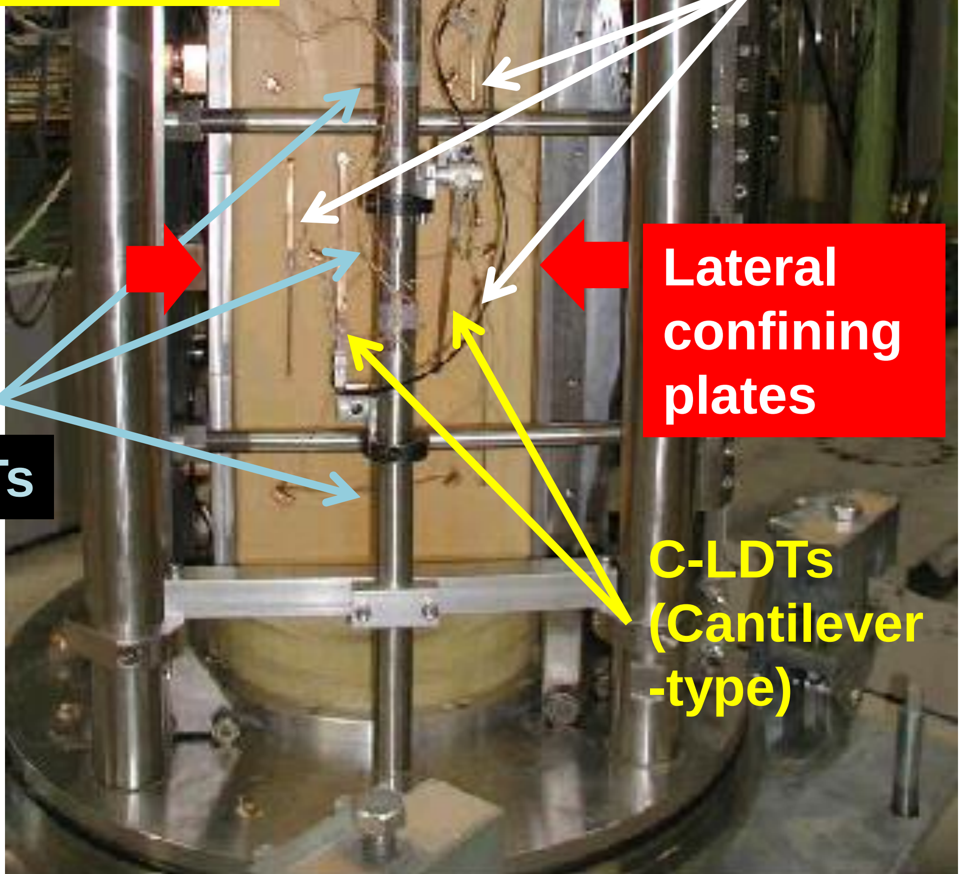

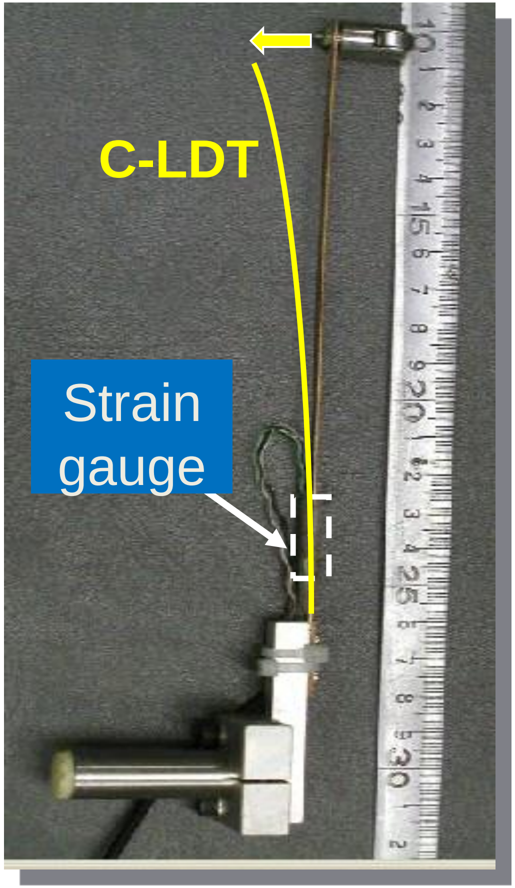

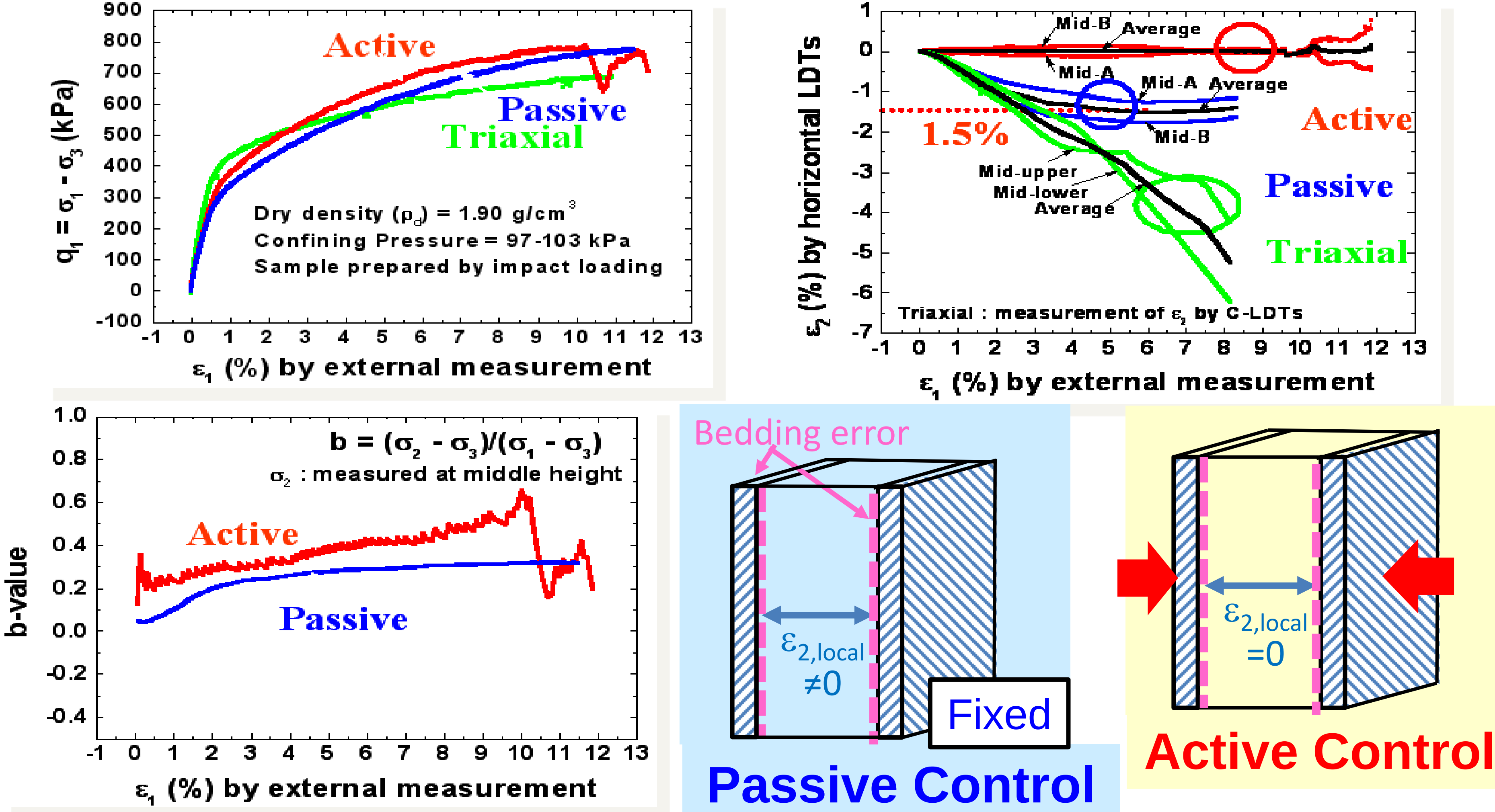

Passive- and active-control "plane strain" compression tests on compacted gravel *(Maqbool and Koseki, 2007)*

2.2 LDTs for hollow cylindrical specimen (torsional shear/triaxial)

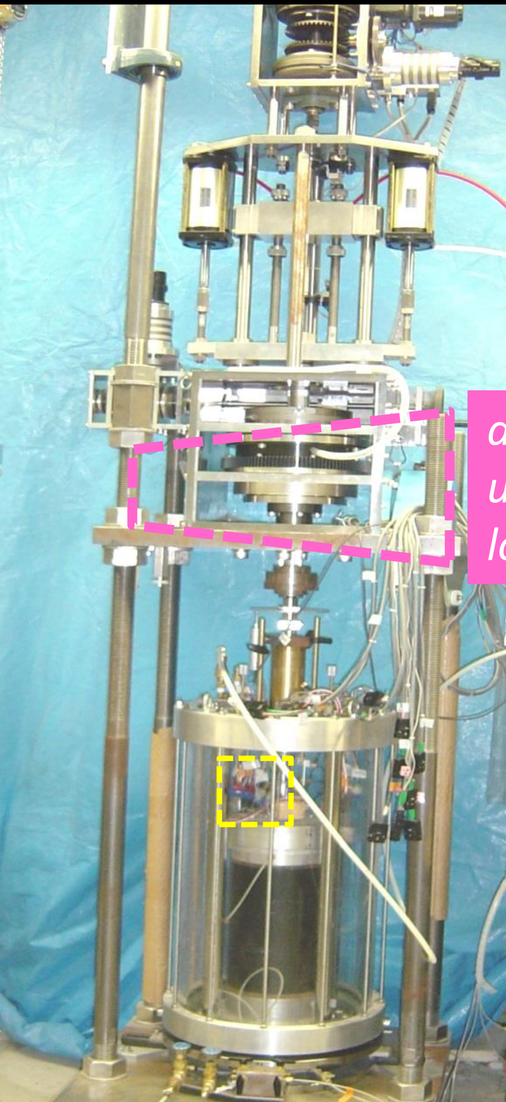

accidentally conducted under misalignment of loading frame

External measurement of axial deformation *(Koseki et al., 2001)*

③Proximity transducer for small vertical displacement
④Proximity transducer for small rotational displacement
⑤Potentiometer for large rotational displacement
⑥High capacity differential pressure transducer for confining stress
⑦Low capacity differential pressure transducer for volume change

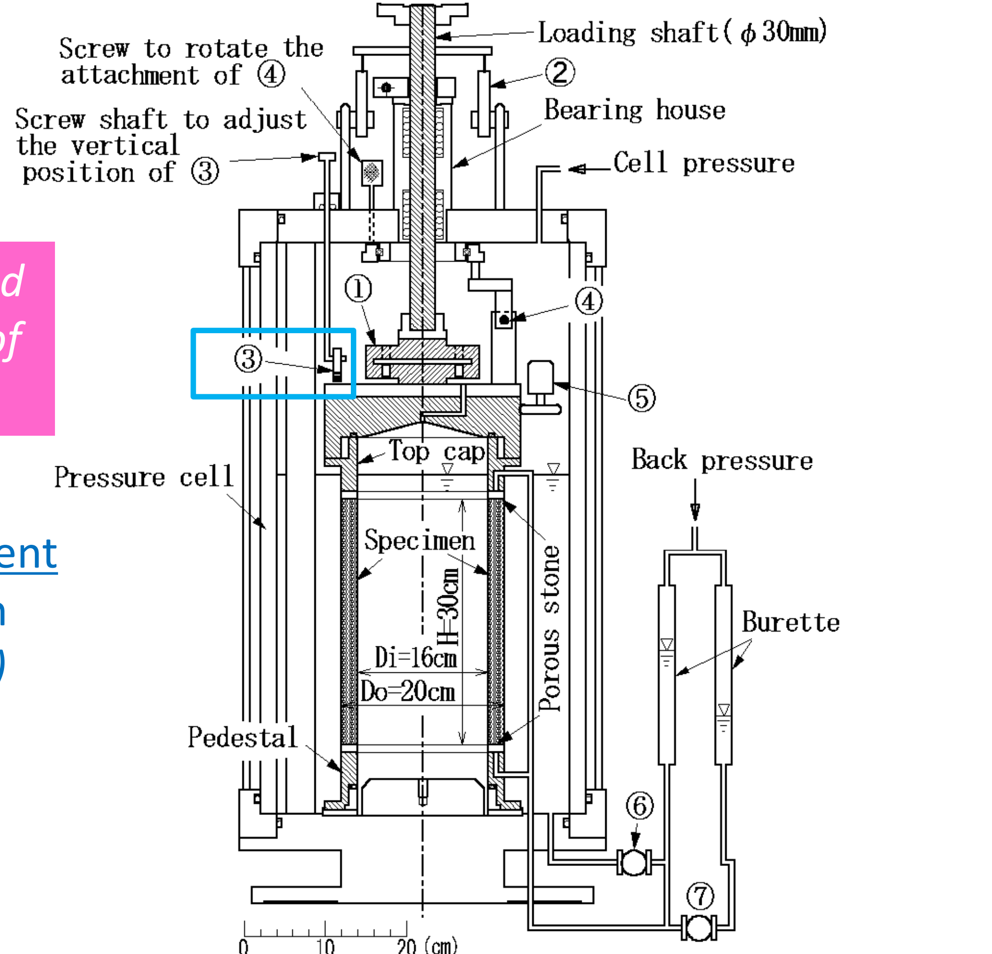

Small unload/reload cycles along different stress paths

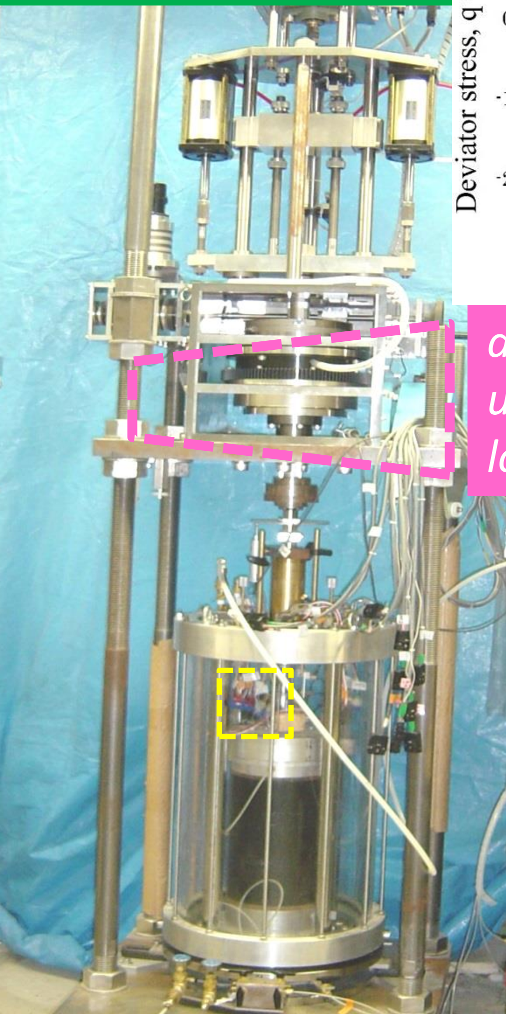

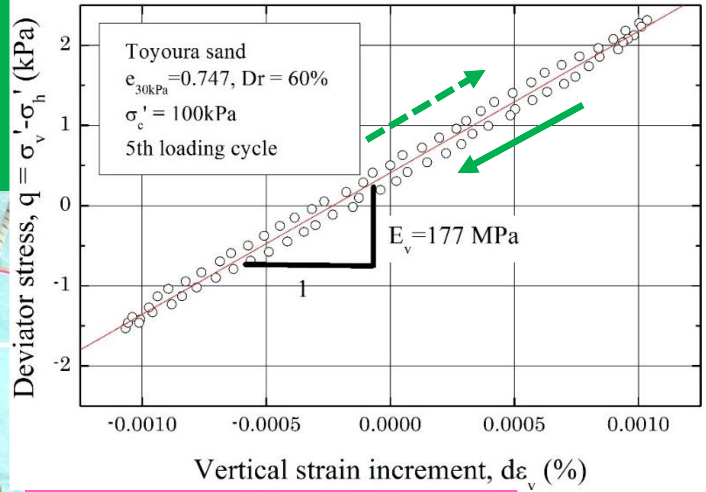

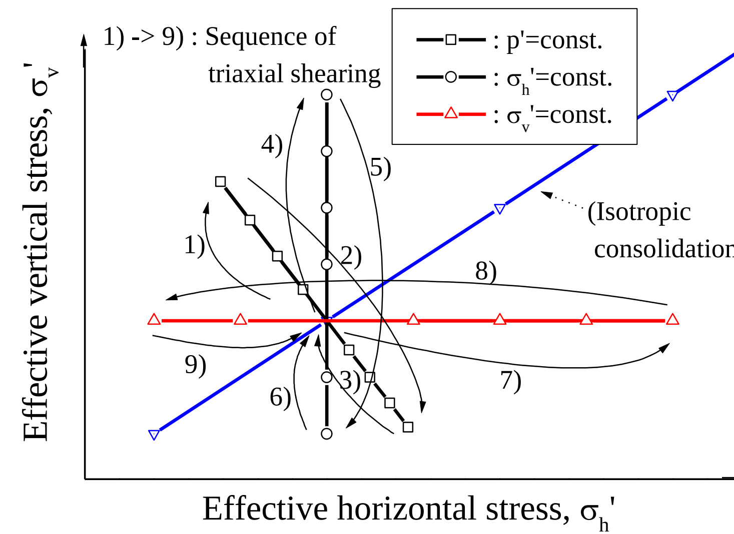

accidentally conducted under misalignment of loading frame

External measurement of axial deformation *(Koseki et al., 2001)*

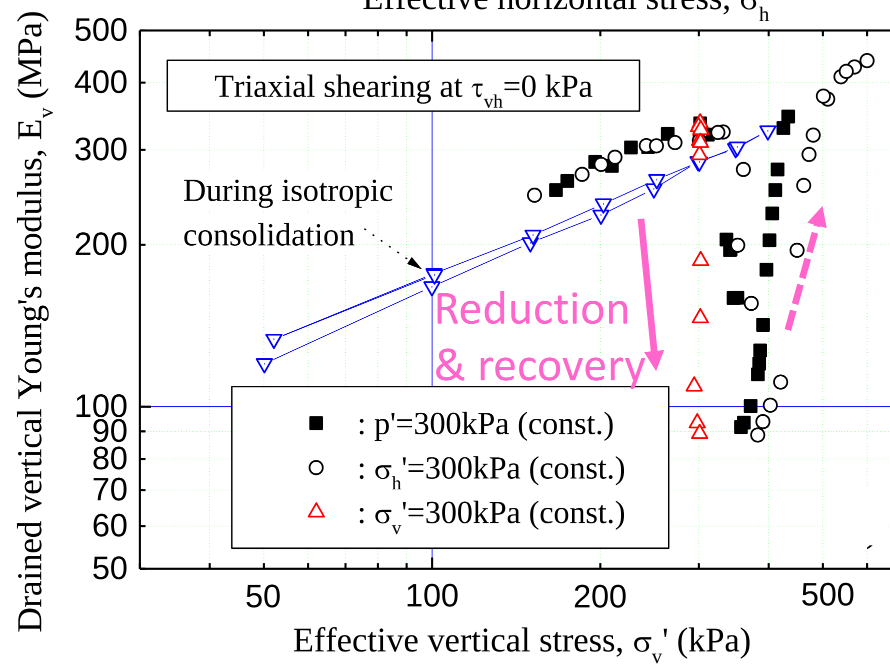

Test results using P-LDTs after fixing misalignment *(HongNam, 2004)*

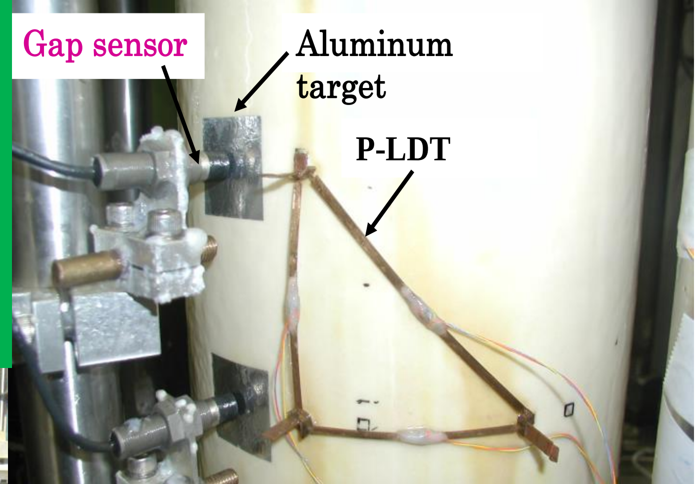

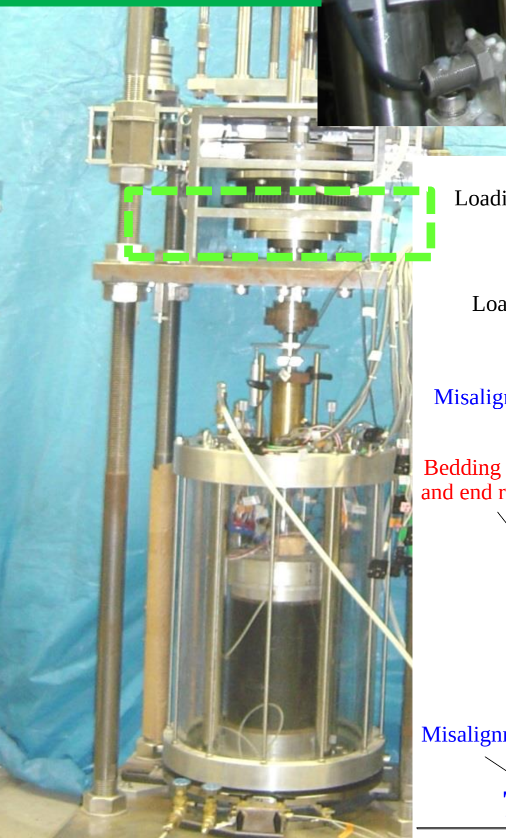

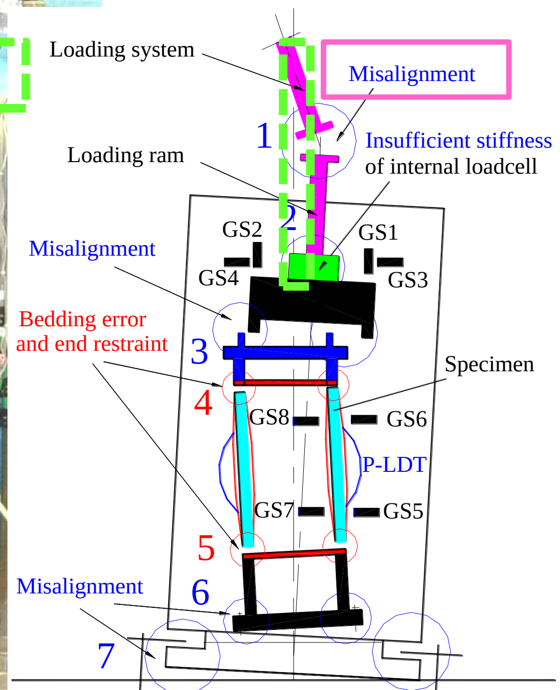

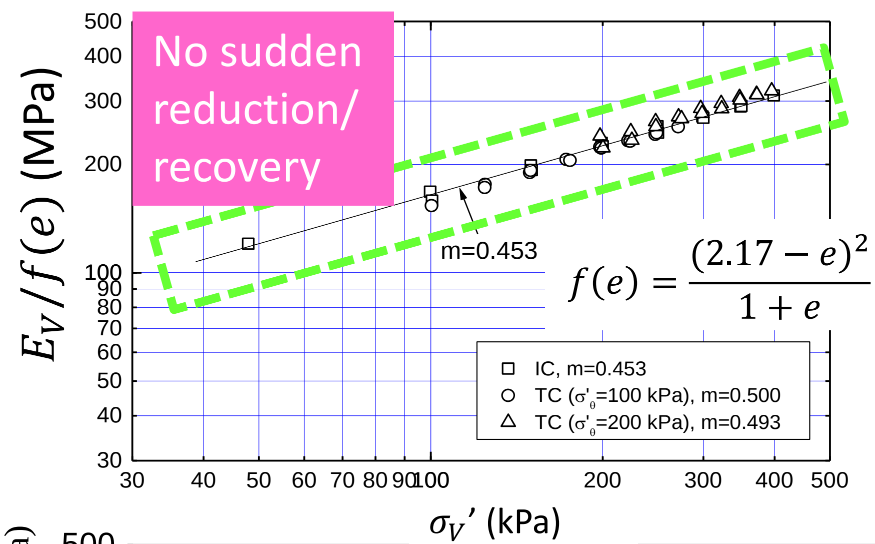

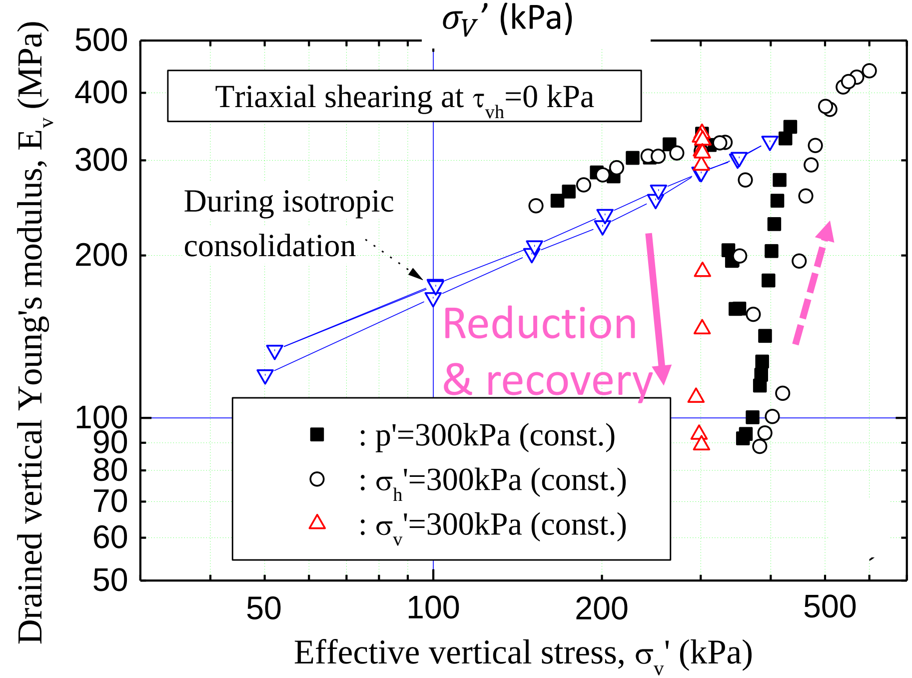

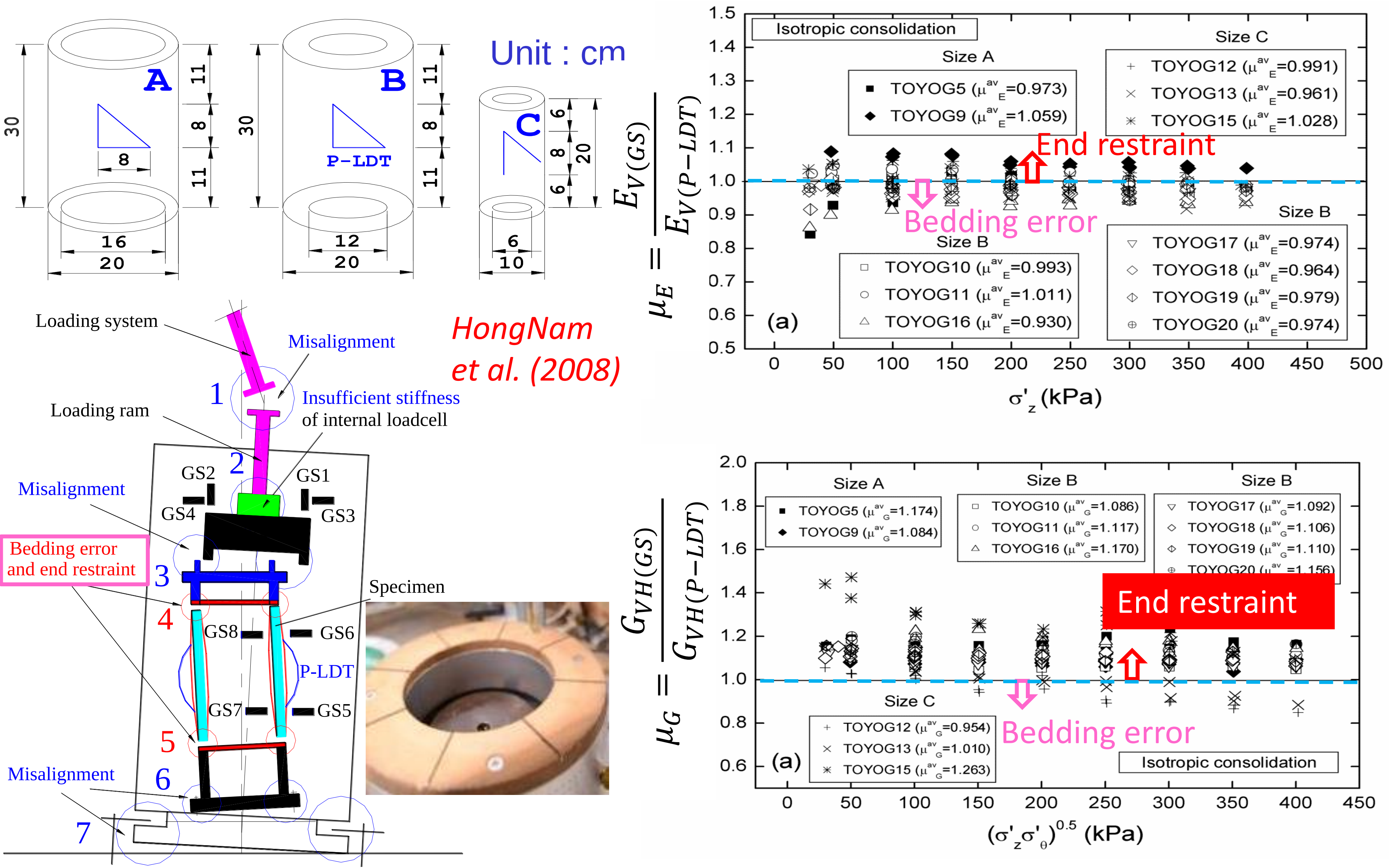

Unit : cm
A
B
C
P-LDT
30
11
8
11
8
16
20
12
20
6
8
6
20
6
10
Loading system
Misalignment
Insufficient stiffness
of internal loadcell
Loading ram
HongNam
et al. (2008)
GS1
GS2
GS3
GS4
GS5
GS6
GS7
GS8
Misalignment
Bedding error
and end restraint
Specimen
P-LDT
Misalignment
1
2
3
4
5
6
7
Isotropic consolidation
Size A
TOYOG5 (μ^{av}_E=0.973)
TOYOG9 (μ^{av}_E=1.059)
Size C
TOYOG12 (μ^{av}_E=0.991)
TOYOG13 (μ^{av}_E=0.961)
TOYOG15 (μ^{av}_E=1.028)
End restraint
Bedding error
Size B
TOYOG10 (μ^{av}_E=0.993)
TOYOG11 (μ^{av}_E=1.011)
TOYOG16 (μ^{av}_E=0.930)
Size B
TOYOG17 (μ^{av}_E=0.974)
TOYOG18 (μ^{av}_E=0.964)
TOYOG19 (μ^{av}_E=0.979)
TOYOG20 (μ^{av}_E=0.974)
(a)
$\mu_E = \frac{E_{V(GS)}}{E_{V(P-LDT)}}$
σ'z (kPa)
Size A
TOYOG5 (μ^{av}_G=1.174)
TOYOG9 (μ^{av}_G=1.084)
Size B
TOYOG10 (μ^{av}_G=1.086)
TOYOG11 (μ^{av}_G=1.117)
TOYOG16 (μ^{av}_G=1.170)
Size B
TOYOG17 (μ^{av}_G=1.092)
TOYOG18 (μ^{av}_G=1.106)
TOYOG19 (μ^{av}_G=1.110)
End restraint
Size C
TOYOG12 (μ^{av}_G=0.954)
TOYOG13 (μ^{av}_G=1.010)
TOYOG15 (μ^{av}_G=1.263)
Bedding error
Isotropic consolidation
(a)
$\mu_G = \frac{G_{VH(GS)}}{G_{VH(P-LDT)}}$
$(\sigma'_z\sigma'_\theta)^{0.5}$ (kPa)

2.3 Local dynamic measurements

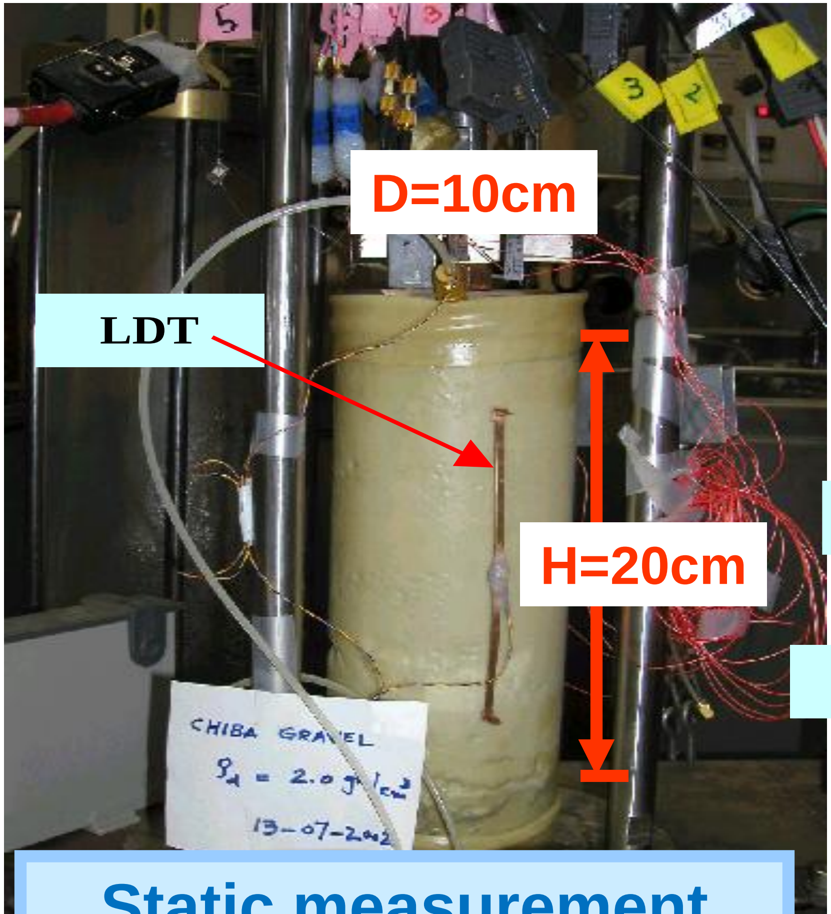

Static measurement

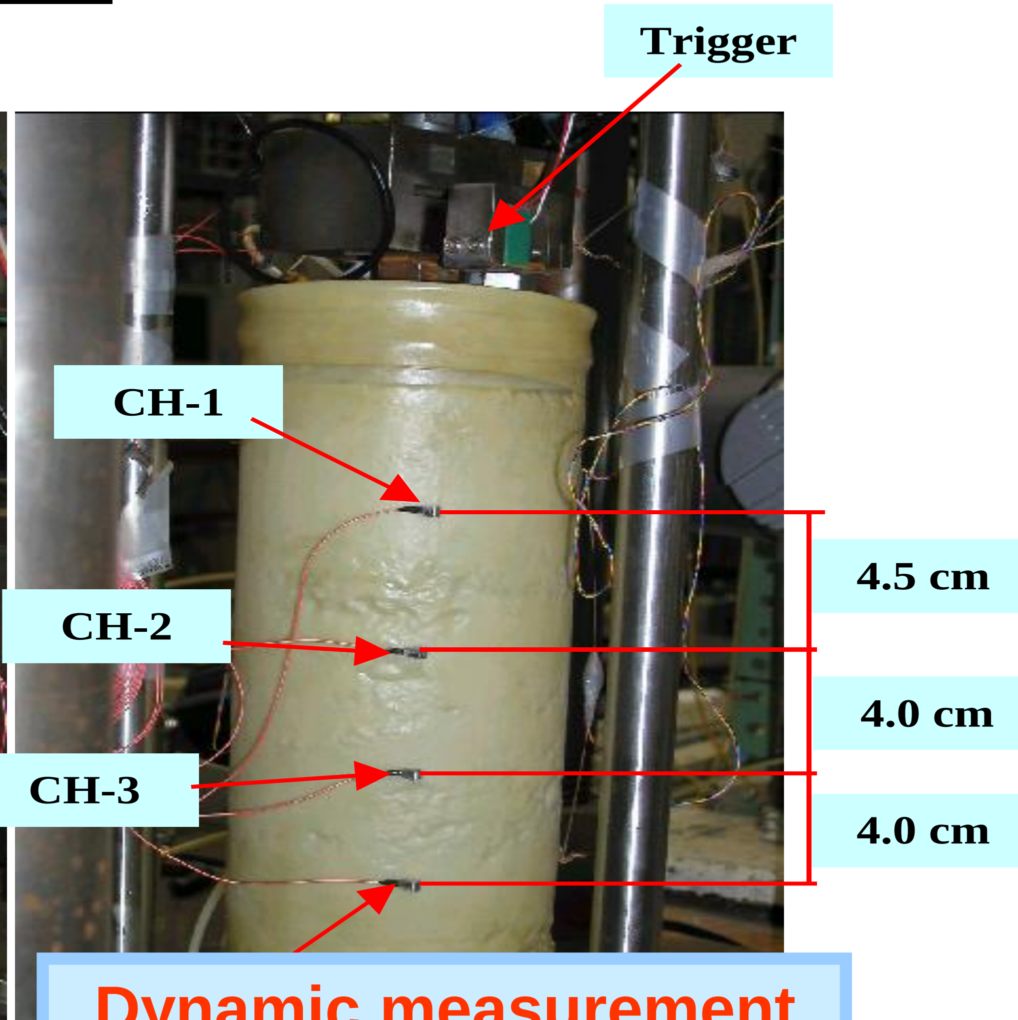

Dynamic measurement

Accelerometers and triggers for wave velocity

$$v = \frac{d_i}{\Delta t_i}$$

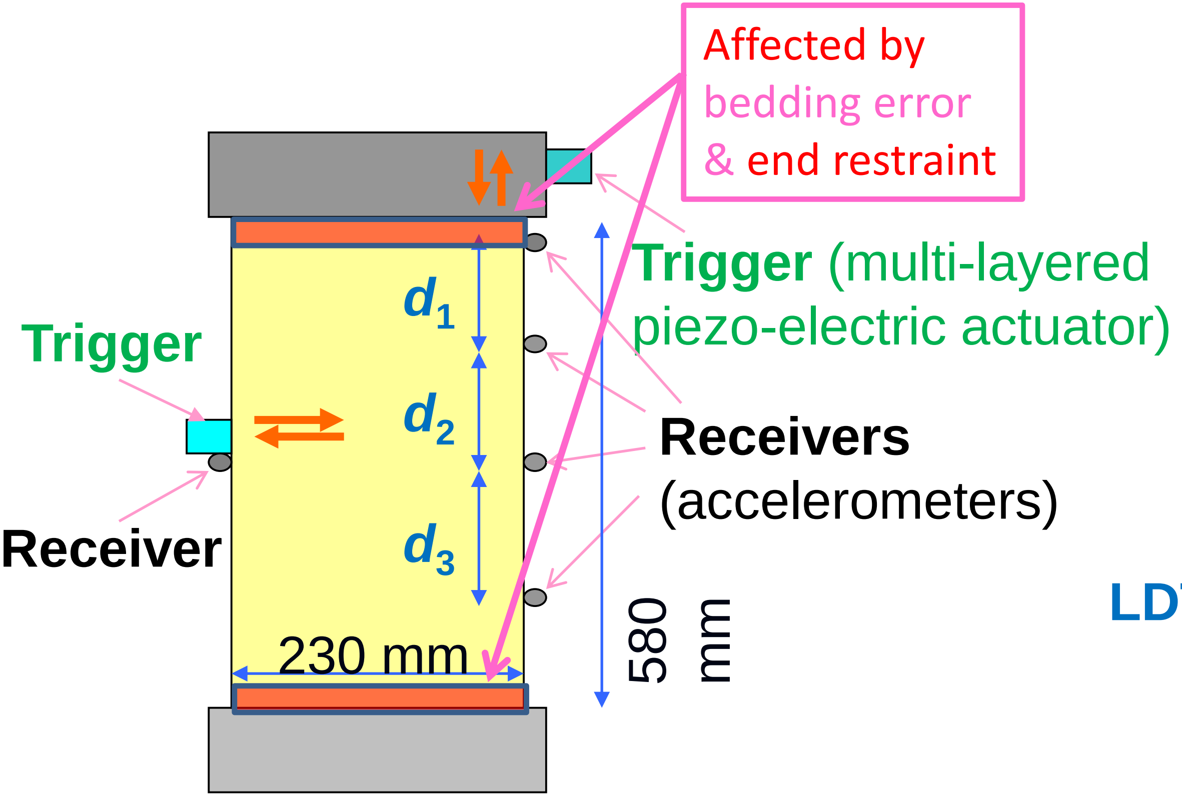

Local dynamic measurement with large prismatic specimen *(modified after AnhDan et al., 2002)*

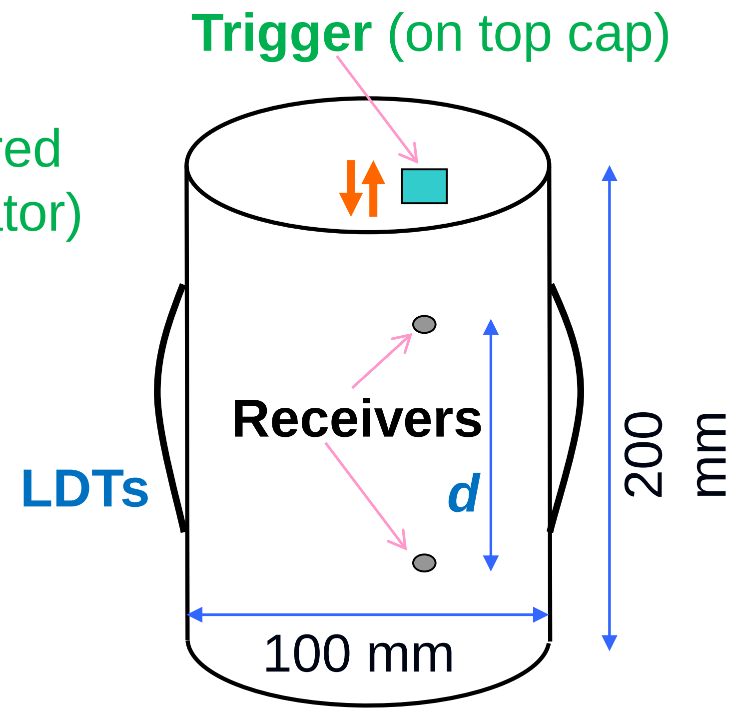

Local dynamic measurement with medium cylindrical specimen *(modified after Maqbool and Koseki, 2011)*

Application to AE (*acoustic emission*) tomography for source location

(modified after Lin et al., 2019)

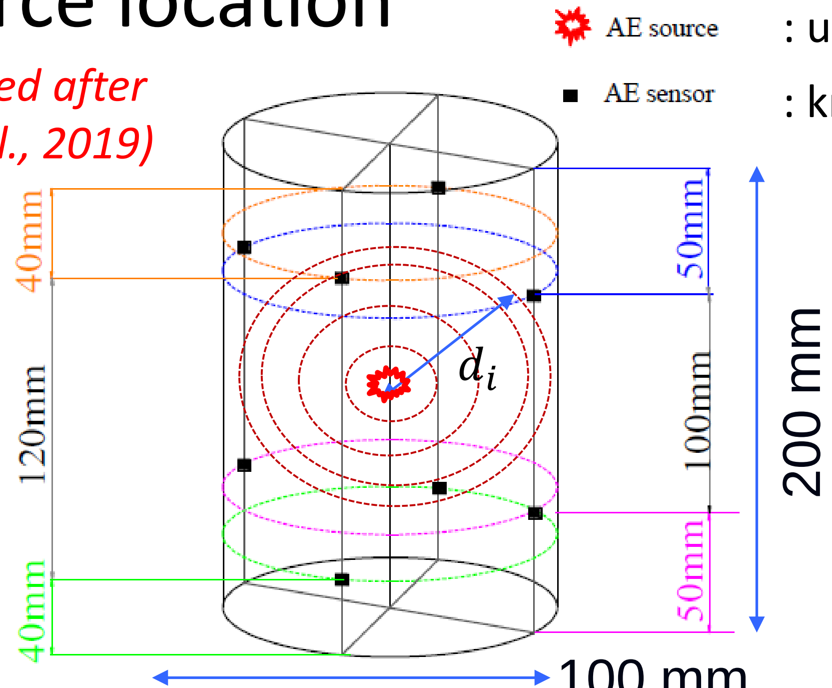

: unknown location (x, y, z) and generation time t

: known location (x_i, y_i, z_i) and arrival time t_i

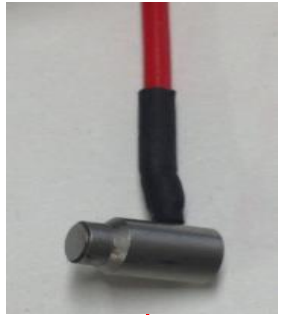

Sensitivity: 115 ± 3 dB (0 dB=1 V/m/s)
Working frequency: 10 kHz to 2 MHz

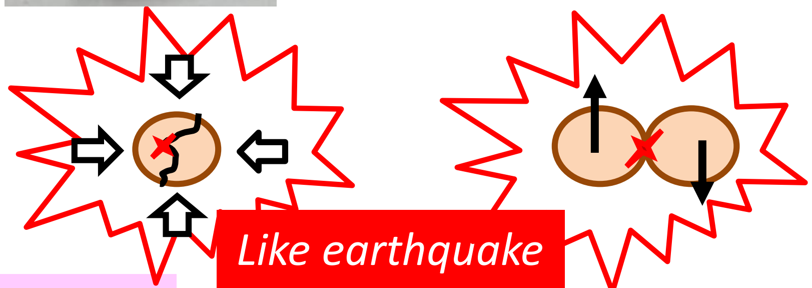

Like earthquake epicenter…

Travel distance between AE source and *i*-th sensor:

$$d_i = (t_i - t) \times v = \sqrt{(x - x_i)^2 + (y - y_i)^2 + (z - z_i)^2}$$

AE wave velocity *(assumed to be 1500 m/sec for saturated sand specimen)*

Typical AE data for 0.5 second at a sampling rate of 2MS/sec

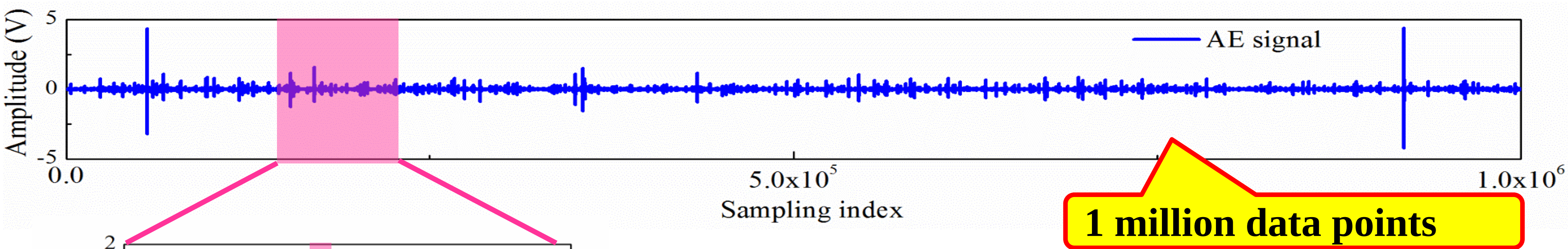

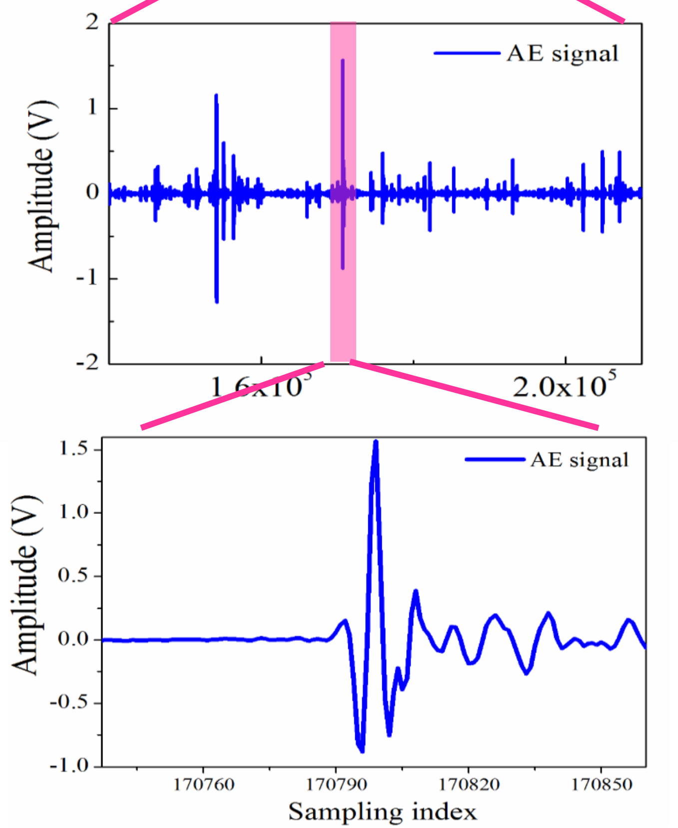

Automatic pick-up based on autoregressive information criteria (AIC) by Akaike (1974)

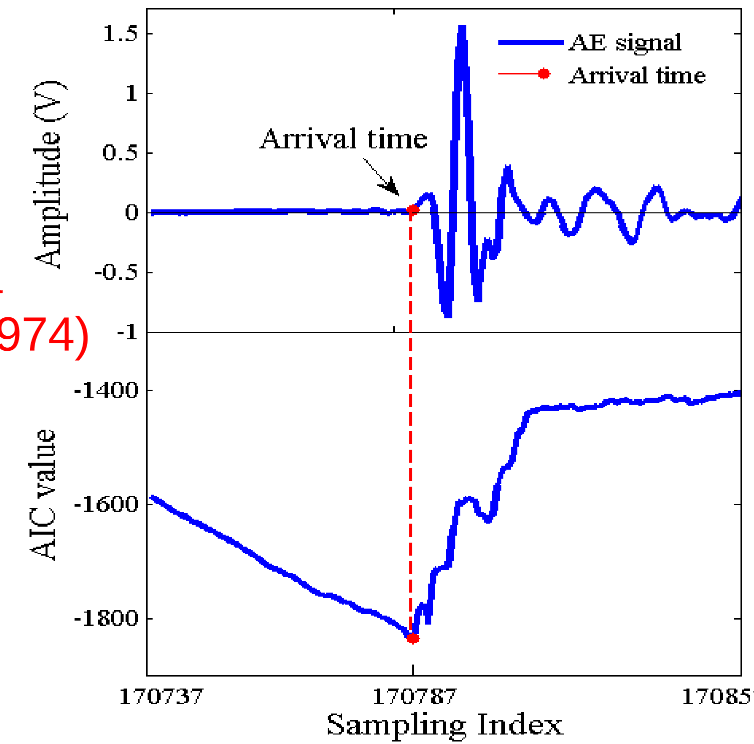

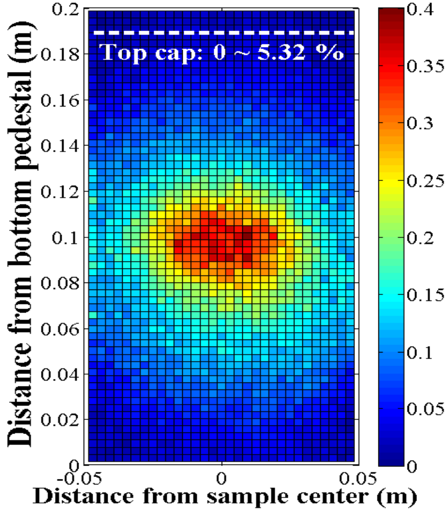

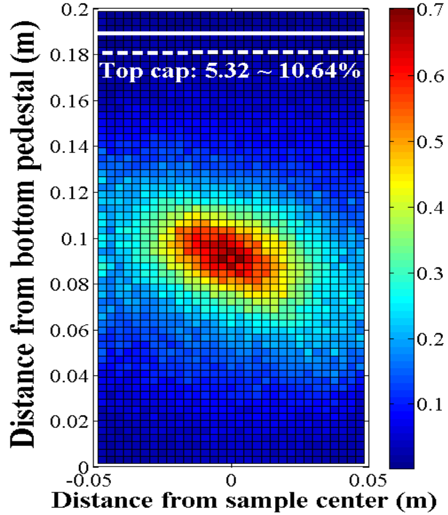

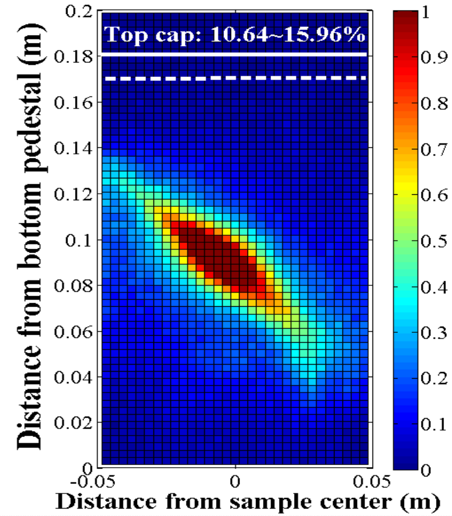

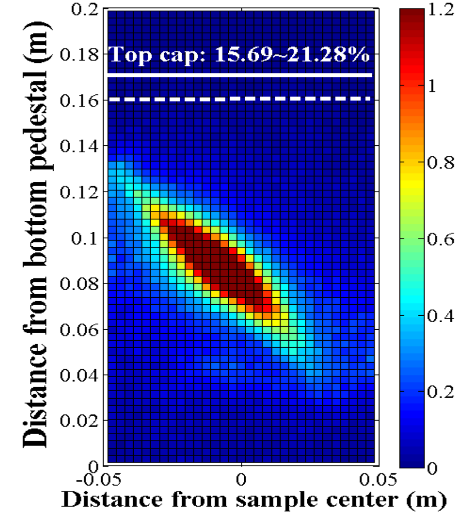

Travel distance:

$$d_i = (t_i - t) \times v_i$$

With dry sand, effects of Inherent & stress-state dependent anisotropies shall be considered.

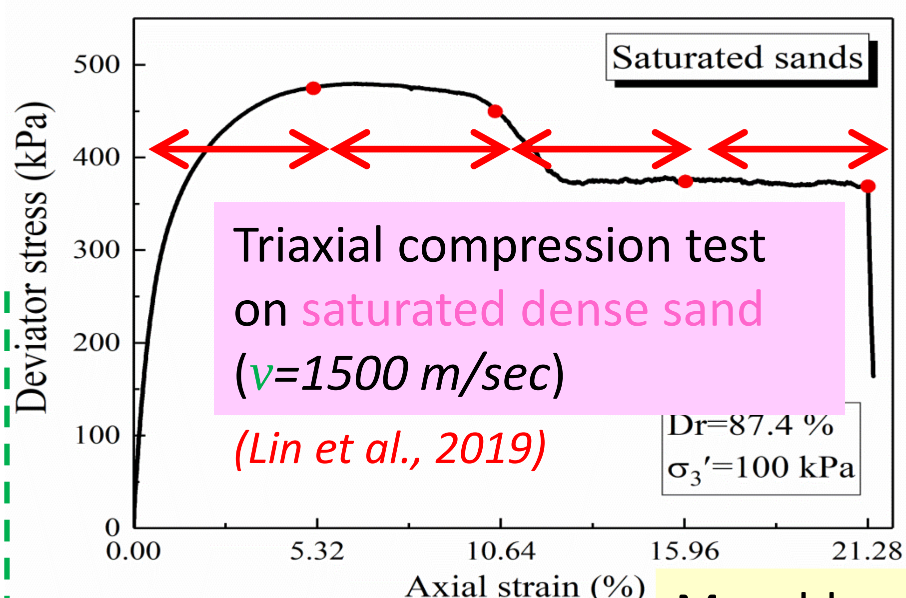

Triaxial compression test on saturated dense sand (v=1500 m/sec)

(Lin et al., 2019)

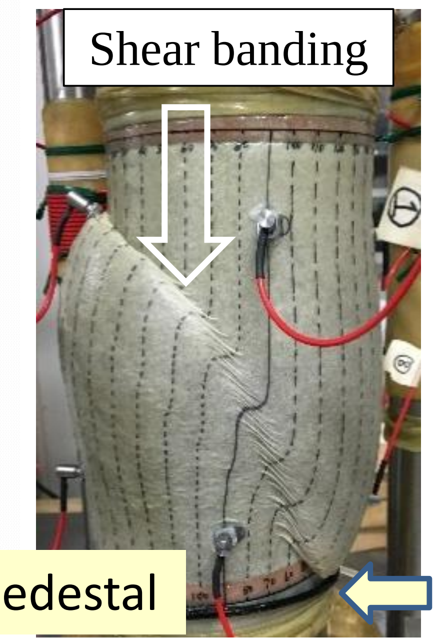

Summary on local measurements (1/2)

- Several types of LDTs have been developed for local static measurements in triaxial, plane strain and torsional shear tests.

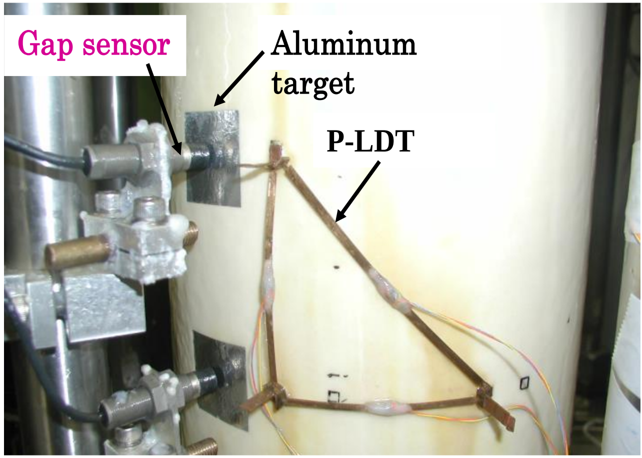

- ✓ They are effective in reducing the effects of bedding error, end restraint and/or system compliance in general.

- ✓ They can be also used to evaluate possible non-uniformities of the local stress/strain distribution induced by system compliance and/or specimen heterogeneity.

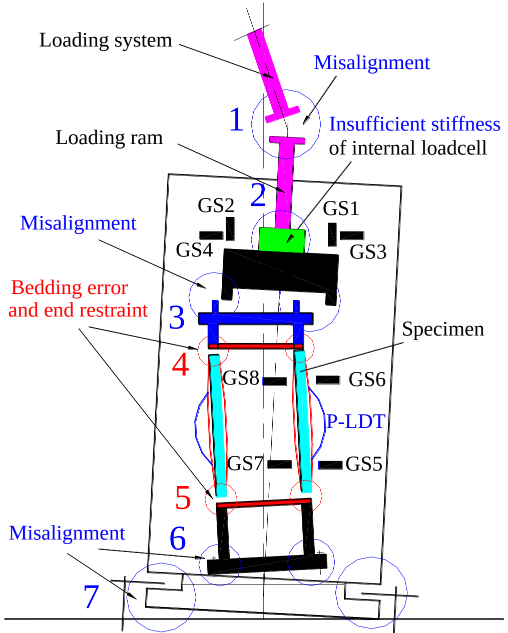

Summary on local measurements (2/2)

- ☐ For local dynamic measurements, accelerometers and AE sensors have been used for evaluation of elastic wave velocities and AE source location, respectively.

- ✓ For non-destructive evaluation of particle crushing and/or sliding, the AE measurement would be promising, while further studies are required on effects of anisotropies.

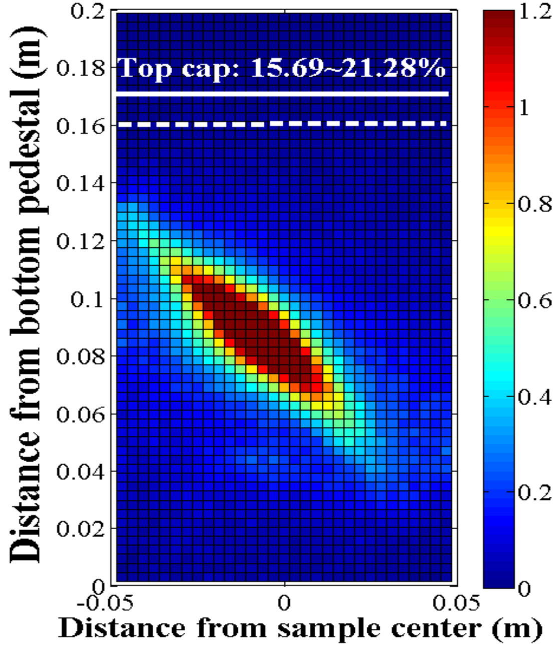

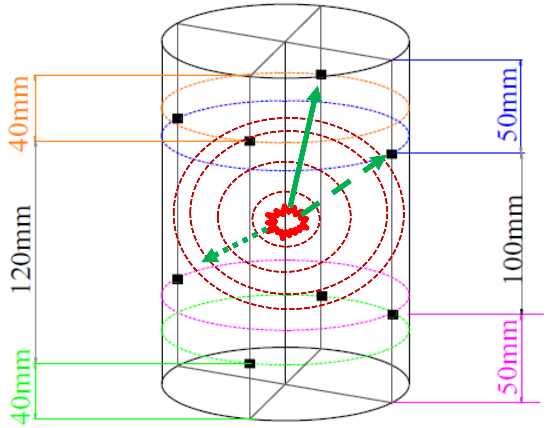

$$d_i = (t_i - t) \times v_i$$

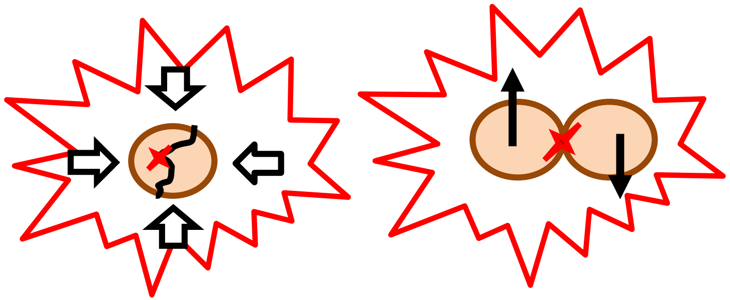

Outline

1. Introduction
2. Local measurements
    - 2.1 LDTs for cylindrical/prismatic specimens (triaxial)
    - 2.2 LDTs for hollow cylindrical specimen (torsional shear/triaxial)
    - 2.3 Local dynamic measurements
3. Unconventional liquefaction tests
    - 3.1 Liquefaction tests using motor-driven loading devices
    - 3.2 Cylindrical/prismatic specimens with thin sandy layer
    - 3.3 Segregated hollow cylindrical specimen
    - 3.4 Direct/indirect evaluation of local deformation during liquefaction
4. Other special tests
    - 4.1 Large deformation tests
    - 4.2 Direct tension tests
    - 4.3 Long-term tests
5. Concluding remarks

Liquefaction tests using motor-driven loading devices

Motor-driven loading device (Zhao, 2018)

Conventional loading device (pneumatic cylinder)

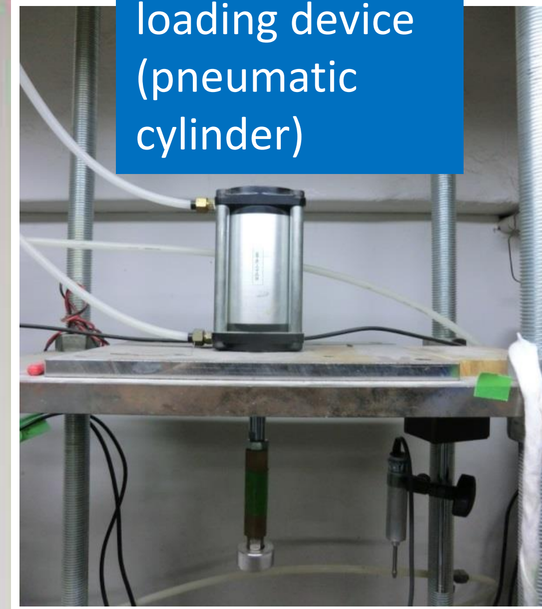

Lee and Seed (1967)

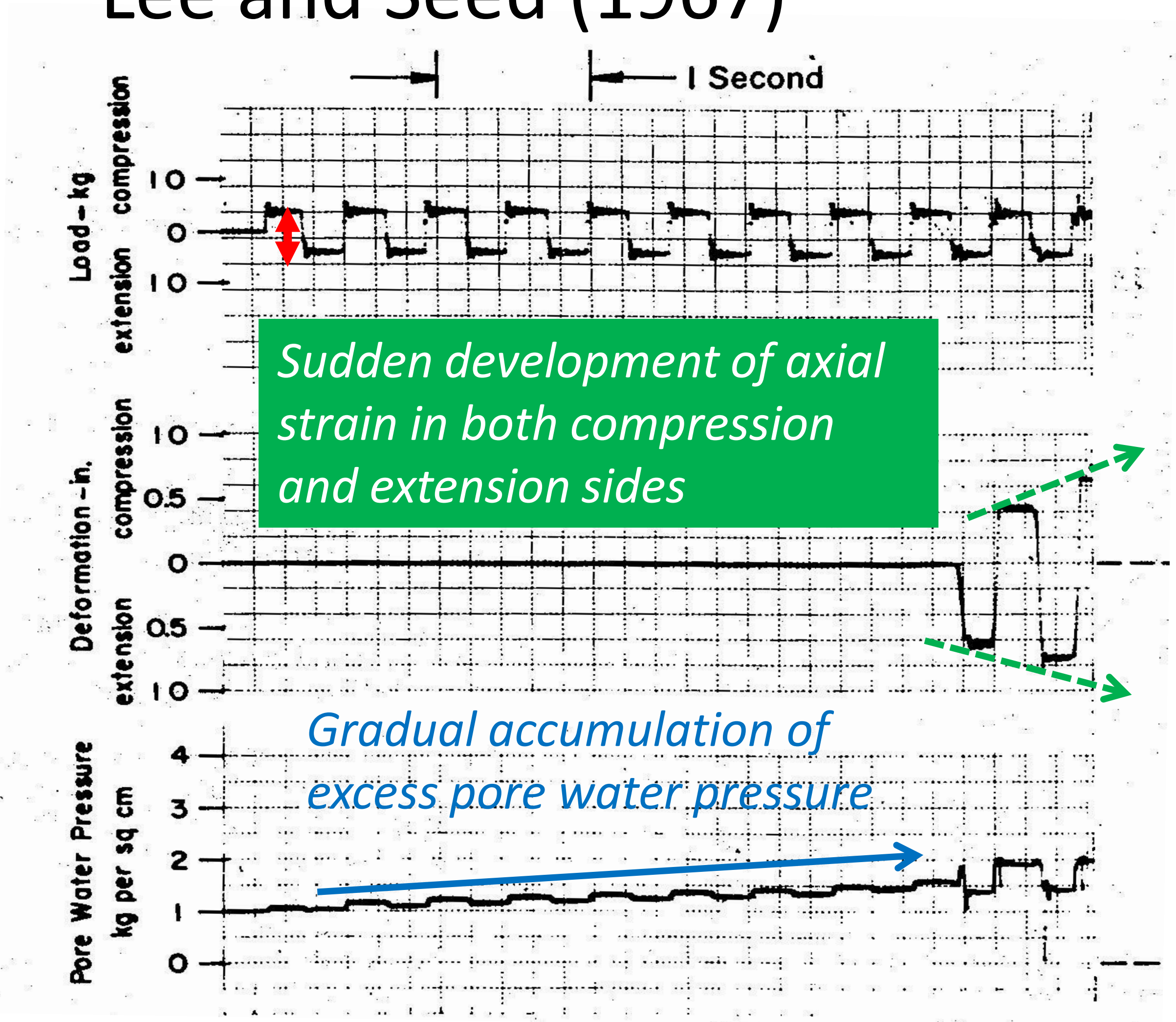

Silica sand No.7

Conventional loading device (pneumatic cylinder)

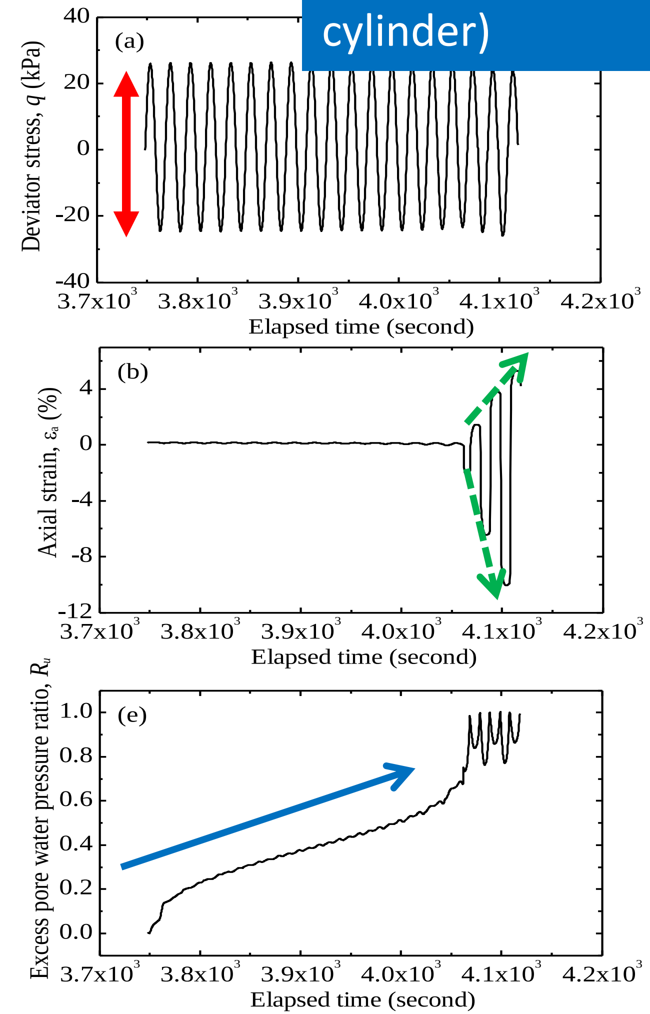

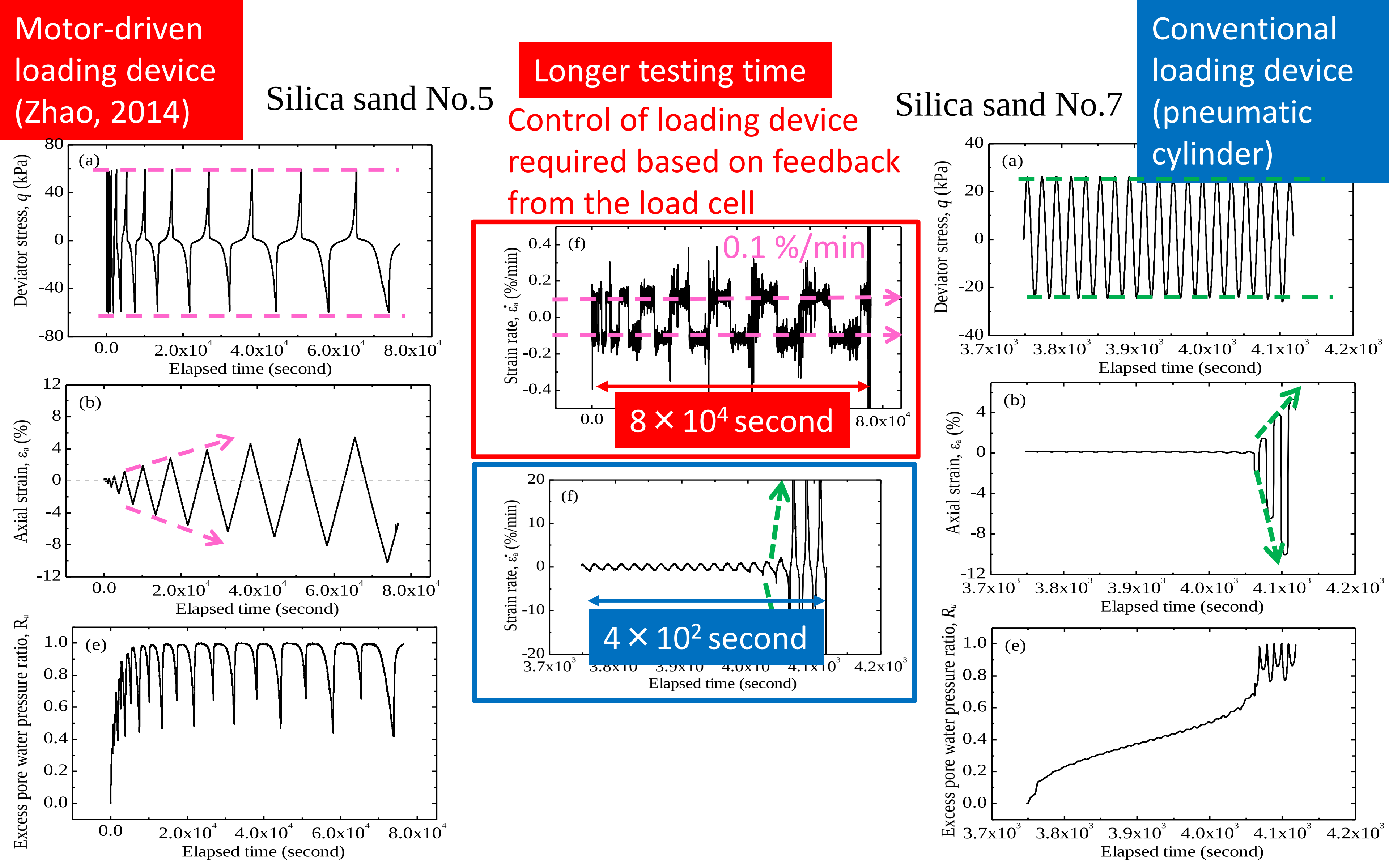
Motor-driven loading device (Zhao, 2014)
Silica sand No.5
Longer testing time
Control of loading device required based on feedback from the load cell
Silica sand No.7
Conventional loading device (pneumatic cylinder)
(a)
Deviator stress, q (kPa)
Elapsed time (second)
(b)
Axial strain, εa (%)
(e)
Excess pore water pressure ratio, Ru
(f)
Strain rate, ε̇a (%/min)
0.1 %/min
8 × 10^4 second
4 × 10^2 second

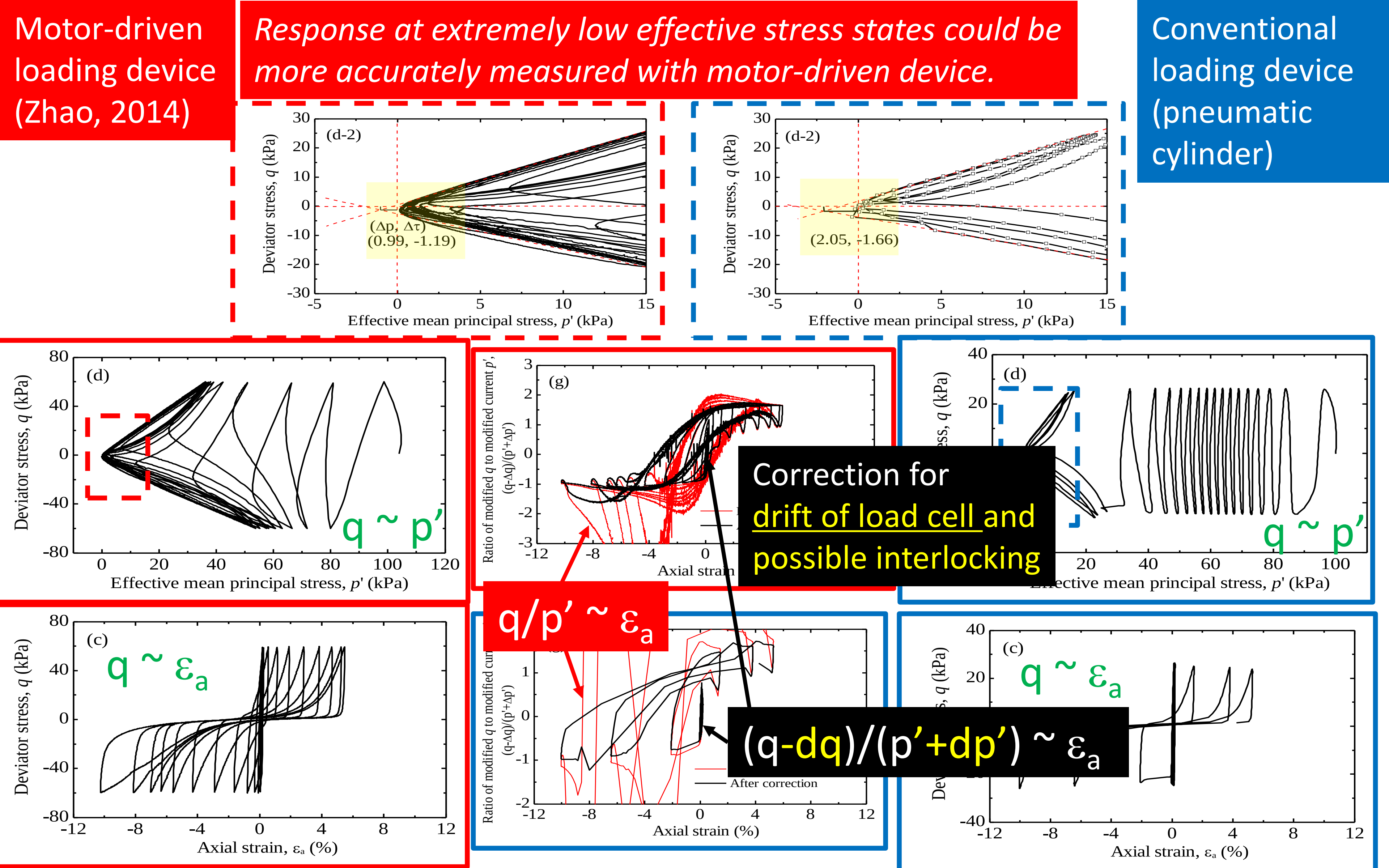

Motor-driven loading device (Zhao, 2014)
Response at extremely low effective stress states could be more accurately measured with motor-driven device.
Conventional loading device (pneumatic cylinder)
(d-2)
Deviator stress, q (kPa)
Effective mean principal stress, p' (kPa)
(Δp, Δτ)
(0.99, -1.19)
(2.05, -1.66)
(d)
q ~ p'
(g)
Ratio of modified q to modified current p', (q-Δq)/(p'+Δp')
Axial strain
Correction for
drift of load cell and
possible interlocking
q/p' ~ εa
(c)
q ~ εa
Axial strain, εa (%)
After correction
Axial strain (%)
(q-dq)/(p'+dp') ~ εa

Cyclic undrained torsional shear tests

With motor-driven loading device *(De Silva et al., 2015)*

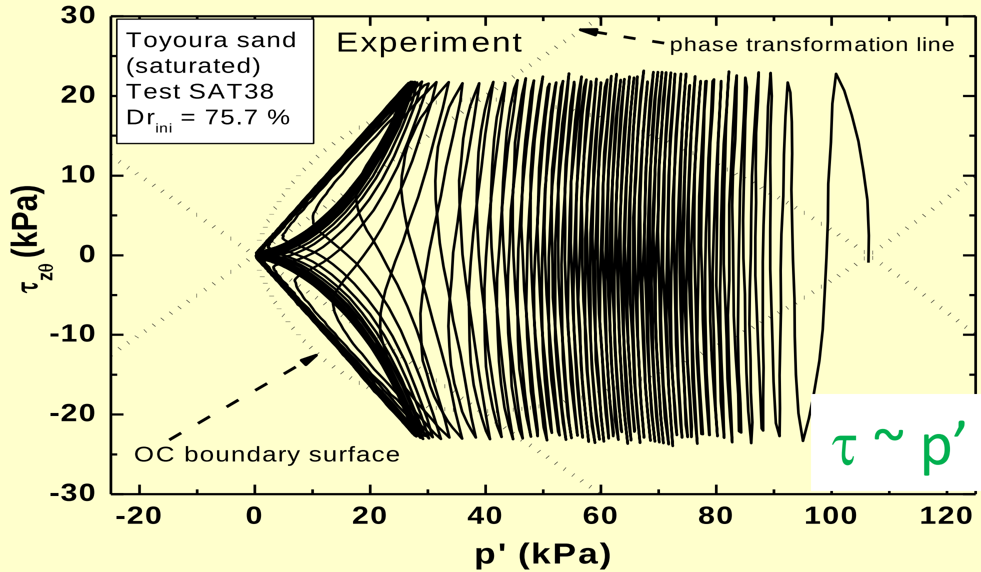

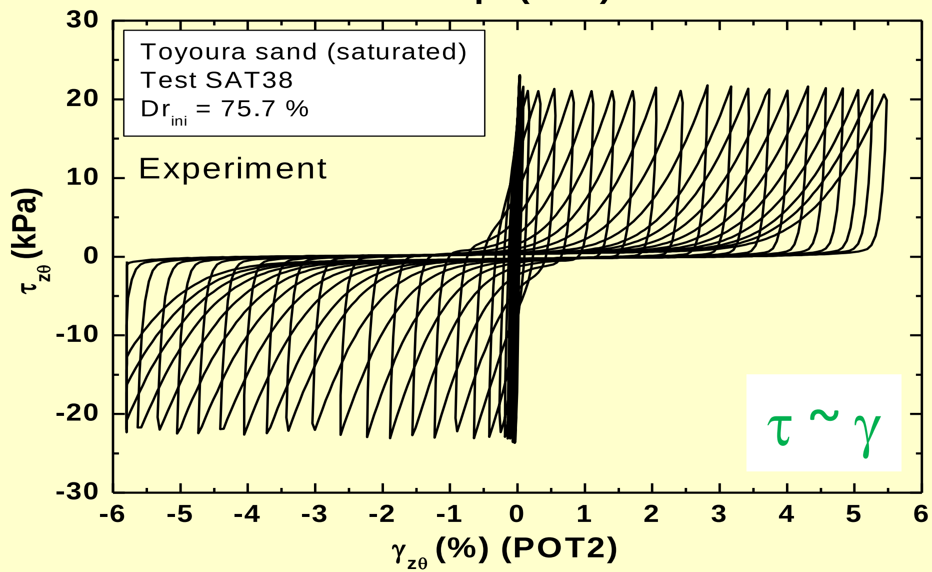

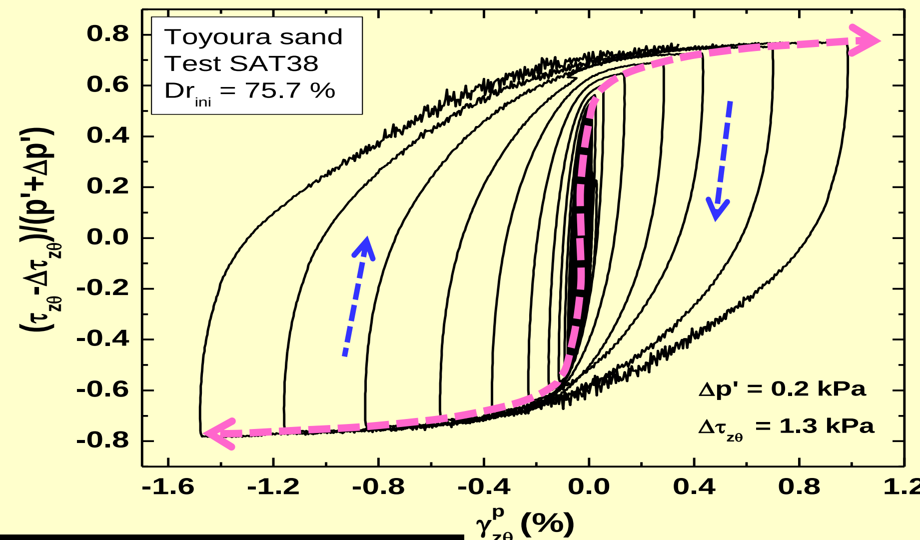

(τ-dτ)/(p’+dp’) ~ γ

Correction for drift of load cell and possible interlocking

3.2 Cylindrical/prismatic specimens with thin sandy layer

Failure of dip slope by 2004 Niigataken-Chuetsu Earthquake

Yokowatashi, Ojiya city, Niigata Prefecture, Japan

Field survey at Yokowatashi

(Deng et al. 2011a)

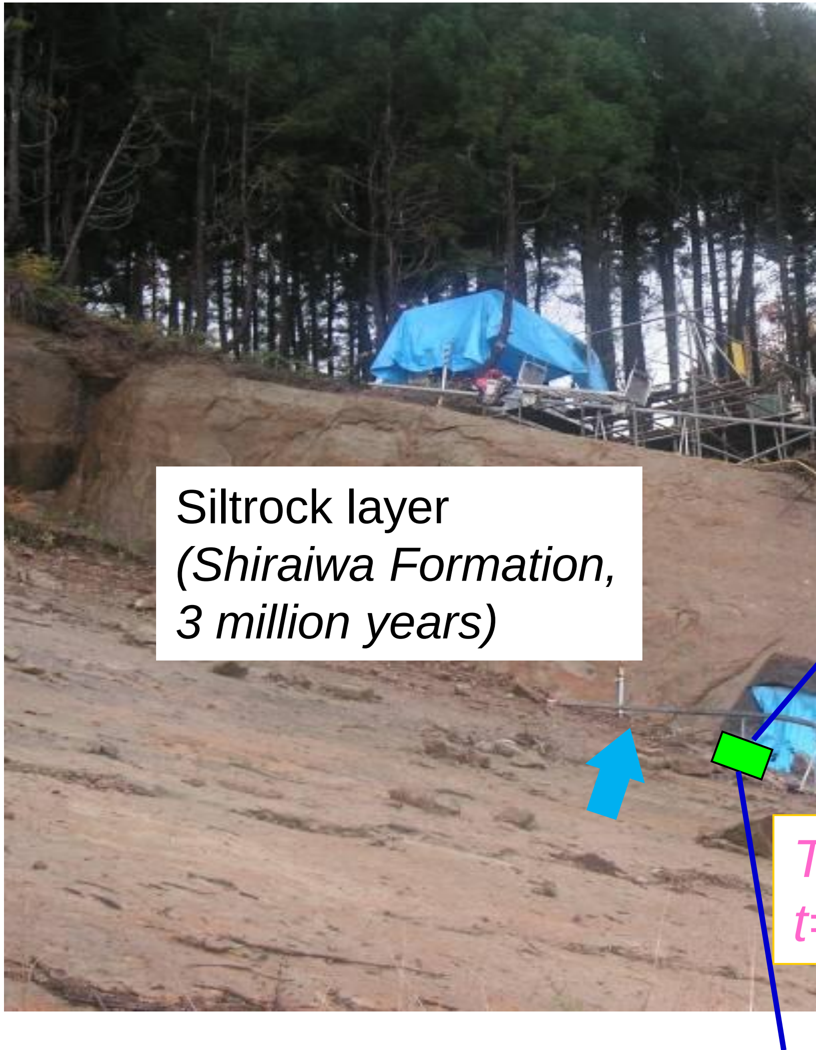

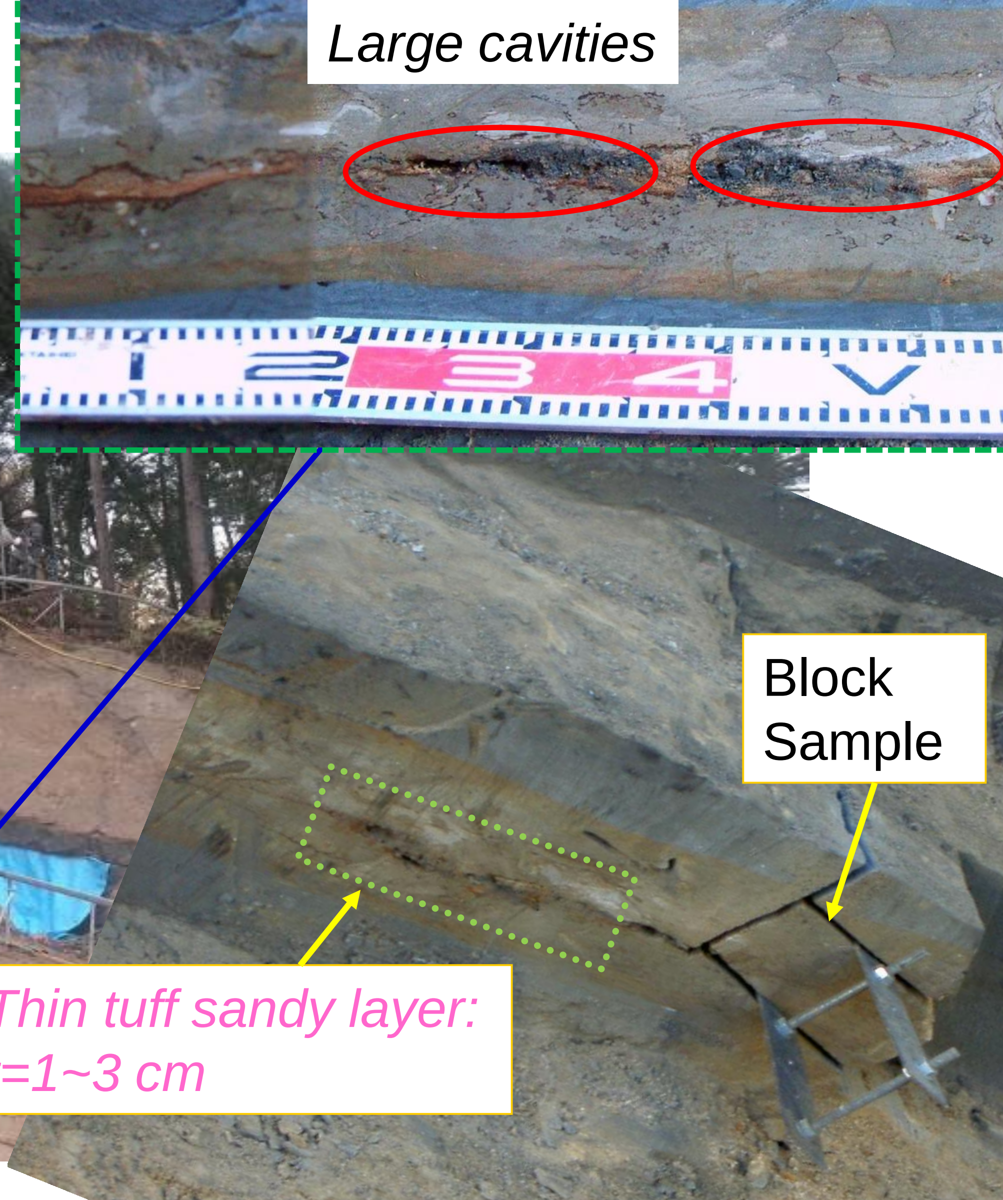

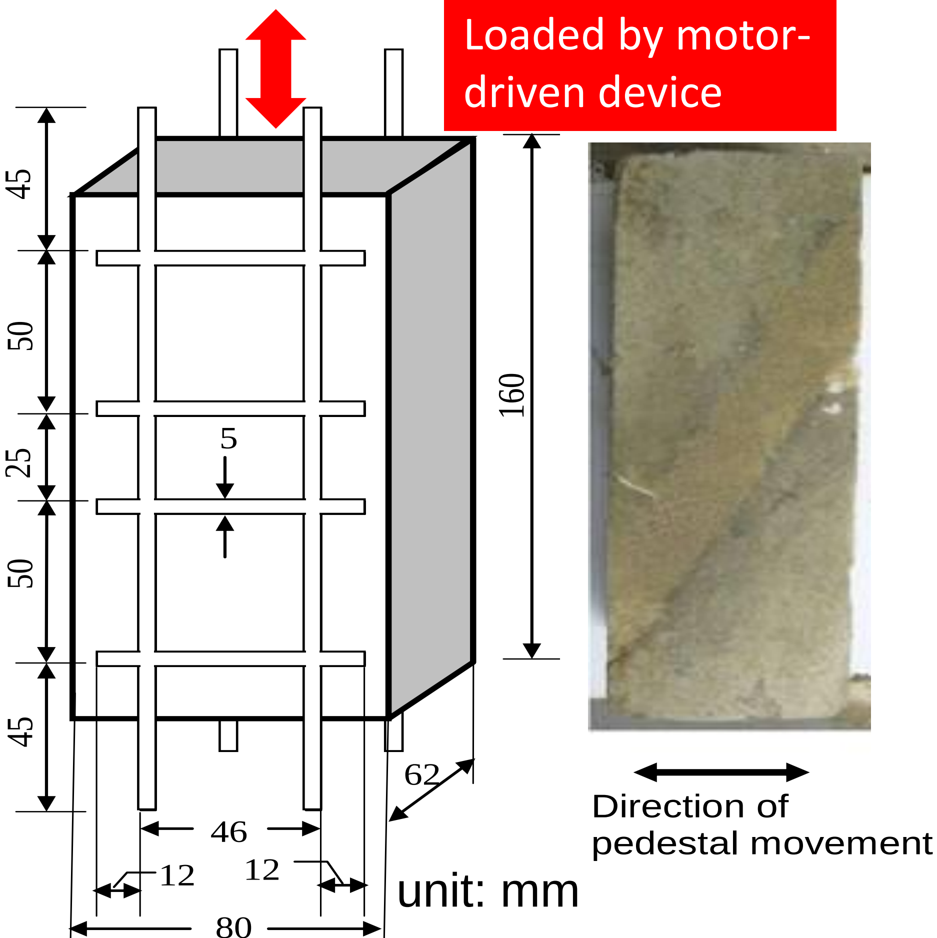

Prismatic interlayered specimen with side filter paper

(Deng et al. 2011b)

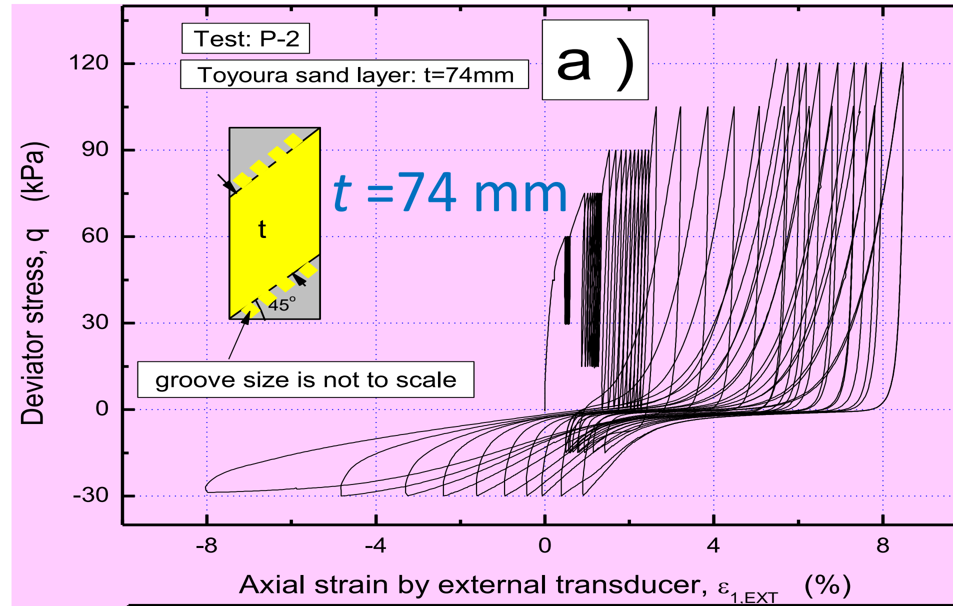

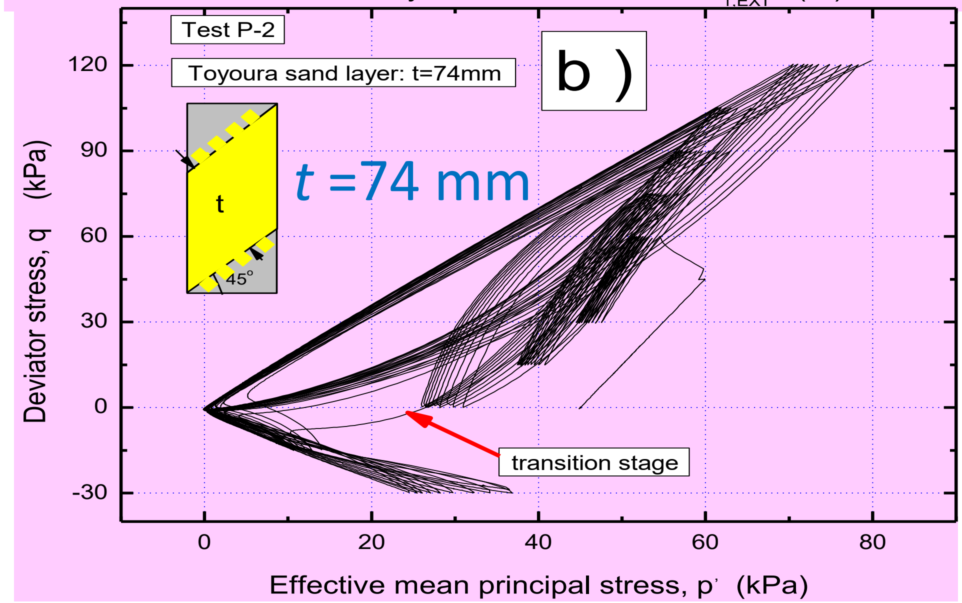

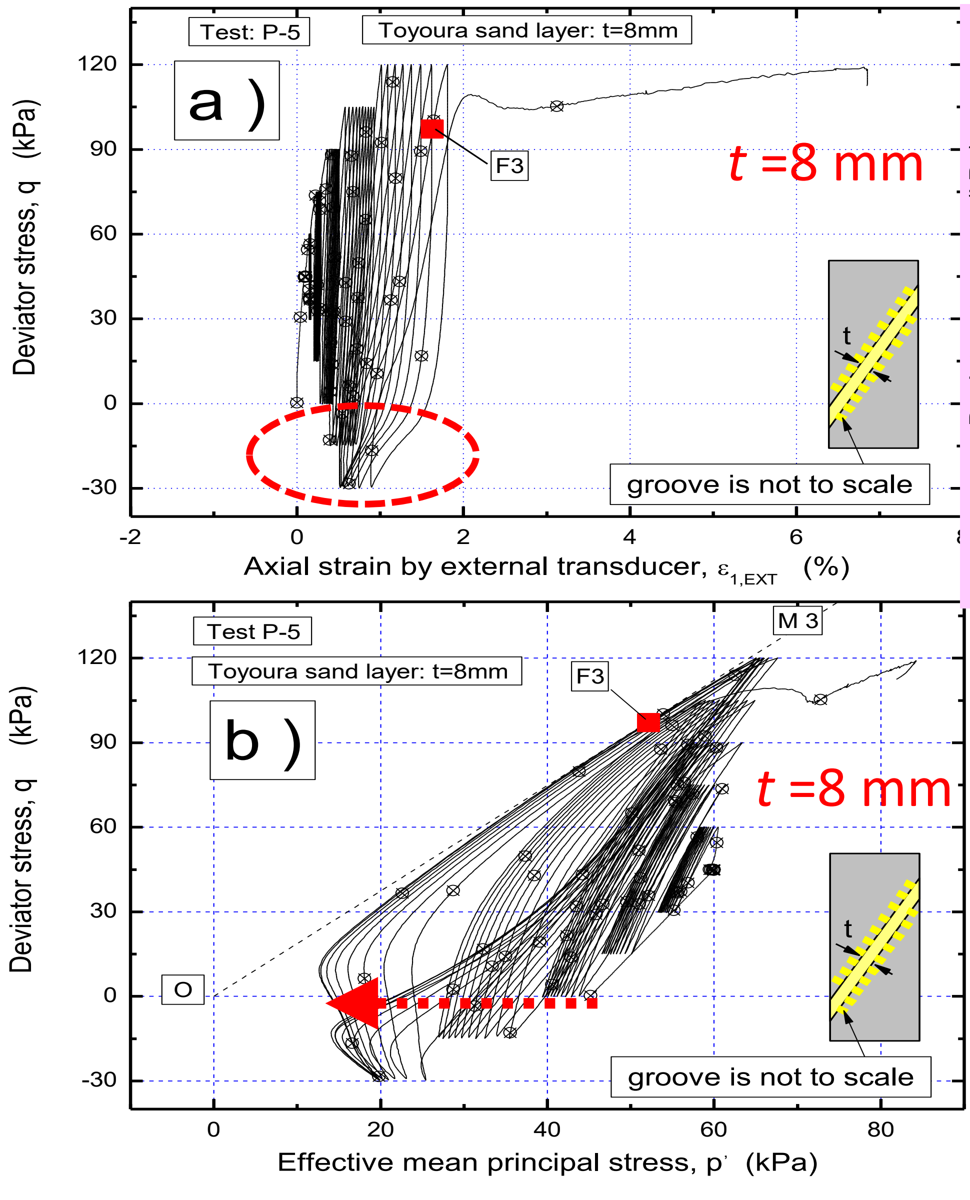

Test: P-5
Toyoura sand layer: t=8mm
a)
F3
t =8 mm
groove is not to scale
t
Deviator stress, q (kPa)
Axial strain by external transducer, $\varepsilon_{1,EXT}$ (%)
Test P-5
Toyoura sand layer: t=8mm
M 3
F3
b)
t =8 mm
O
groove is not to scale
Deviator stress, q (kPa)
Effective mean principal stress, p' (kPa)

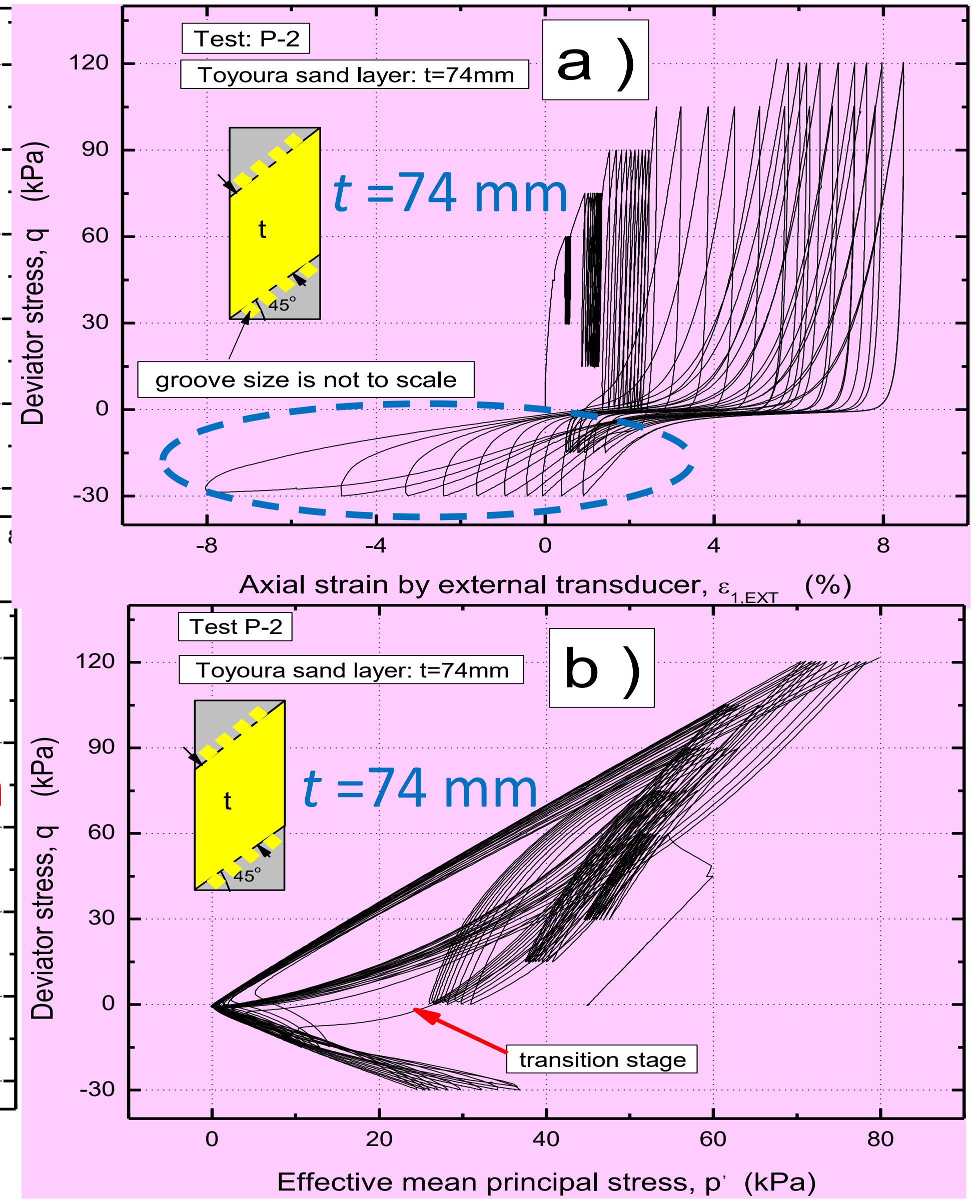

Test: P-2
Toyoura sand layer: t=74mm
a)
t =74 mm
t
45°
groove size is not to scale
Deviator stress, q (kPa)
Axial strain by external transducer, $\varepsilon_{1,EXT}$ (%)
Test P-2
Toyoura sand layer: t=74mm
b)
t =74 mm
t
45°
transition stage
Deviator stress, q (kPa)
Effective mean principal stress, p' (kPa)

AS: Air servo;
LCDPT: Low capacity differential pressure transducer;
HCDPT: High capacity differential pressure transducer;
V_i : Volume of injected water;
CP_c: Current effective confining pressure;
V_n : Volume of needed water to inject;
ΔV: Volume increment of injected water at the next step;
E.C.P.: Effective confining pressure;
V.W.F.: Apparent volume change due to system compliance.

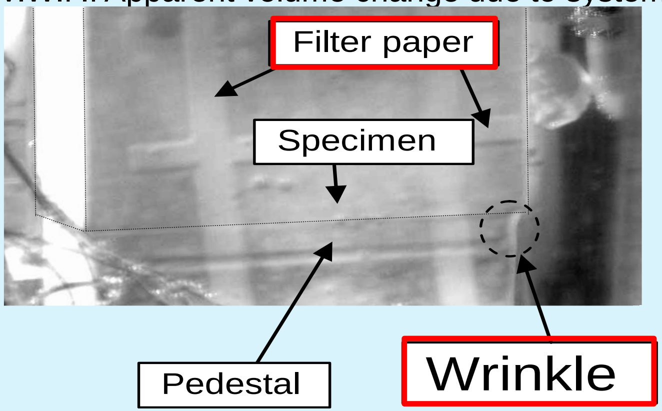

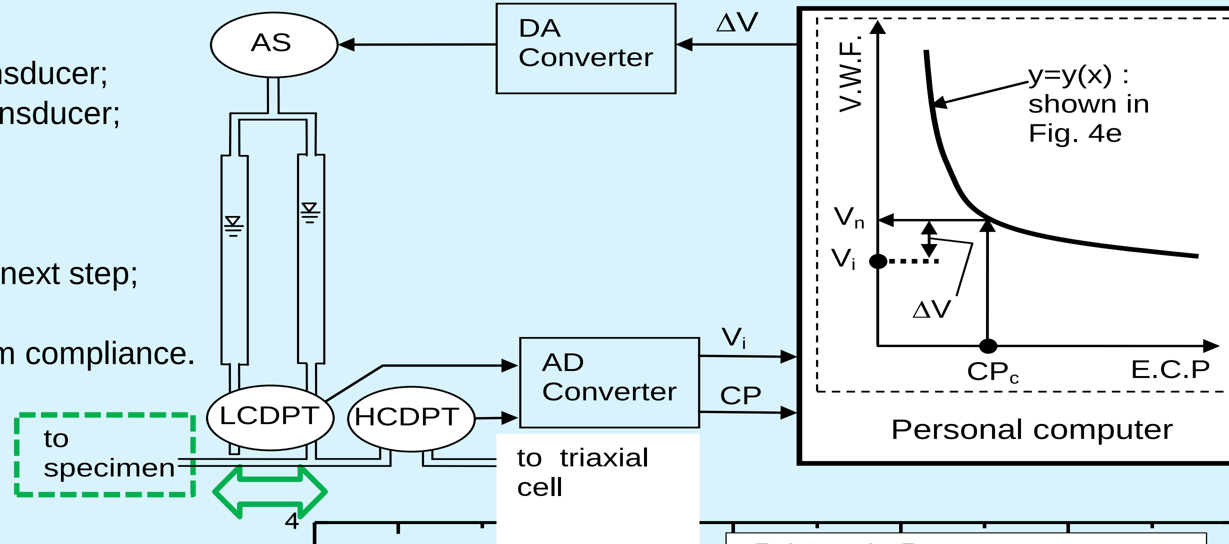

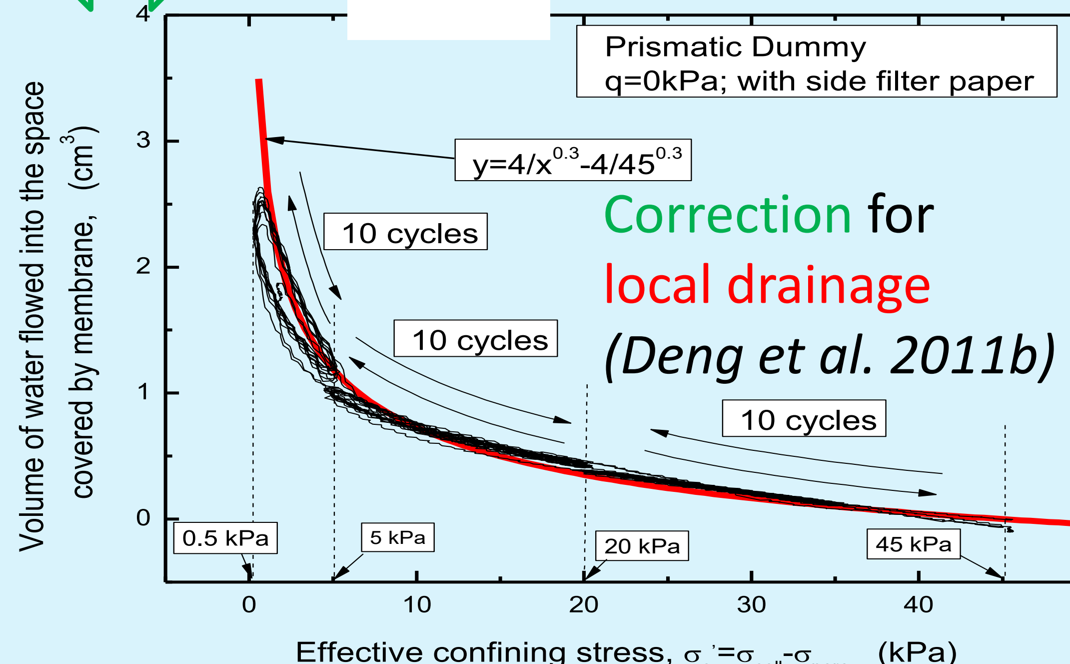

Correction for local drainage *(Deng et al. 2011b)*

Sources for local drainage

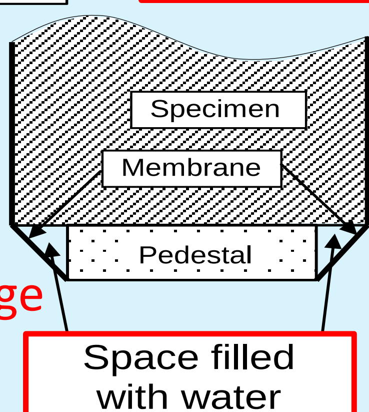

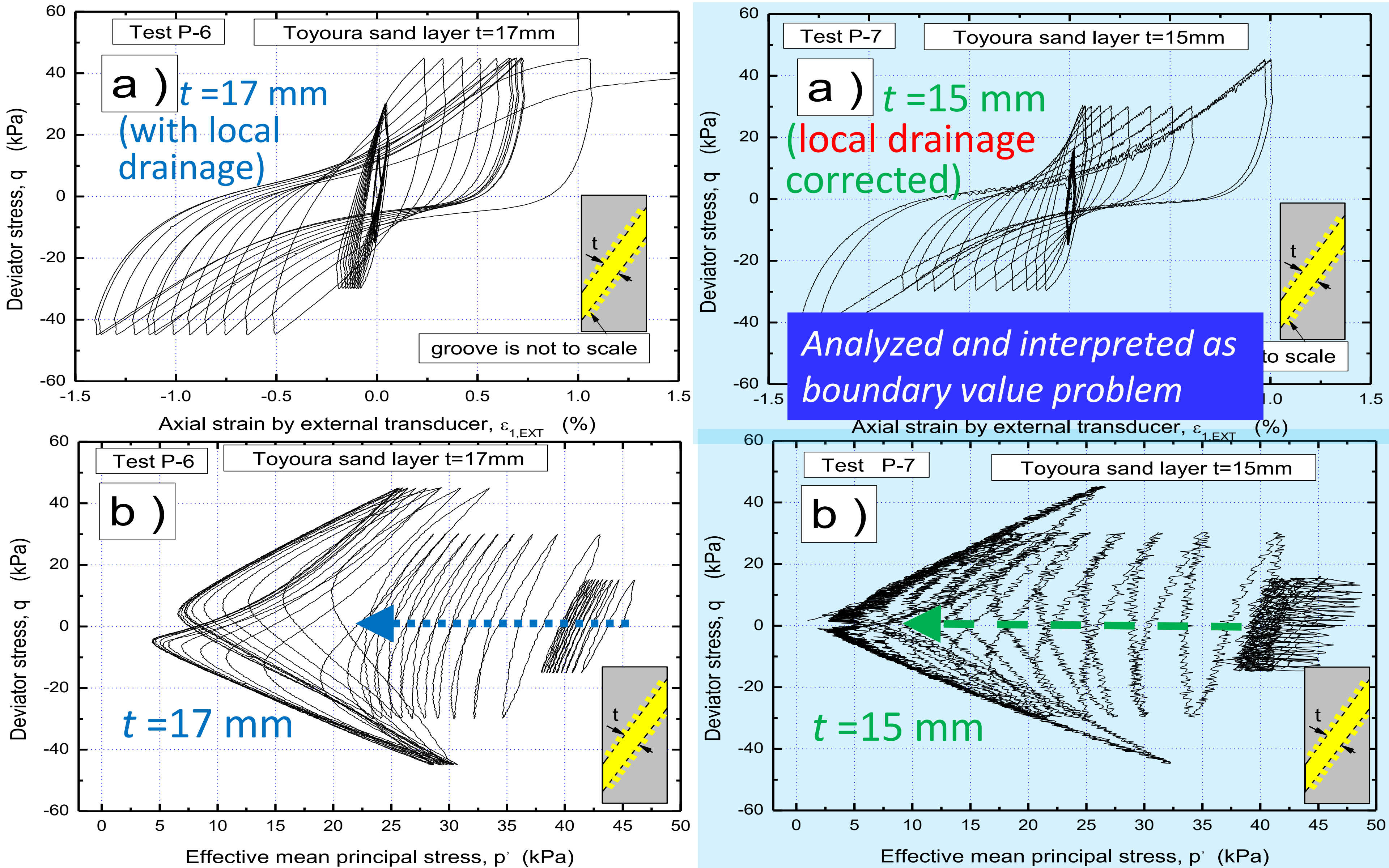
Test P-6
Toyoura sand layer t=17mm
a)
t =17 mm
(with local drainage)
groove is not to scale
Deviator stress, q (kPa)
Axial strain by external transducer, ε1,EXT (%)
Test P-7
Toyoura sand layer t=15mm
a)
t =15 mm
(local drainage corrected)
to scale
Analyzed and interpreted as boundary value problem
Deviator stress, q (kPa)
Axial strain by external transducer, ε1,EXT (%)
Test P-6
Toyoura sand layer t=17mm
b)
t =17 mm
Deviator stress, q (kPa)
Effective mean principal stress, p' (kPa)
Test P-7
Toyoura sand layer t=15mm
b)
t =15 mm
Deviator stress, q (kPa)
Effective mean principal stress, p' (kPa)

3.3 Segregated hollow cylindrical specimen

Liquefaction by 2011 off the Pacific coast of Tohoku Earthquake

Land development works in Kuki city, Saitama prefecture, using dredged sandy soils *(Koseki et al., 2015)*

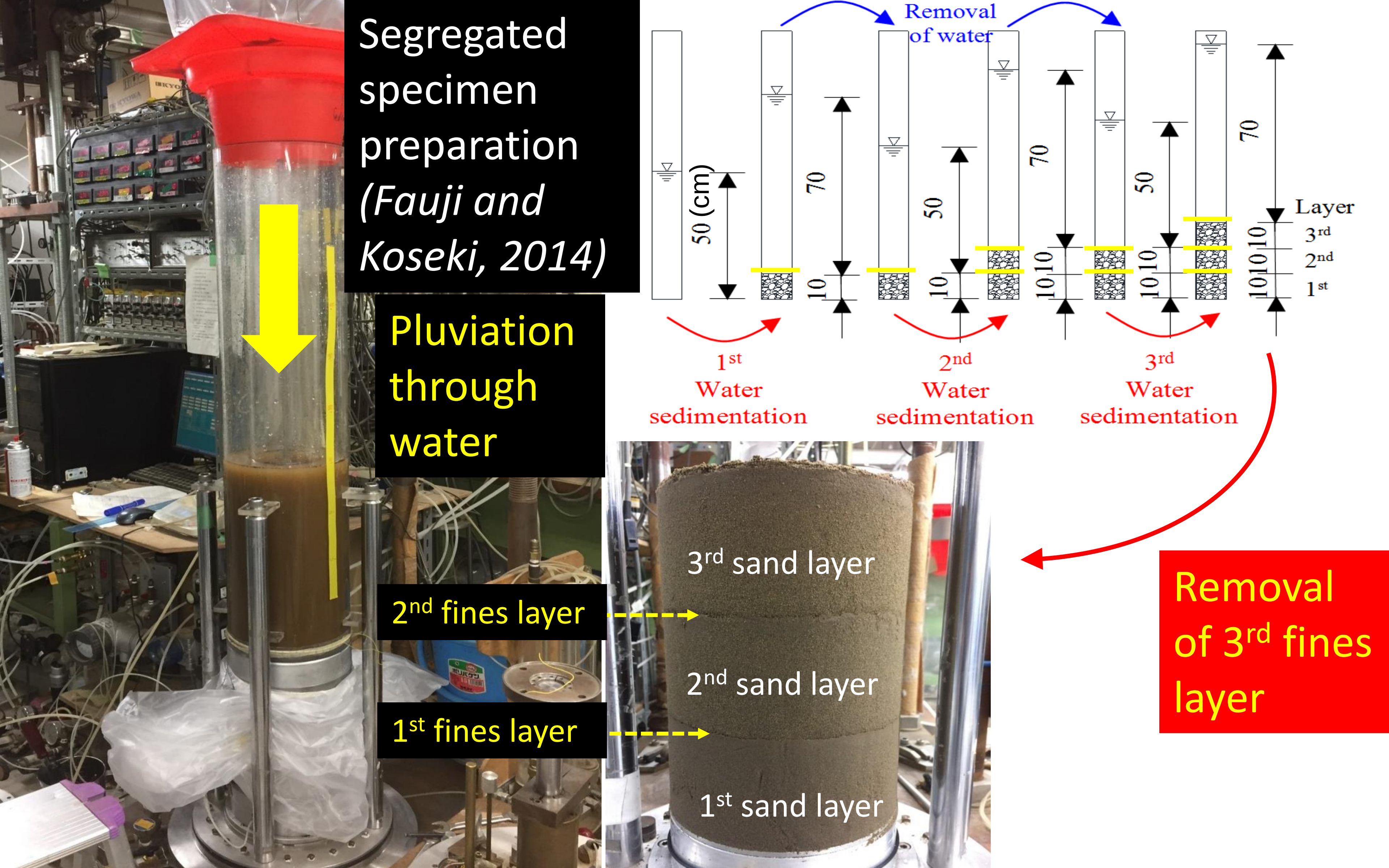

Segregated specimen preparation (Fauji and Koseki, 2014)
Pluviation through water
2nd fines layer
1st fines layer
Removal of water
50 (cm)
70
10
50
70
10
10
50
10
10
70
10
10
10
Layer
3rd
2nd
1st
1st Water sedimentation
2nd Water sedimentation
3rd Water sedimentation
3rd sand layer
2nd sand layer
1st sand layer
Removal of 3rd fines layer

Observation of water film below fines layer in 1-D column test *(modified after Fauji, 2015)*

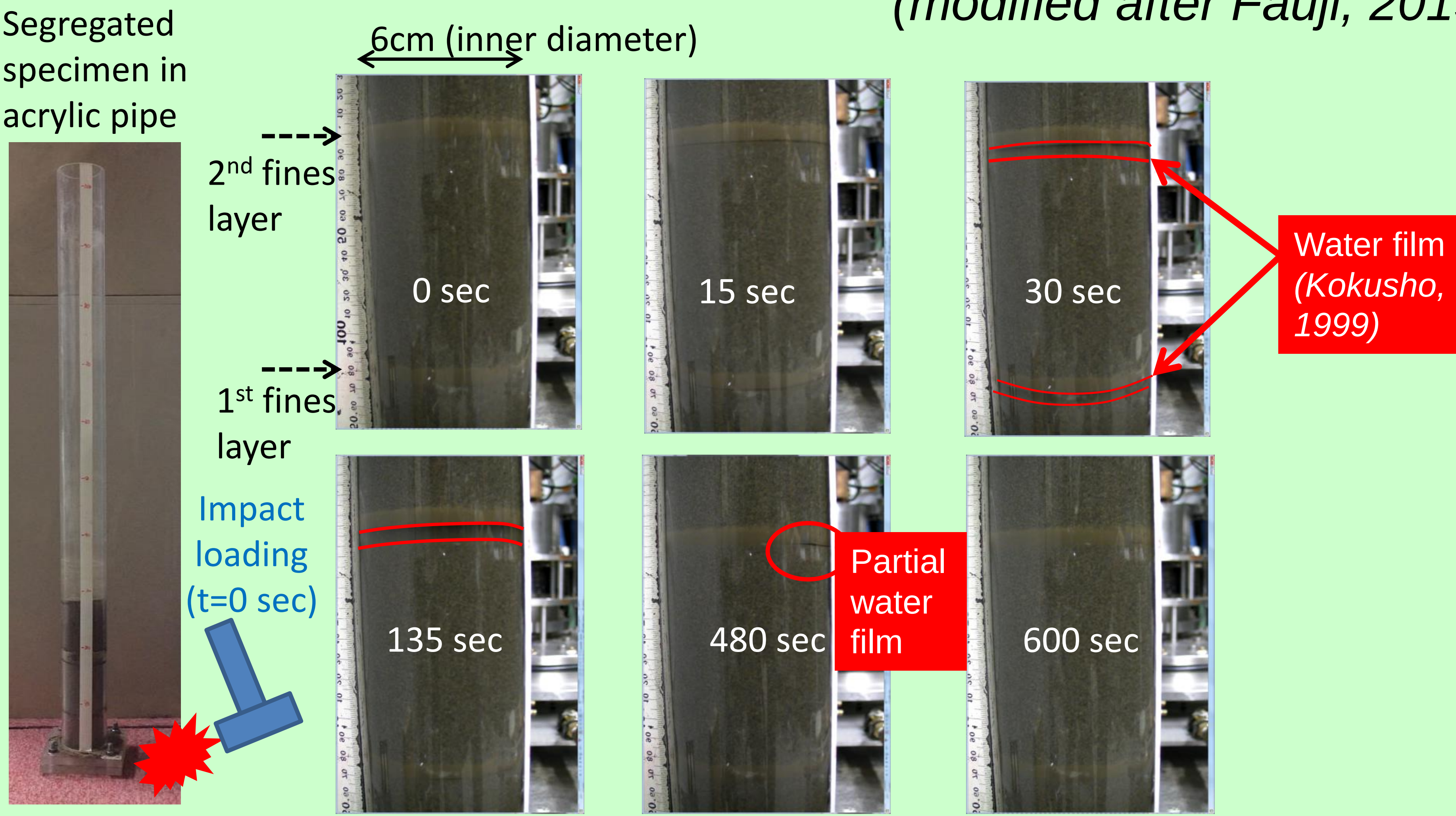

Undrained cyclic torsional shear test on segregated hollow cylindrical specimen *(modified after Fauji and Koseki, 2014)*

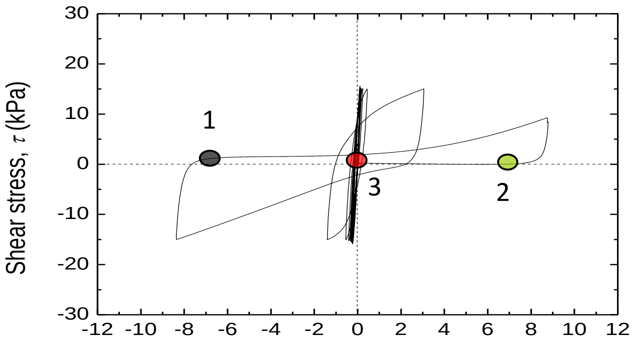

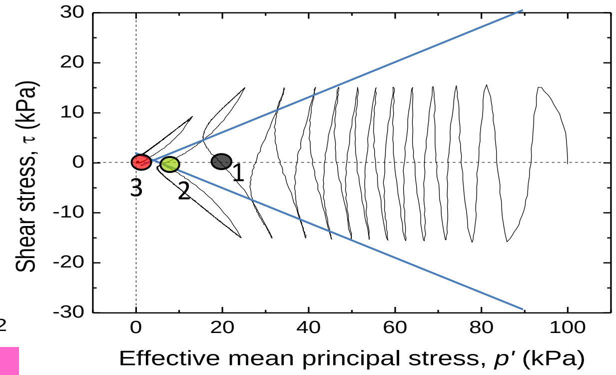

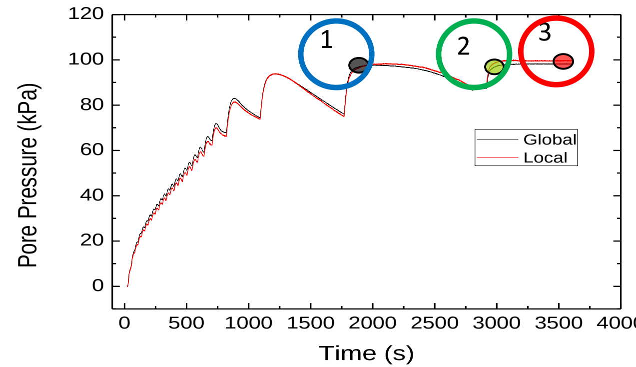

Gap formed during consolidation.

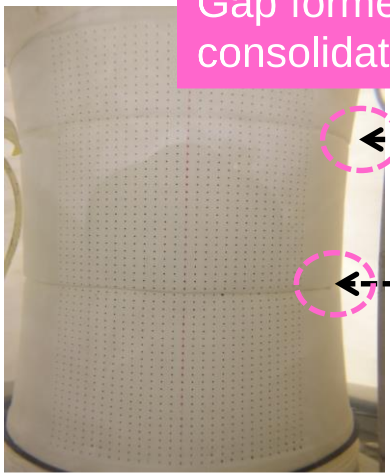

2nd fines layer

1st fines layer

Before cyclic loading

At state 1

At state 2

At state 3

Membrane wrinkles appeared across the gap during cyclic loading.

As compared to <u>uniformly-mixed and moist-tamped</u> specimen, no significant effect of possible water film formation was observed.

Attempts to observe water film in cyclic torsional shear test on segregated hollow cylindrical specimen *(modified after Fauji, 2015)*

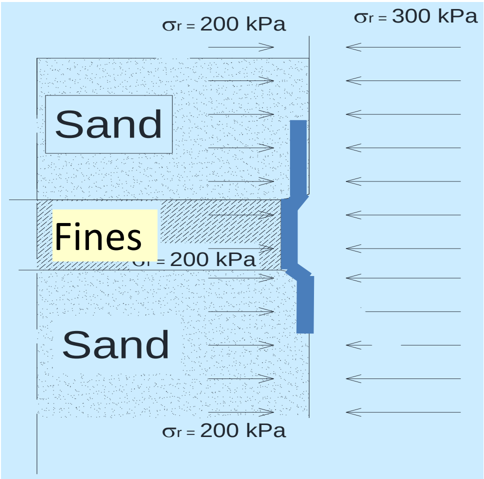

Another membrane glued in advance

a) Reinforcement of membrane

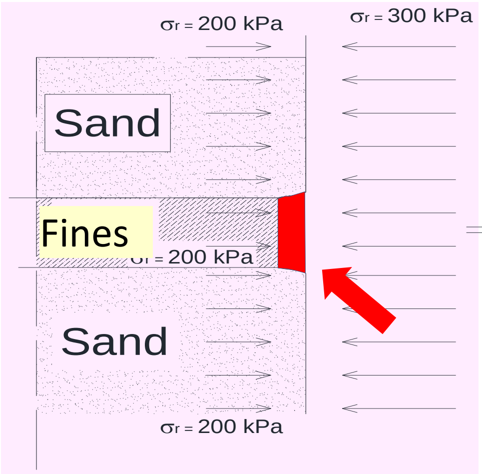

Silicone sealant added after consolidation

b) Gap filling

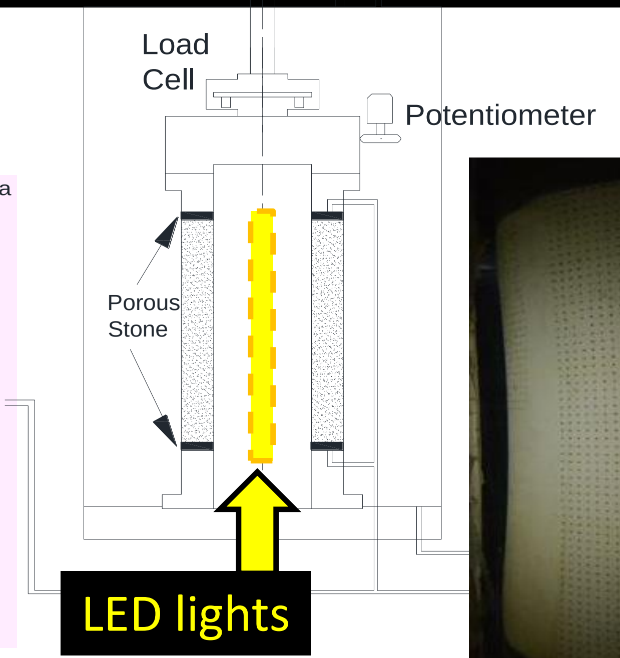

c) LED lights installation

Confirmation of light transmission through water specimen

Still, no significant effect of possible water film formation was observed.

3.4 Direct/indirect evaluation of local deformation

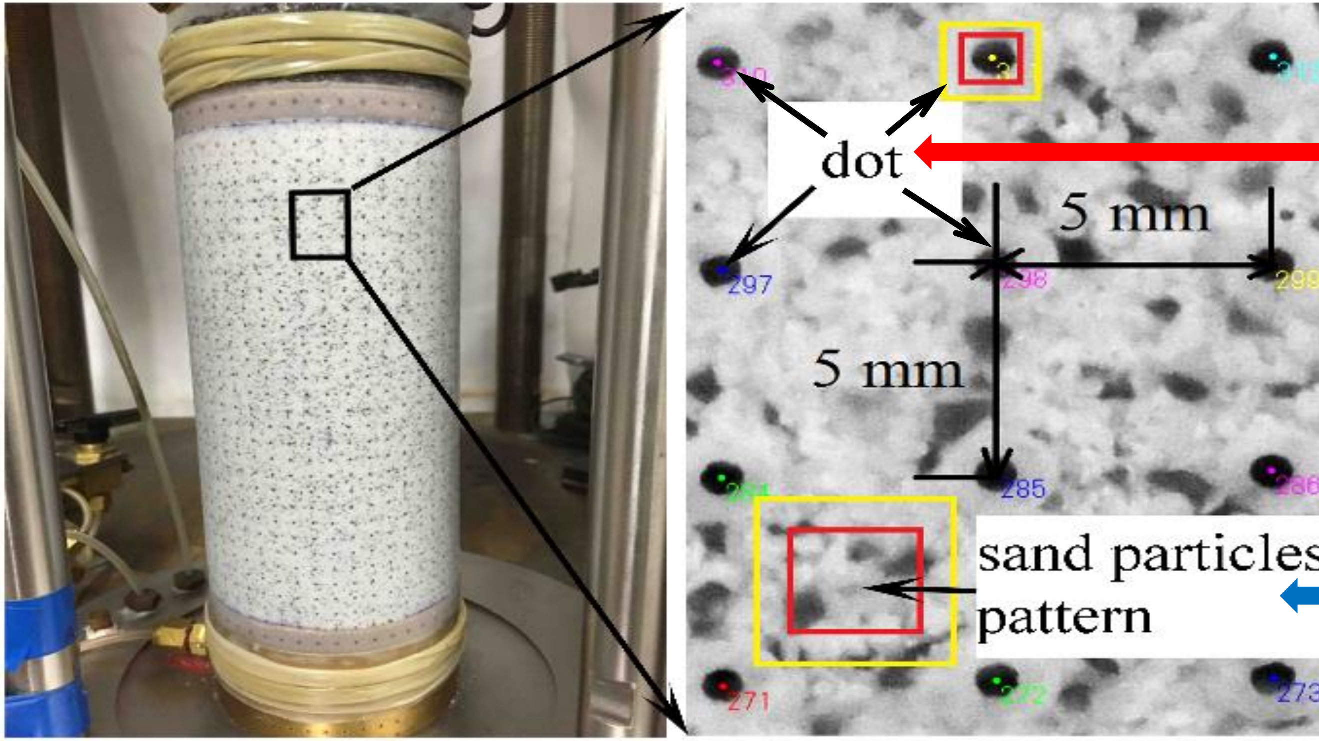

Pasted in advance on membrane and analyzed as indirect evaluation

Observed through transparent membrane and analyzed as direct evaluation

Cylindrical specimen using transparent membrane and colored sand particles *(modified after Zhao et al., 2018)*

Undrained cyclic triaxial test results on moist-tamped silica sand specimen *(modified after Zhao et al., 2018)*

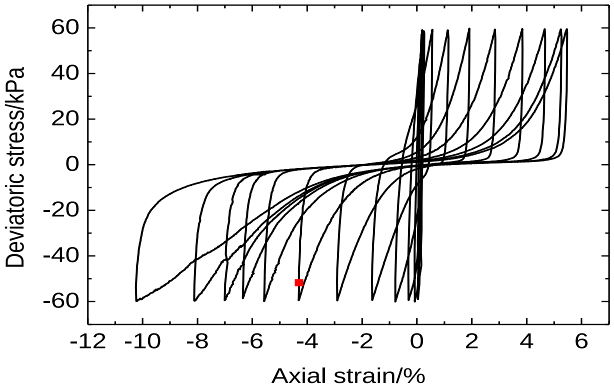

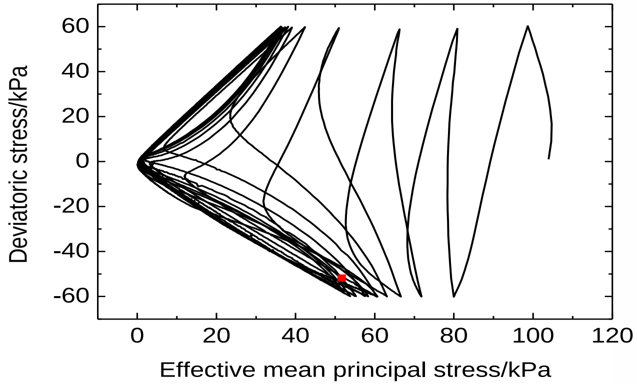

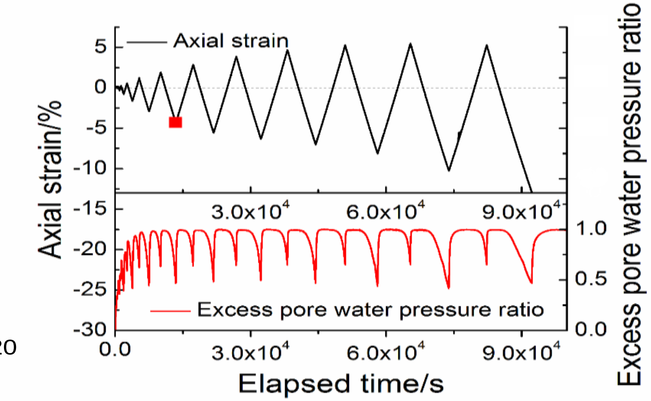

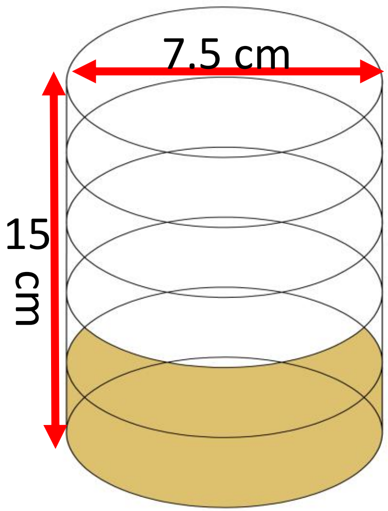

Moist tamping

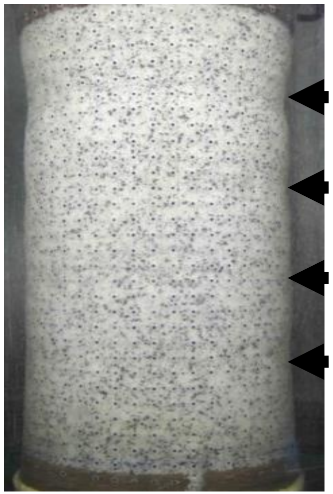

Original photo

Interfaces between tamped layers

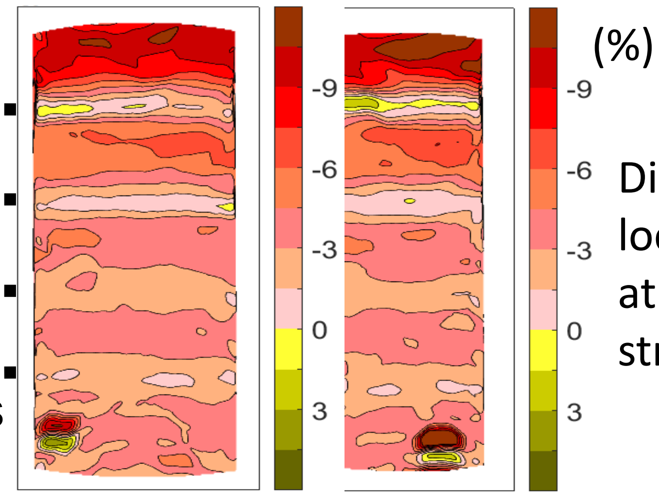

Indirect and direct evaluation results

Distribution of local axial strain at global axial strain of -4.3%

Vertical slippage accumulation during liquefaction of silica sand

(modified after Zhao et al., 2018)

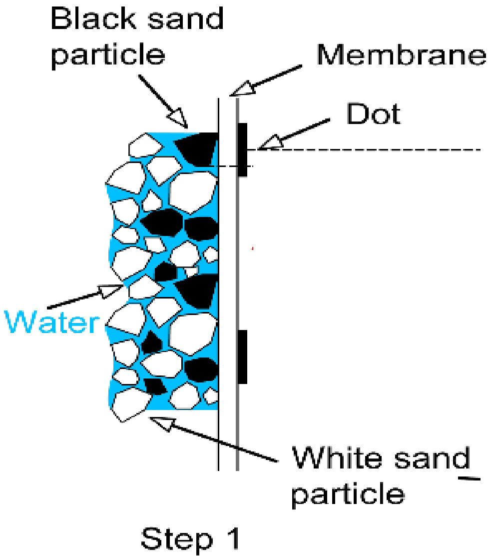

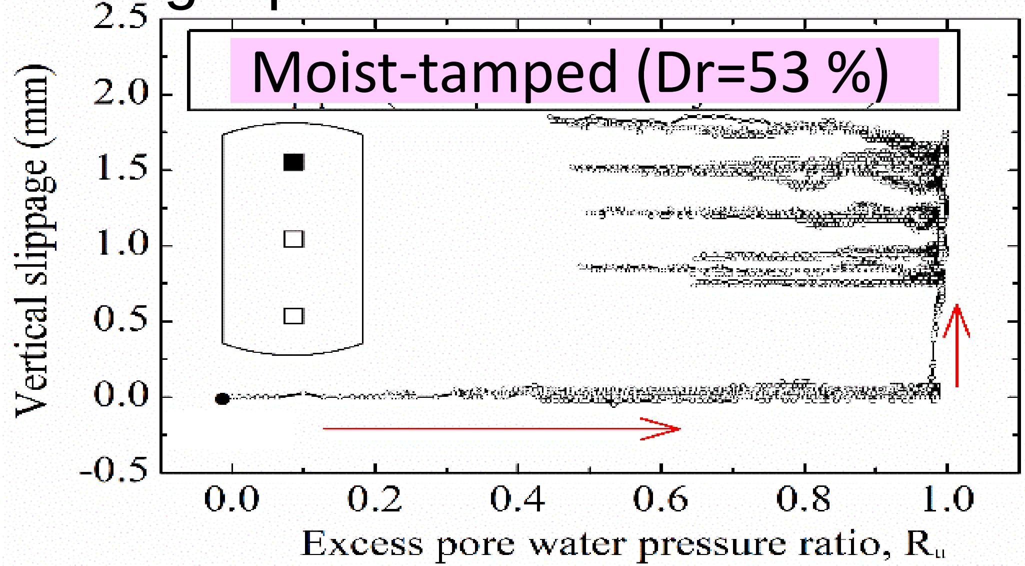

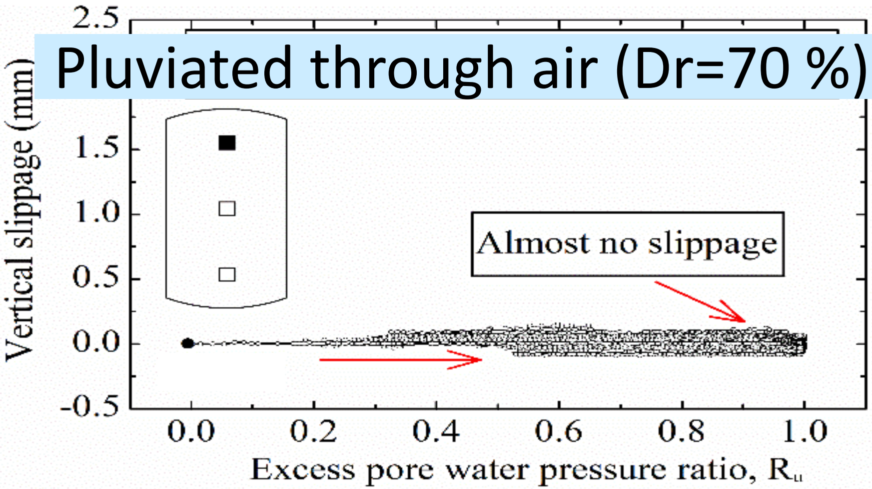

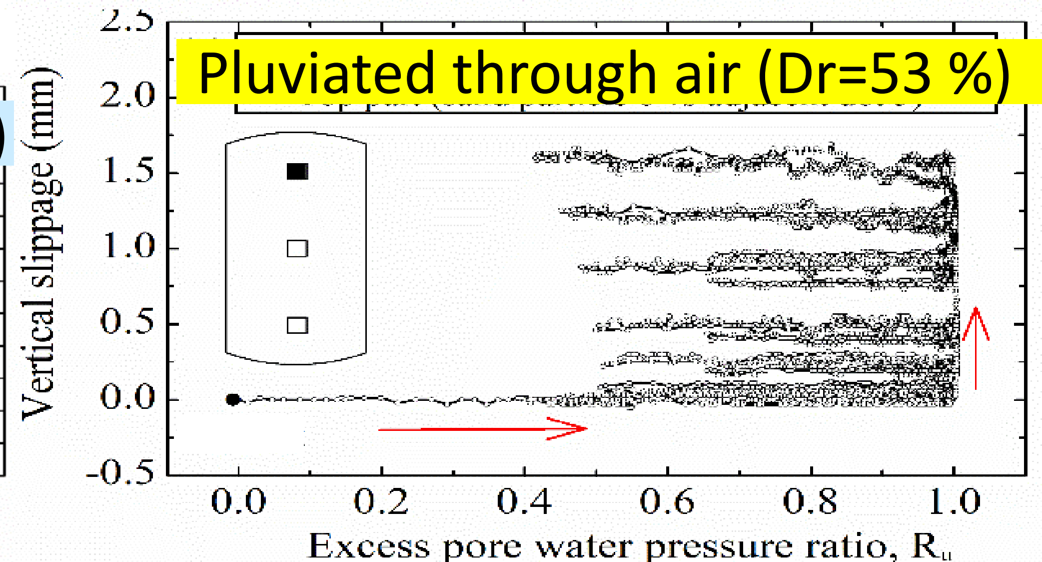

Summary on unconventional liquefaction tests (1/2)

- Liquefaction tests using motor-driven loading devices can reveal more clearly the specimen response at extremely low effective stress states, though they require longer testing time and special feedback control.

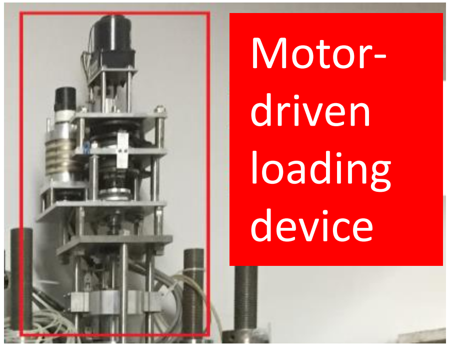

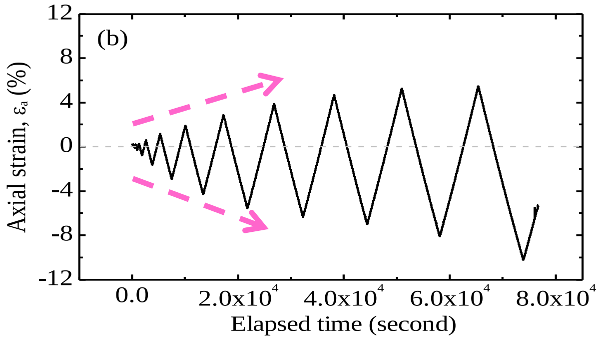

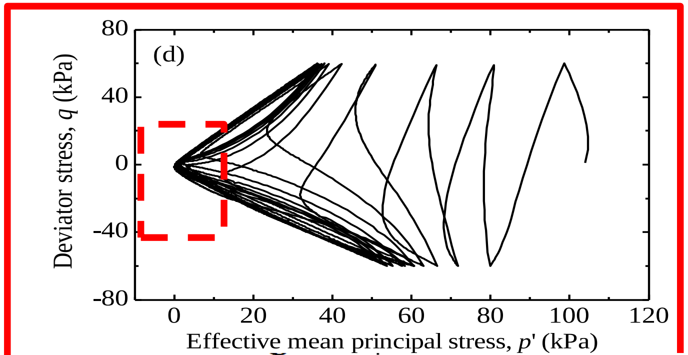

✓ They are also effective in conducting image analysis of the specimen deformation during liquefaction, by which local deformation can be directly evaluated using colored sand particles and transparent membrane.

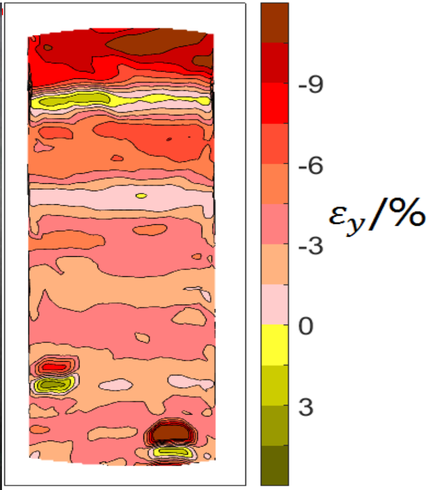

Summary on unconventional liquefaction tests (2/2)

- Liquefaction test results on segregated specimen and interlayered specimen shall be analyzed and interpreted as boundary value problems.

✓ Effects of system compliance need to be considered properly, including drift of load cell output and local drainage due to membrane penetration/wrinkling as well as filter paper deformation.

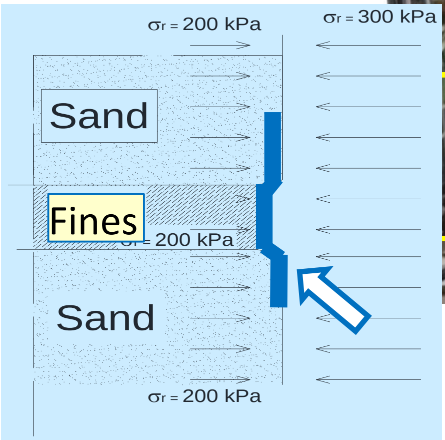

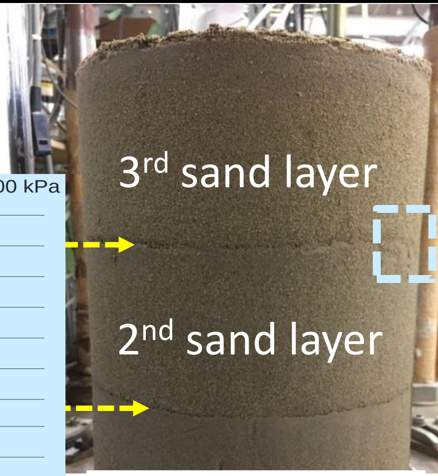

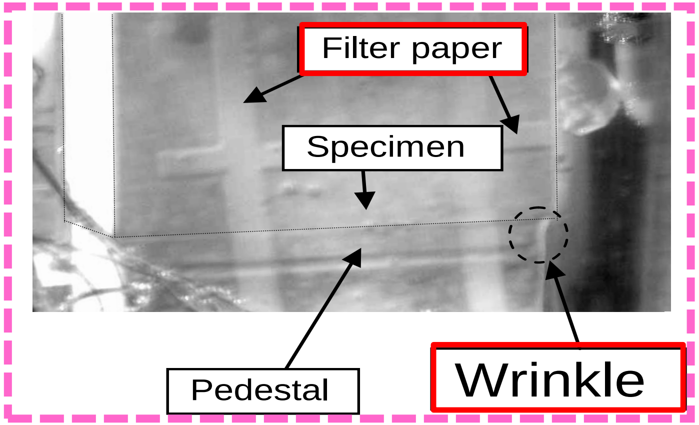

Outline

1. Introduction
2. Local measurements
    2.1 LDTs for cylindrical/prismatic specimens (triaxial)
    2.2 LDTs for hollow cylindrical specimen (torsional shear/triaxial)
    2.3 Local dynamic measurements
3. Unconventional liquefaction tests
    3.1 Liquefaction tests using motor-driven loading devices
    3.2 Cylindrical/prismatic specimens with thin sandy layer
    3.3 Segregated hollow cylindrical specimen
    3.4 Direct/indirect evaluation of local deformation during liquefaction
4. Other special tests
    4.1 Large deformation tests
    4.2 Direct tension tests
    4.3 Long-term tests
5. Concluding remarks

Large deformation of liquefied soils

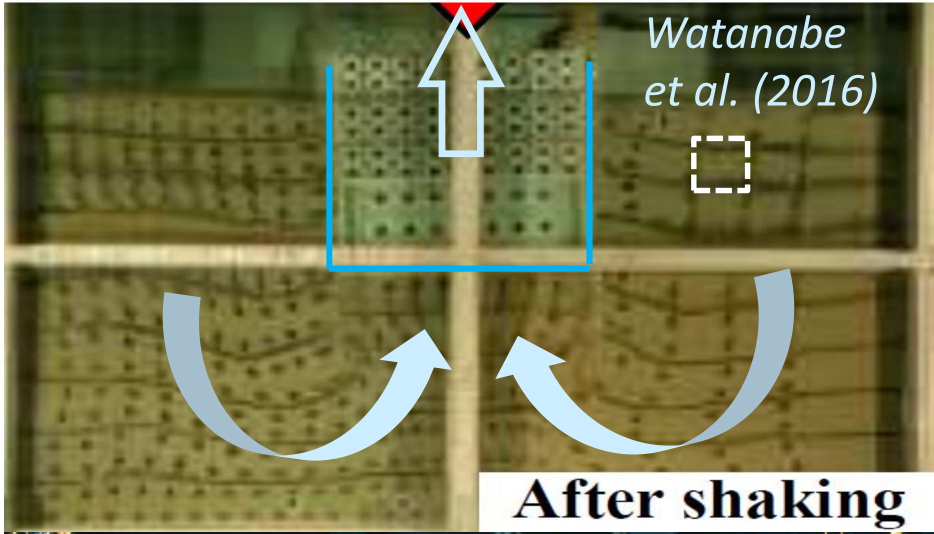

Large deformation torsional shear liquefaction tests

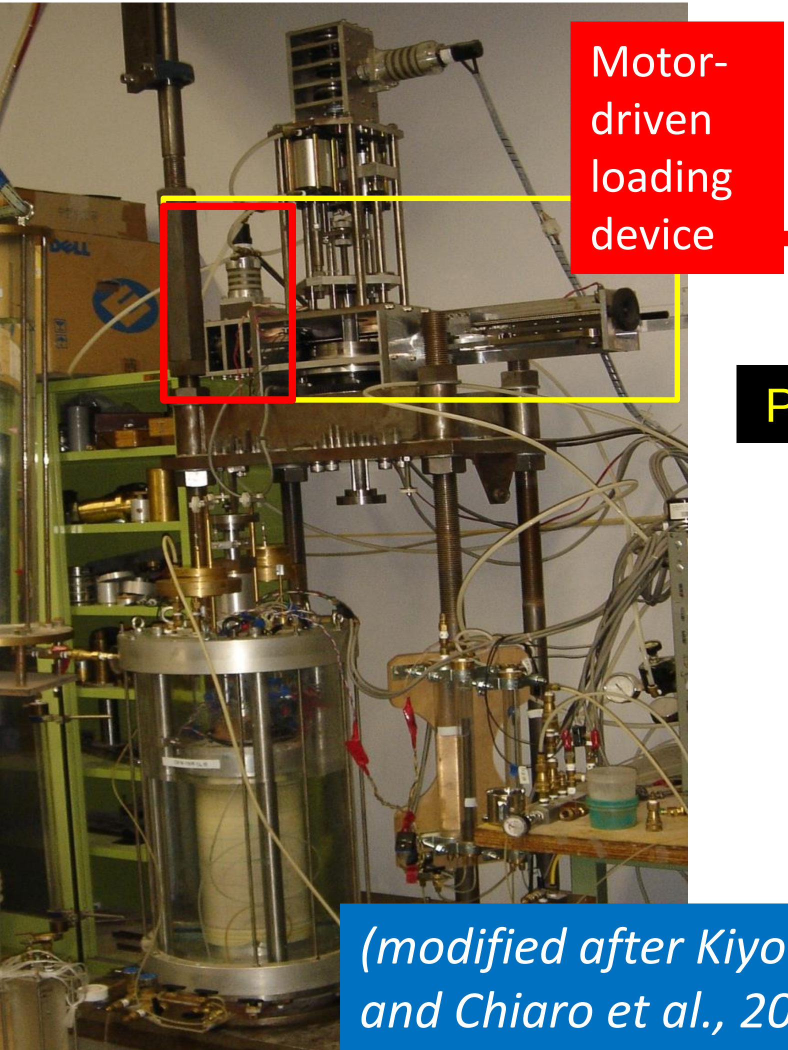

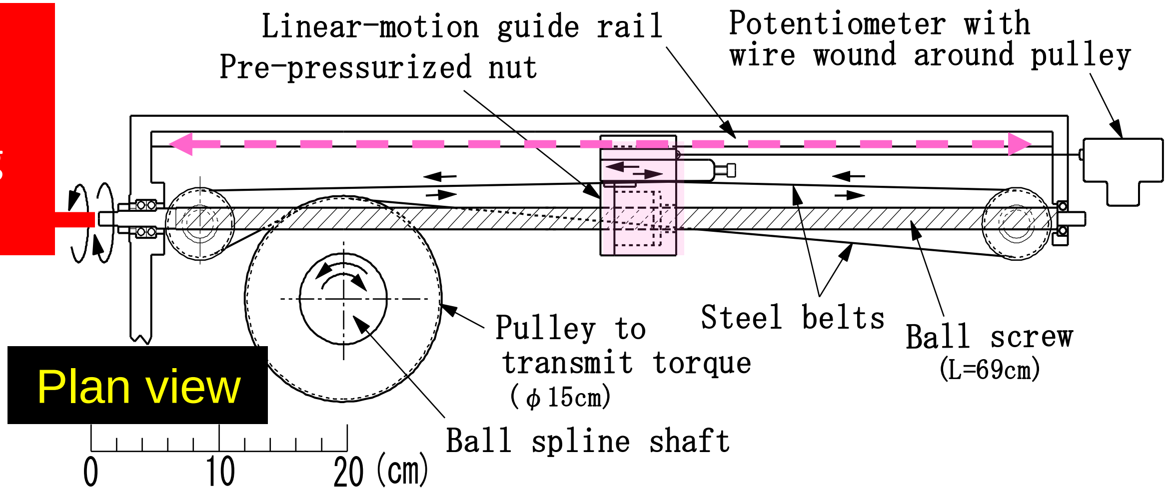

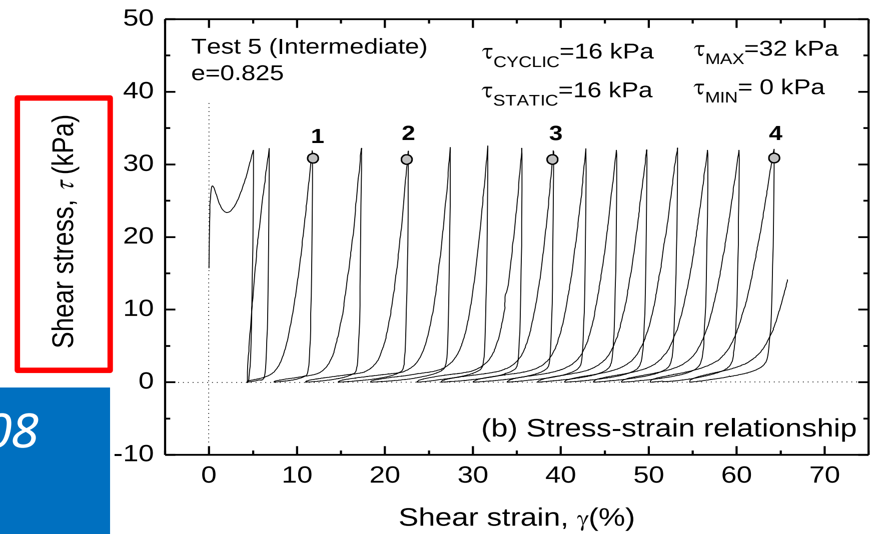

(modified after Kiyota et al., 2008 and Chiaro et al., 2012, 2013)

Correction for effect of membrane force *(Chiaro et al., 2012)*

$$\tau = \tau_{total} - \tau_{memb}$$

Detected by torque load cell

Computed

$$\tau_{memb} = \frac{t_{memb} E_{memb} (r_o^3 + r_i^3)\,\theta}{H (r_o^3 - r_i^3)}$$

Measured in calibration test

By filling water between inner and outer membranes and shearing it under undrained condition

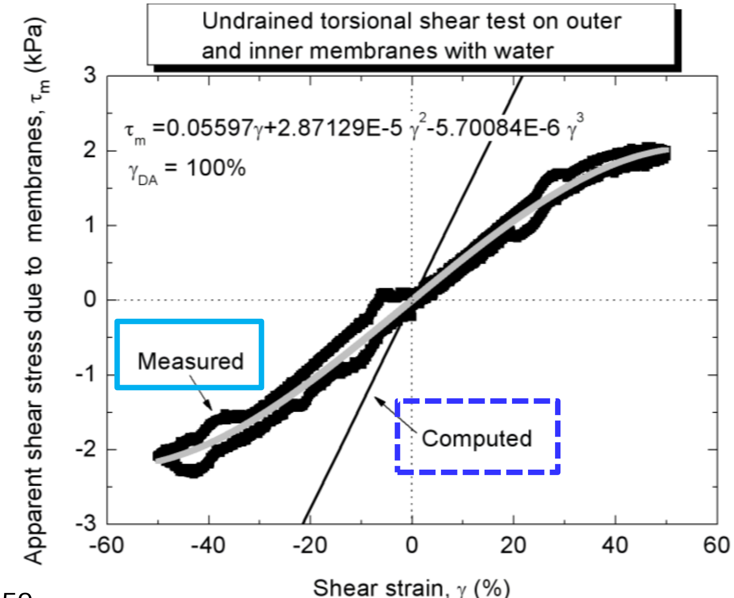

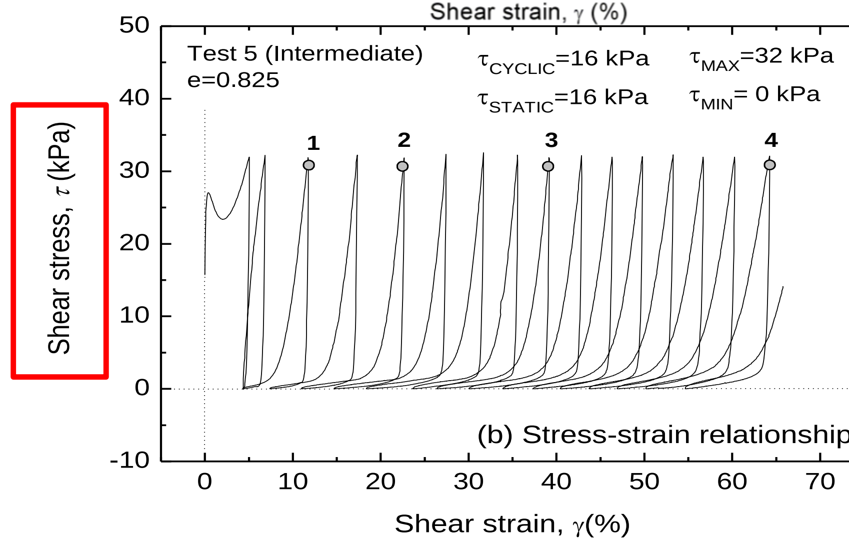

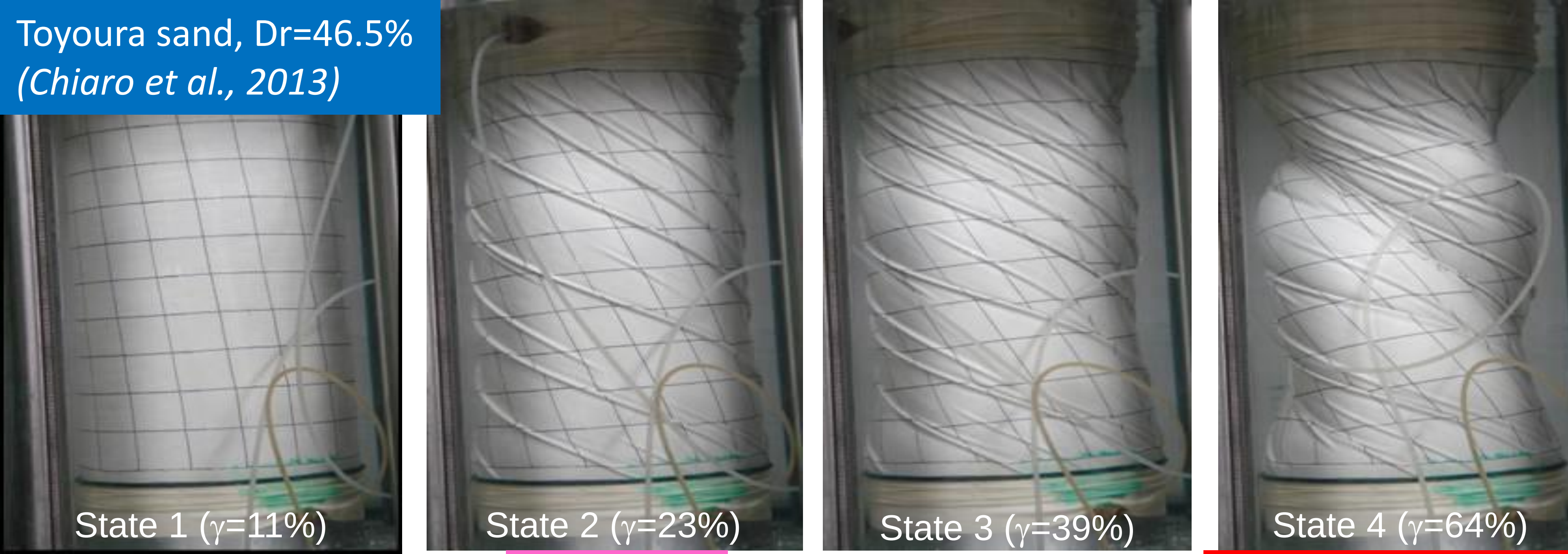

Toyoura sand, Dr=46.5%
(Chiaro et al., 2013)
State 1 (γ=11%)
State 2 (γ=23%)
State 3 (γ=39%)
State 4 (γ=64%)

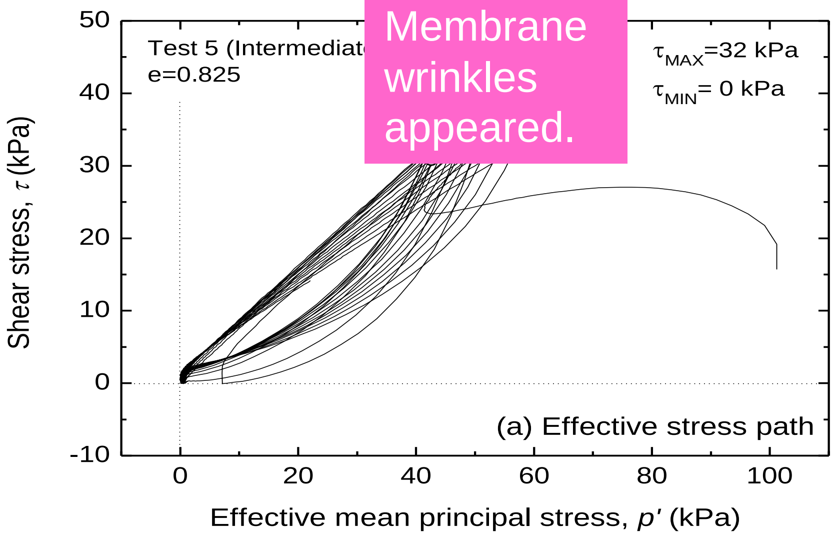

Membrane wrinkles appeared.
Test 5 (Intermediat
e=0.825
τMAX=32 kPa
τMIN= 0 kPa
Shear stress, τ (kPa)
Effective mean principal stress, p' (kPa)
(a) Effective stress path

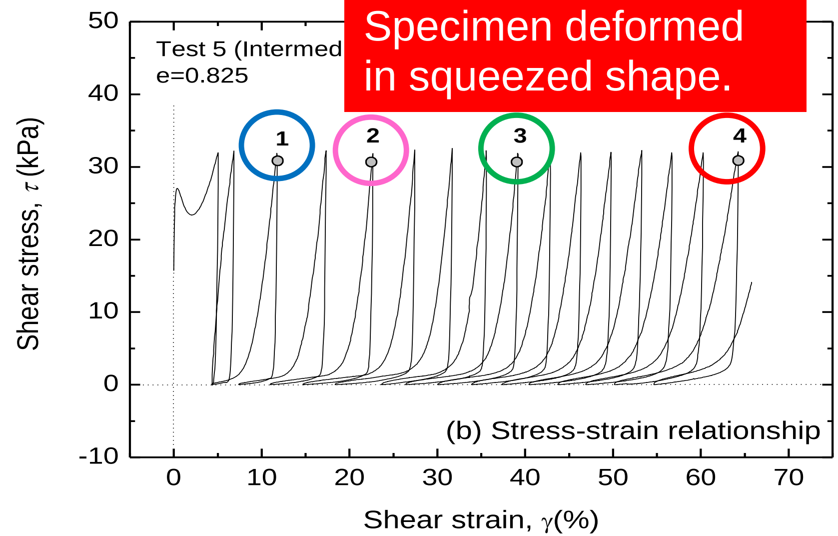

Specimen deformed in squeezed shape.
Test 5 (Intermed
e=0.825
1
2
3
4
Shear stress, τ (kPa)
Shear strain, γ(%)
(b) Stress-strain relationship

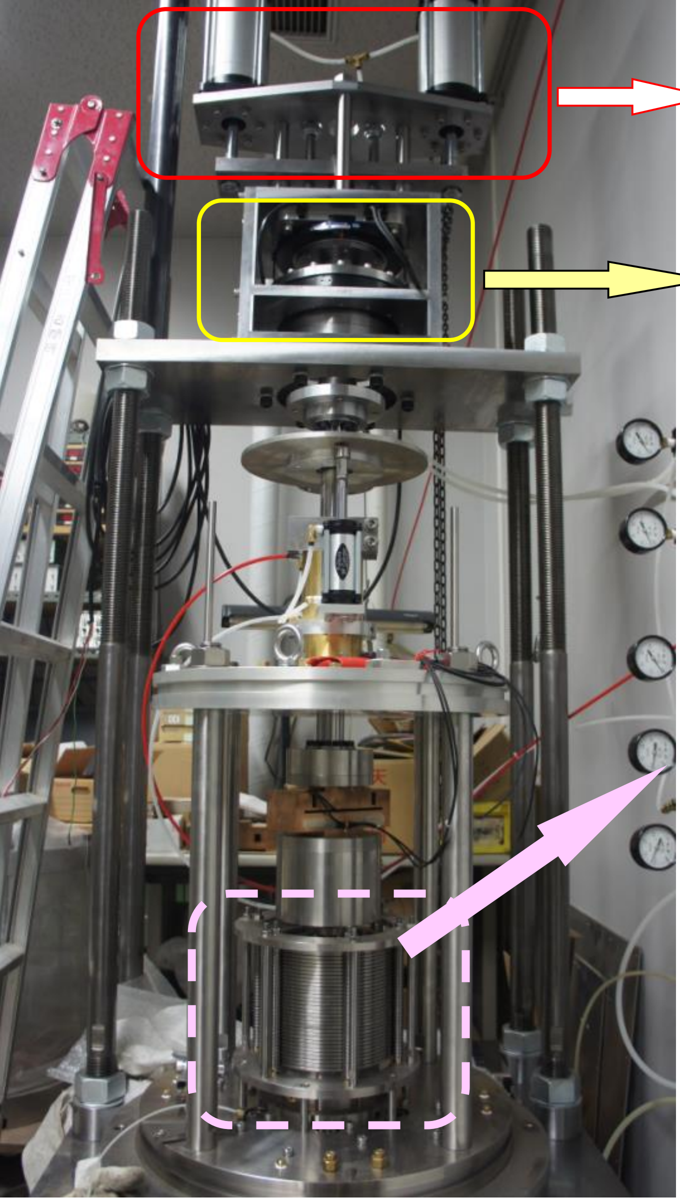

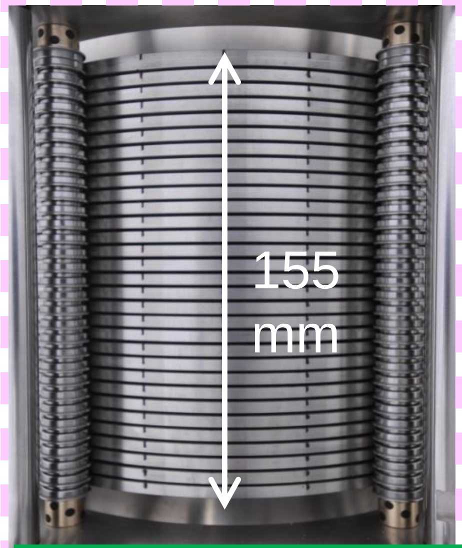

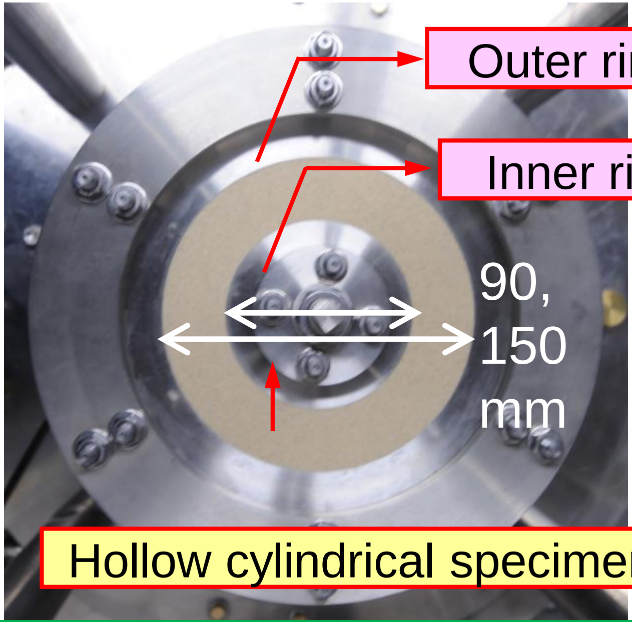

Modified after Wahyudi et al. (2015)

Stacked-ring torsional shear apparatus

to maintain the same specimen shape & dimensions even after large deformation

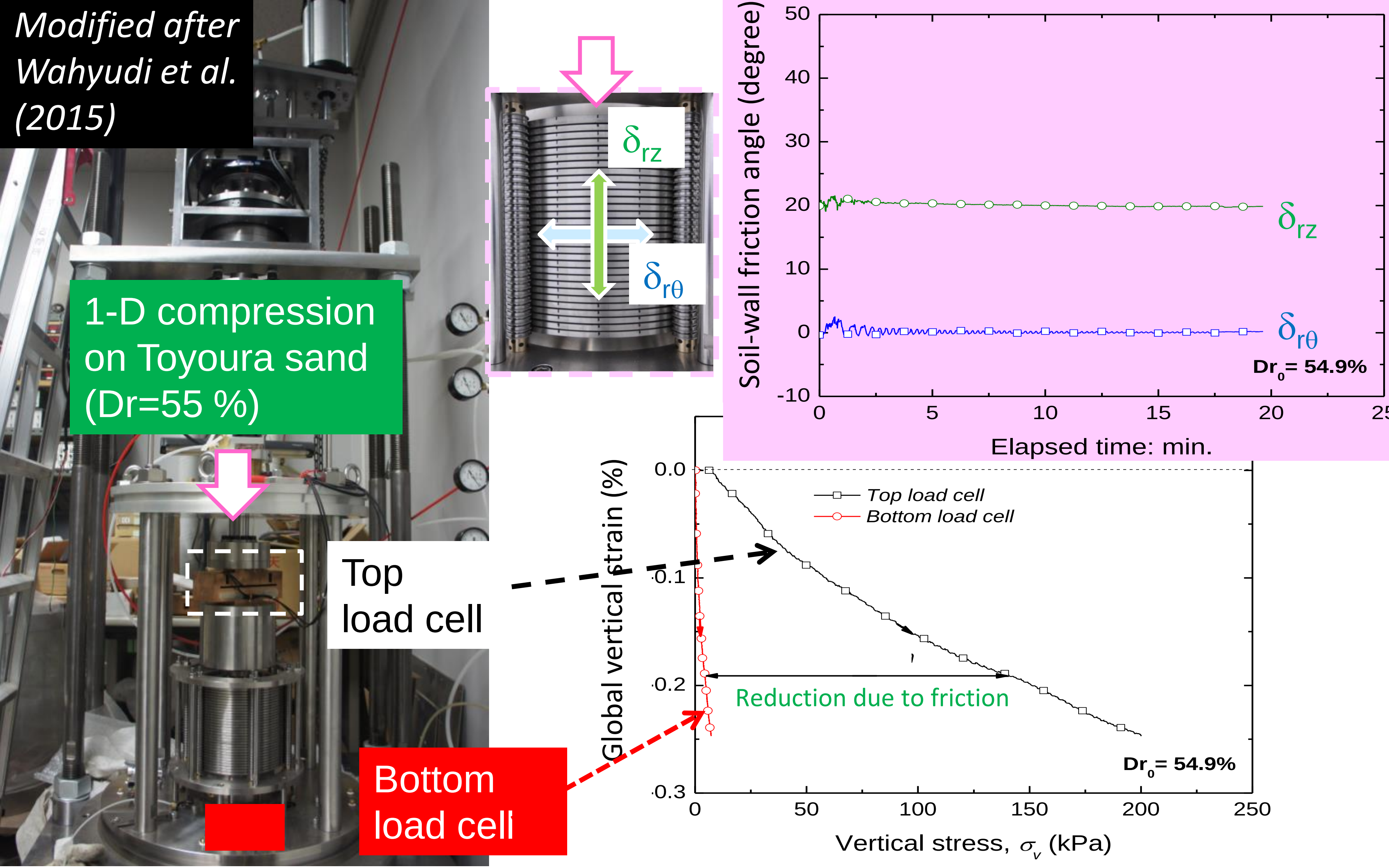
Modified after Wahyudi et al. (2015)
1-D compression on Toyoura sand (Dr=55 %)
δrz
δrθ
Top load cell
Bottom load cell
Soil-wall friction angle (degree)
Elapsed time: min.
Dr0= 54.9%
Global vertical strain (%)
Vertical stress, σv (kPa)
Top load cell
Bottom load cell
Reduction due to friction
Dr0= 54.9%

Stacked-ring shear apparatus after reduction of specimen height and typical constant-volume cyclic shear test results on dry Toyoura sand

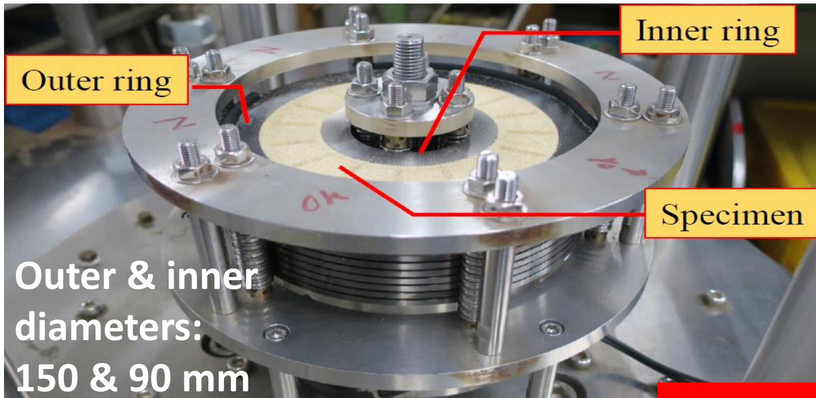

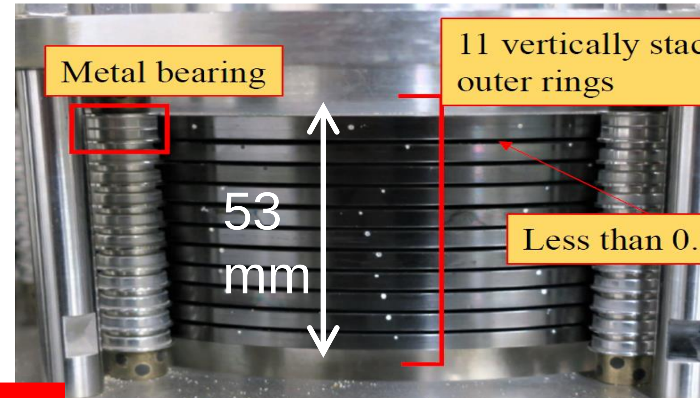

Modified after Wahyudi et al. (2016)

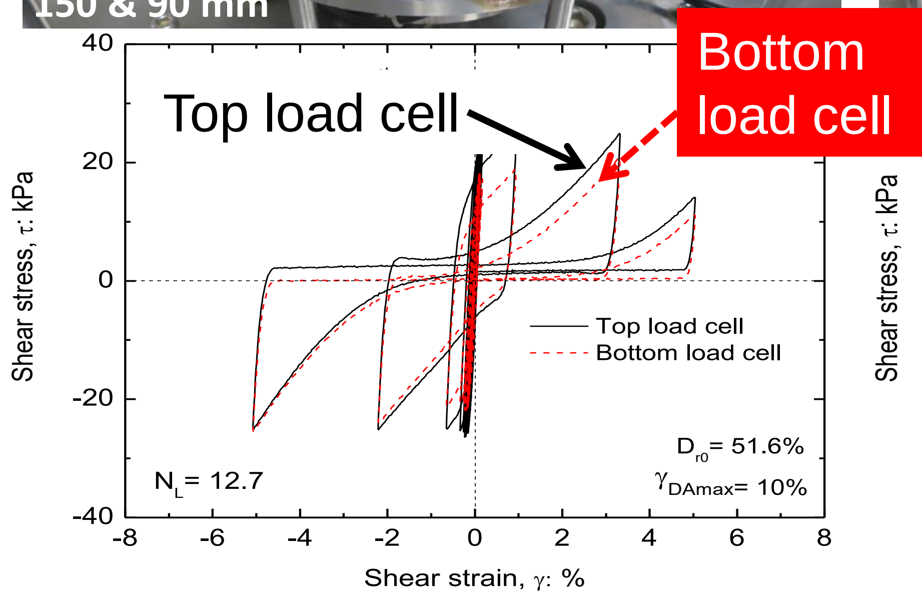

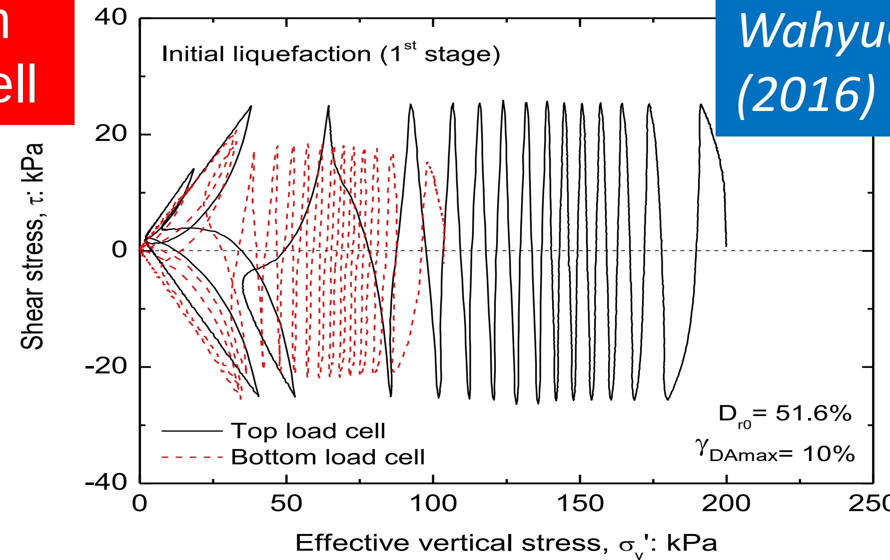

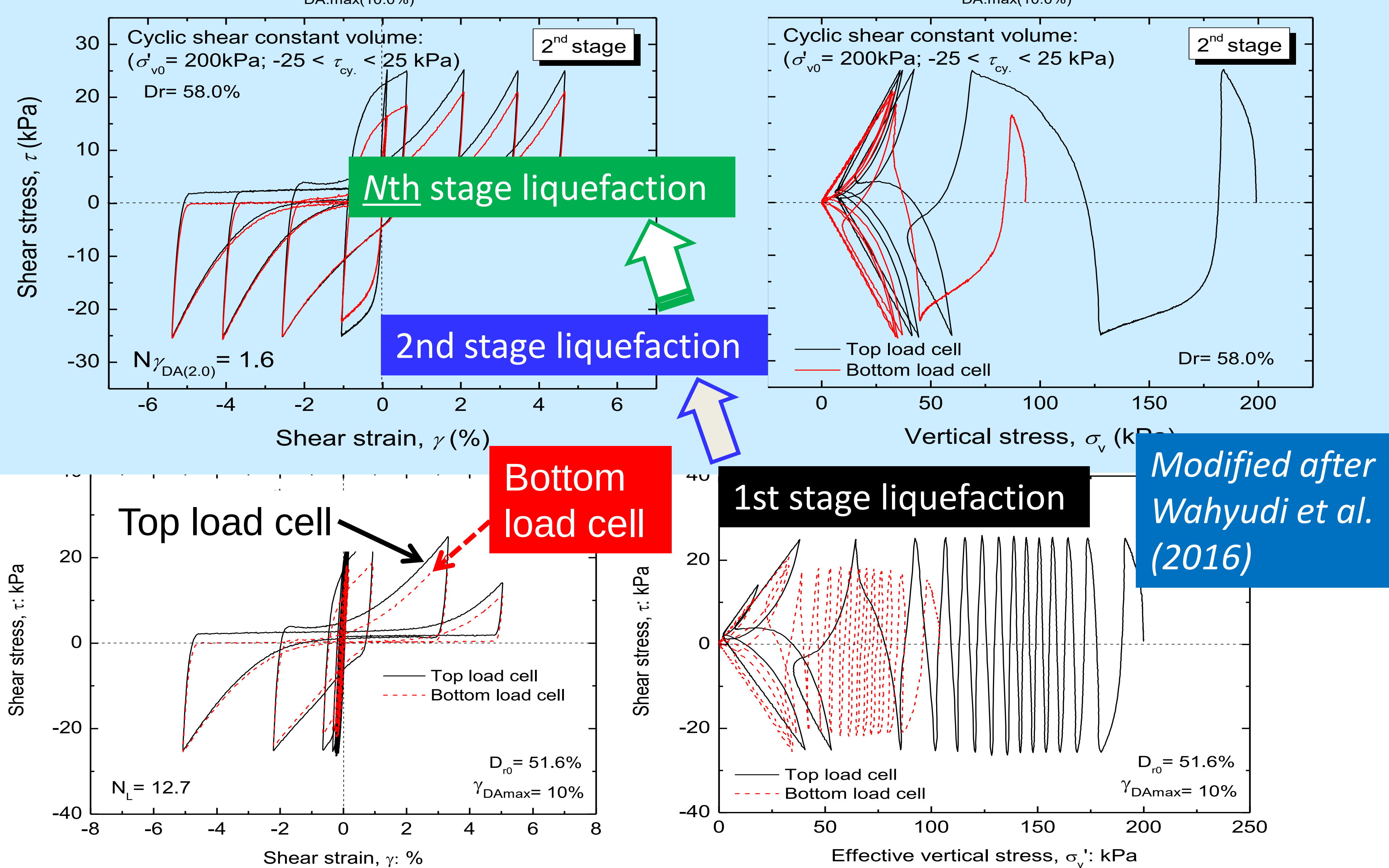
Cyclic shear constant volume:
(σ'_{v0}= 200kPa; -25 < $\tau_{cy.}$ < 25 kPa)
Dr= 58.0%
2^{nd} stage
$N\gamma_{DA(2.0)}$= 1.6
Shear stress, τ (kPa)
Shear strain, γ (%)
Cyclic shear constant volume:
(σ'_{v0}= 200kPa; -25 < $\tau_{cy.}$ < 25 kPa)
2^{nd} stage
Top load cell
Bottom load cell
Dr= 58.0%
Vertical stress, σ_v (kPa)
Nth stage liquefaction
2nd stage liquefaction
Bottom load cell
Top load cell
1st stage liquefaction
Modified after Wahyudi et al. (2016)
Shear stress, τ: kPa
Top load cell
Bottom load cell
D_{r0}= 51.6%
N_L= 12.7
γ_{DAmax}= 10%
Shear strain, γ: %
Shear stress, τ: kPa
Top load cell
Bottom load cell
D_{r0}= 51.6%
γ_{DAmax}= 10%
Effective vertical stress, σ_v': kPa

Constant-volume monotonic shear on Aso pumice

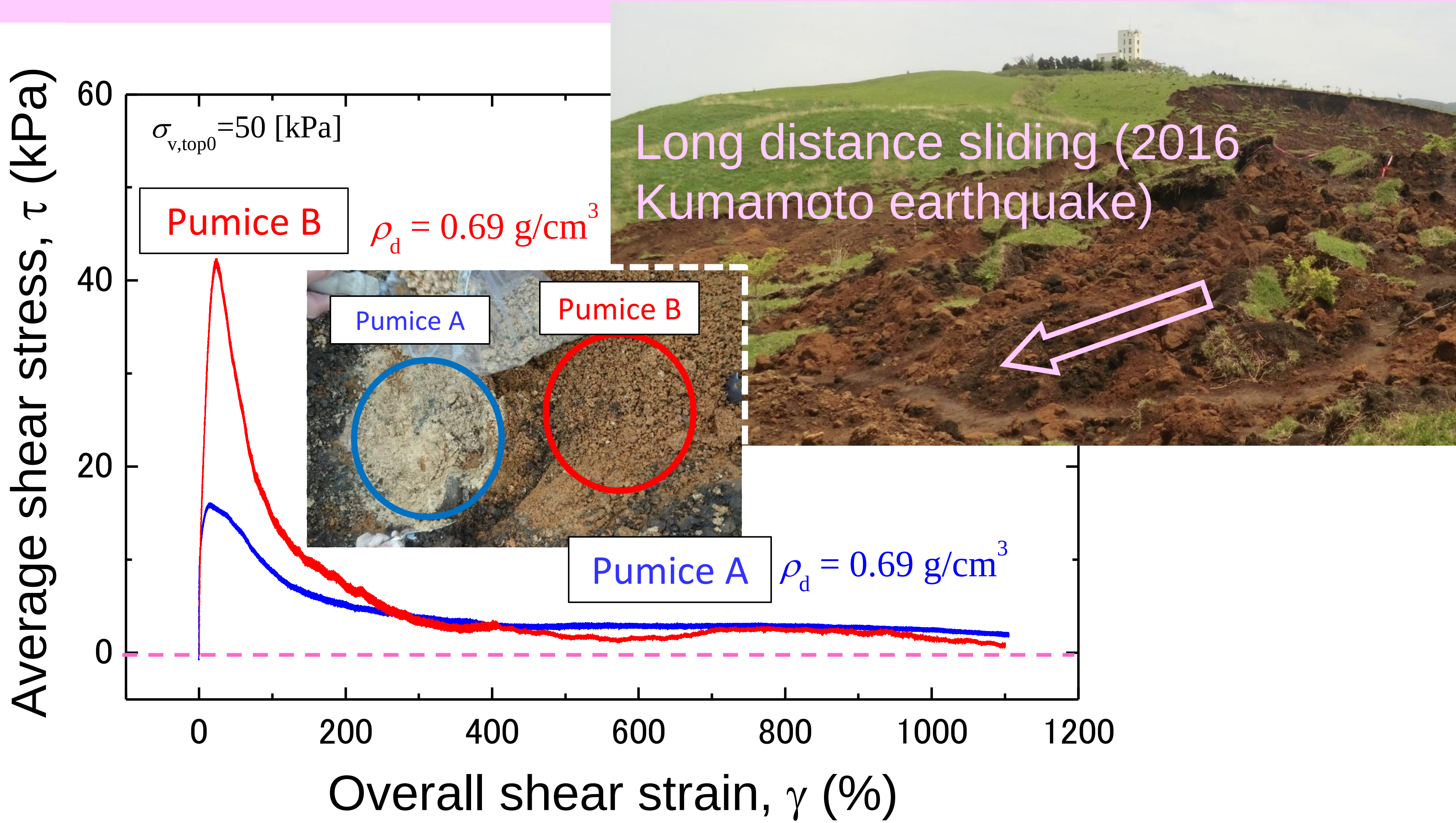

Constant-volume monotonic shear on Toyoura sand

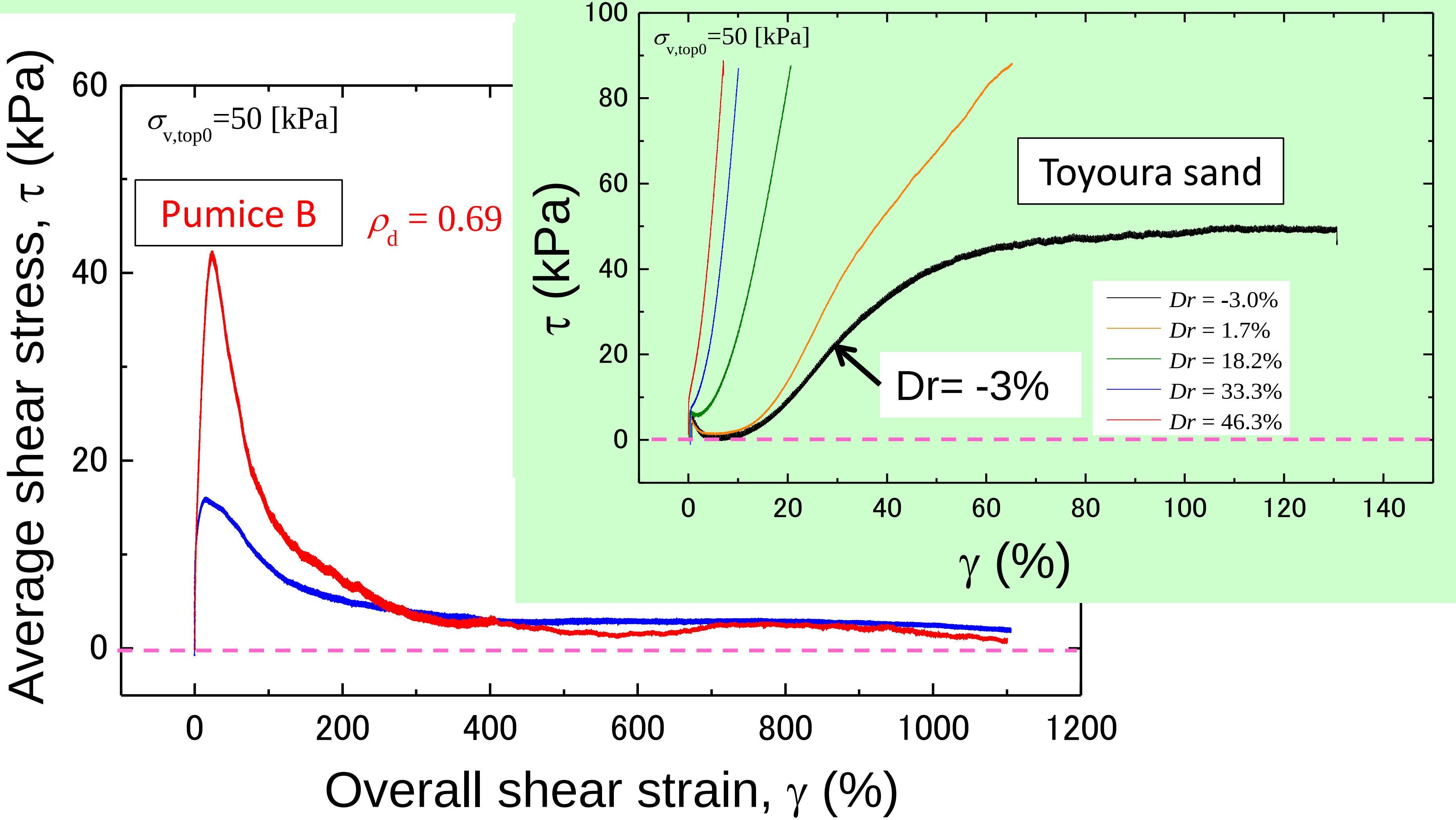

4.2 Tension tests

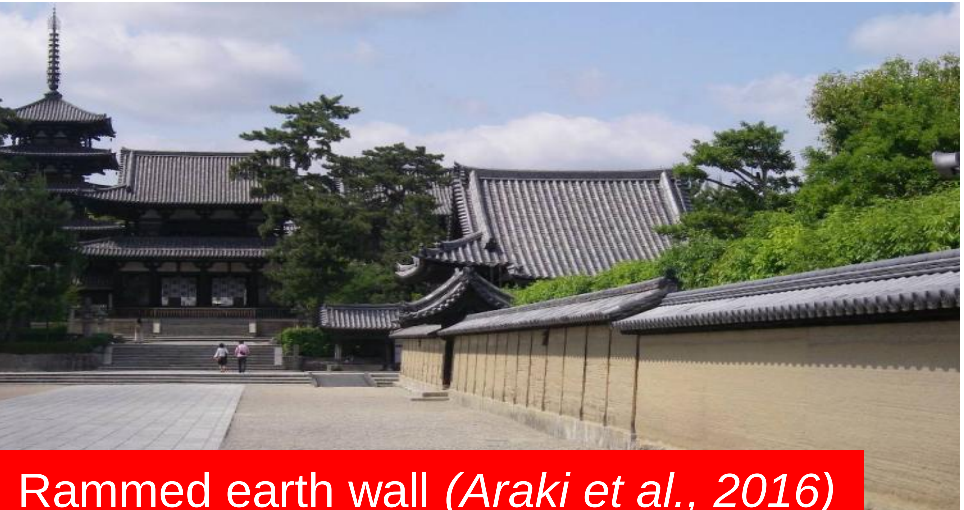

Rammed earth wall *(Araki et al., 2016)*

Lattice-shaped ground improvement by in-situ cement mixing as liquefaction countermeasure *(Namikawa et al., 2007)*

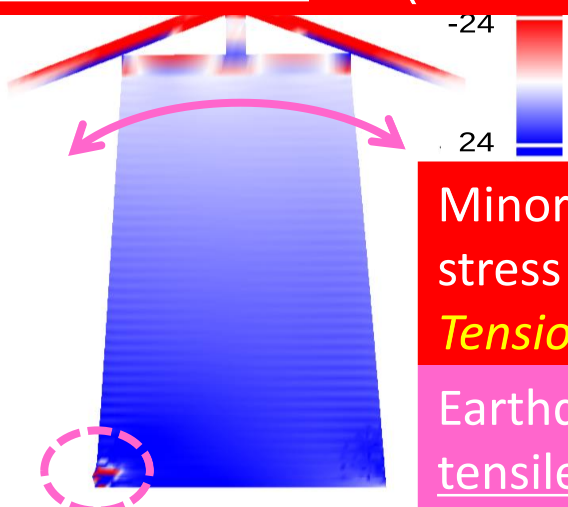

Minor principal stress (kPa) :
Tension in red

Earthquake-induced tensile failure due to excessive bending

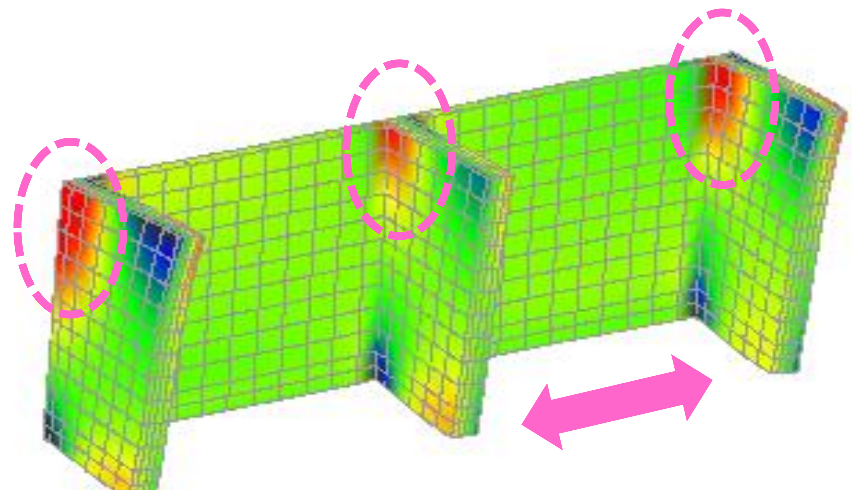

4.2 Tension tests

Namikawa and Koseki (2007)

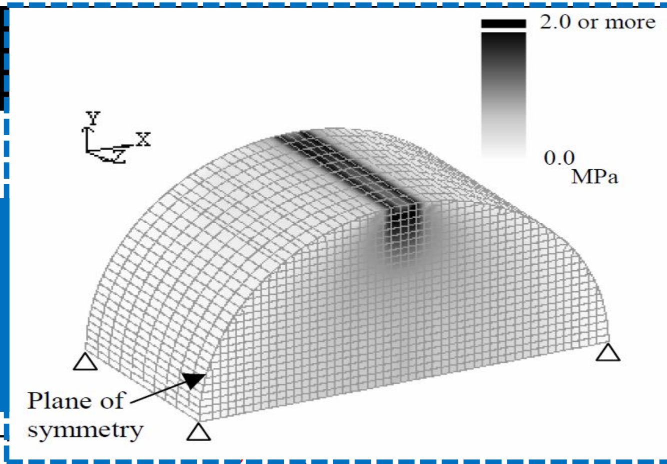

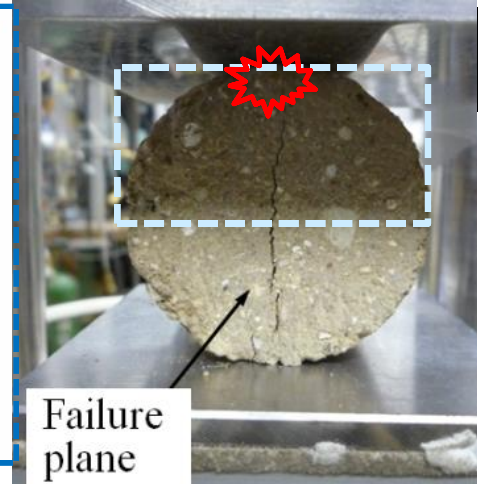

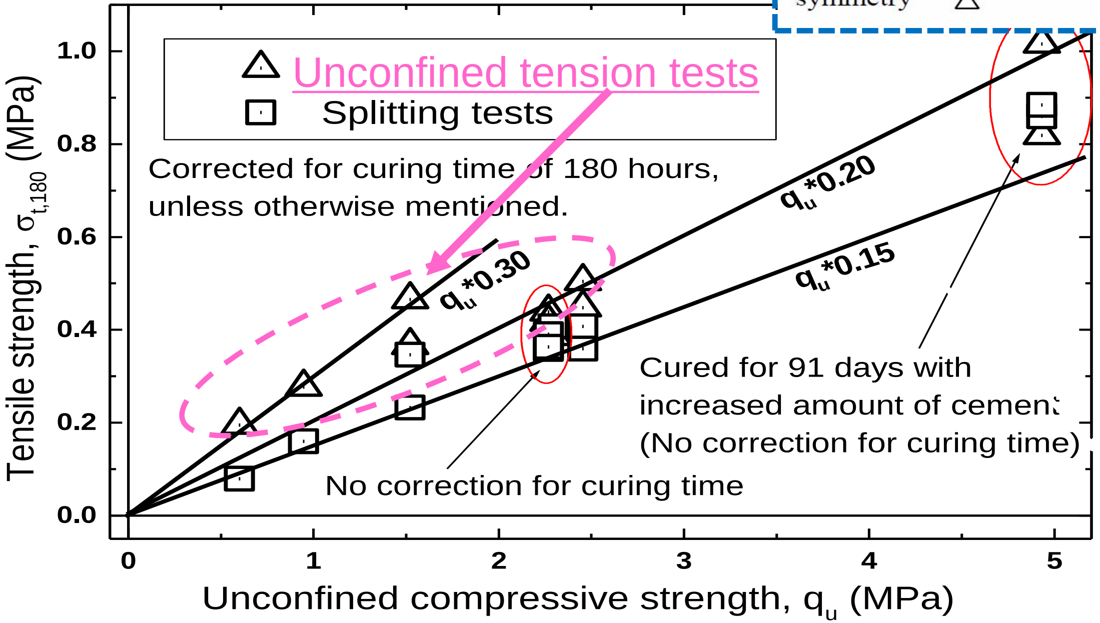

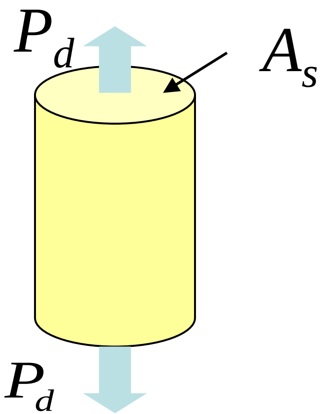

$$\sigma_t = \frac{P_d}{A_s}$$

Unconfined tension test

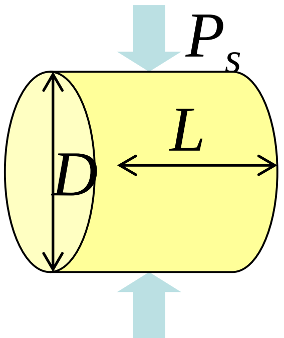

$$\sigma_t = -\frac{2P_s}{\pi LD}$$

Splitting test

Comparison of tensile strengths of cement-treated sand obtained by splitting (*Brazilian*) & unconfined direct tension tests *(Koseki et al., 2005)*

Trimmed cylindrical specimen for unconfined tension test

(Namikawa and Koseki, 2007)

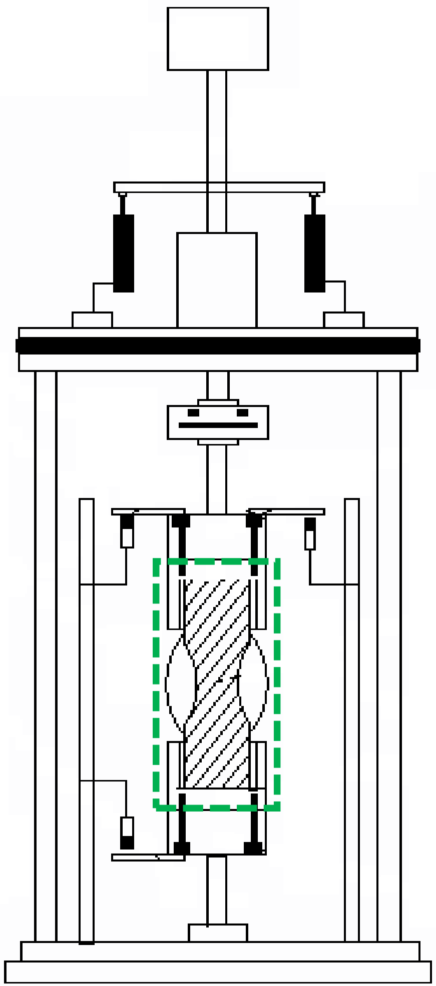

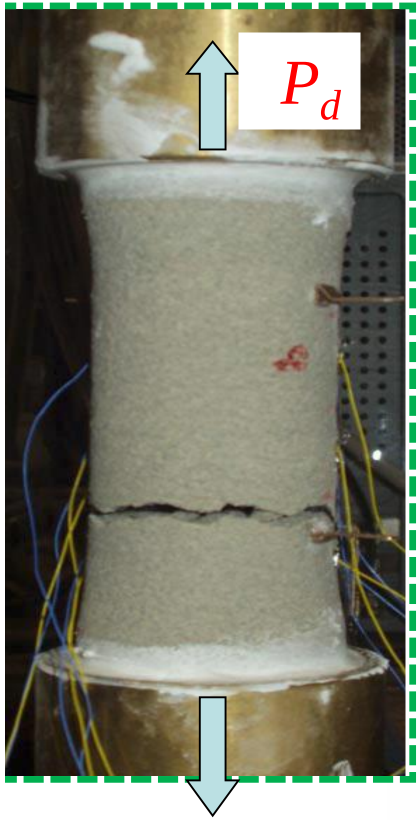

$$\sigma_t = \frac{P_d}{As}$$

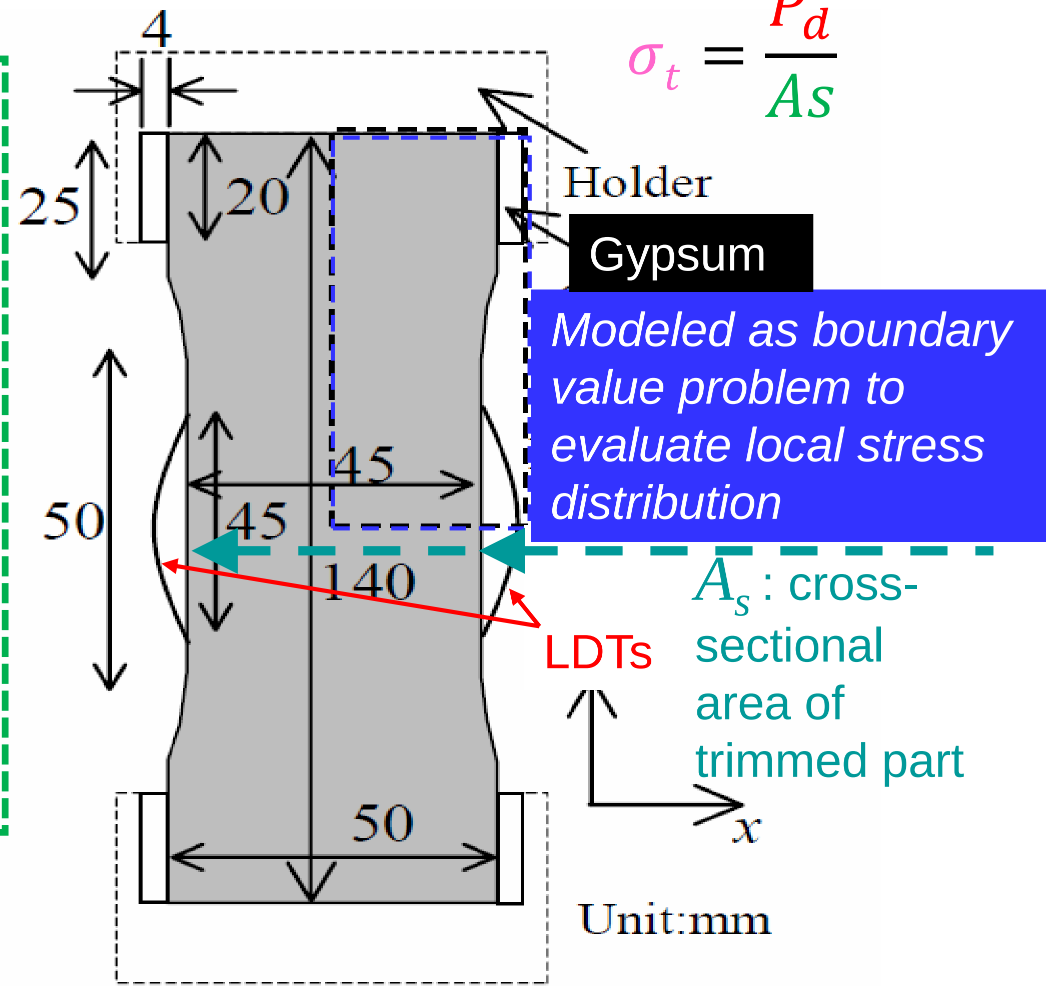

Unconfined tension test result on cement-treated sand with several types of axial strain measurement

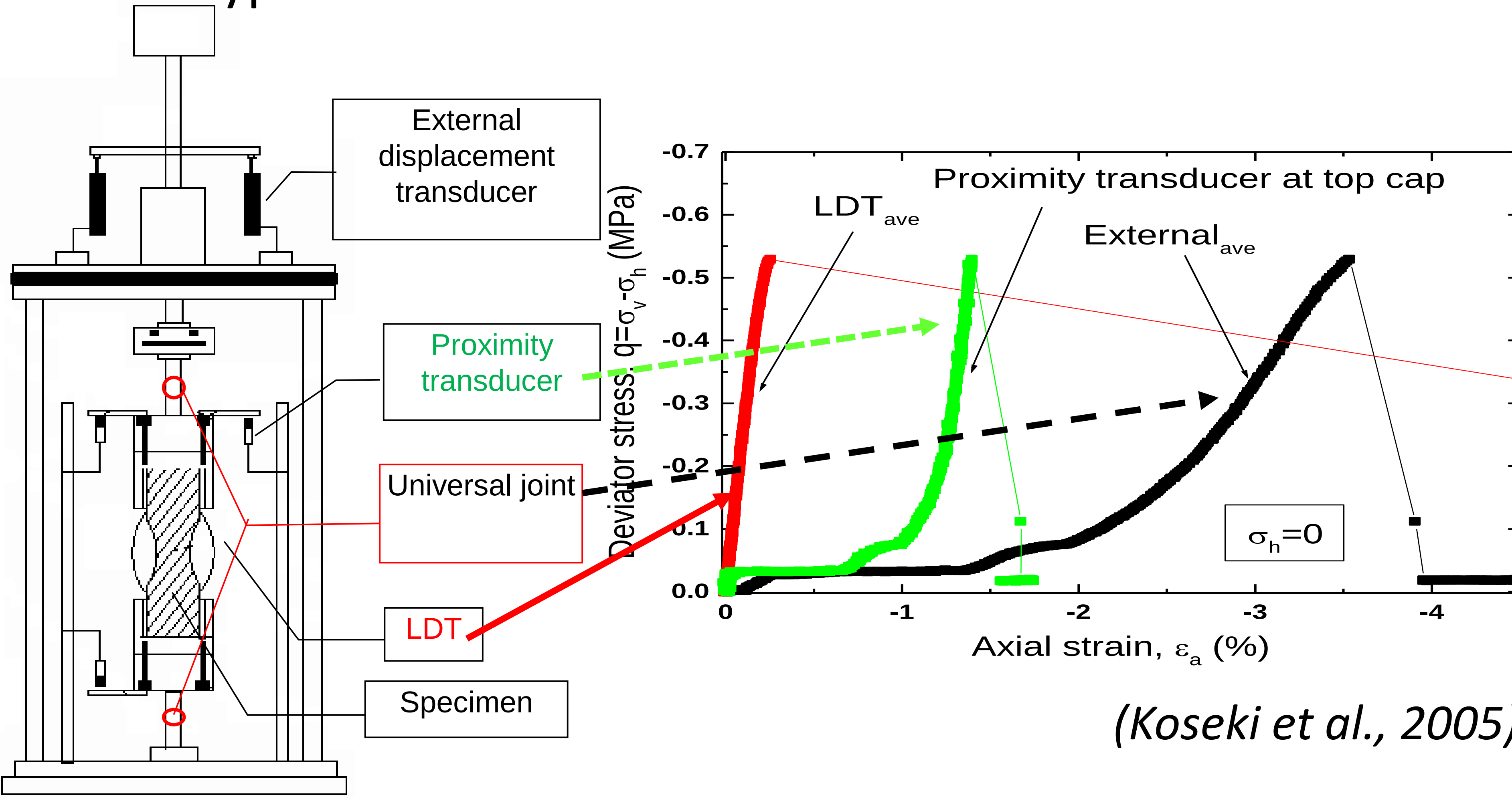

(Koseki et al., 2005)

Typical condition of failed specimens in unconfined tension and splitting tests on unsaturated rammed earth material

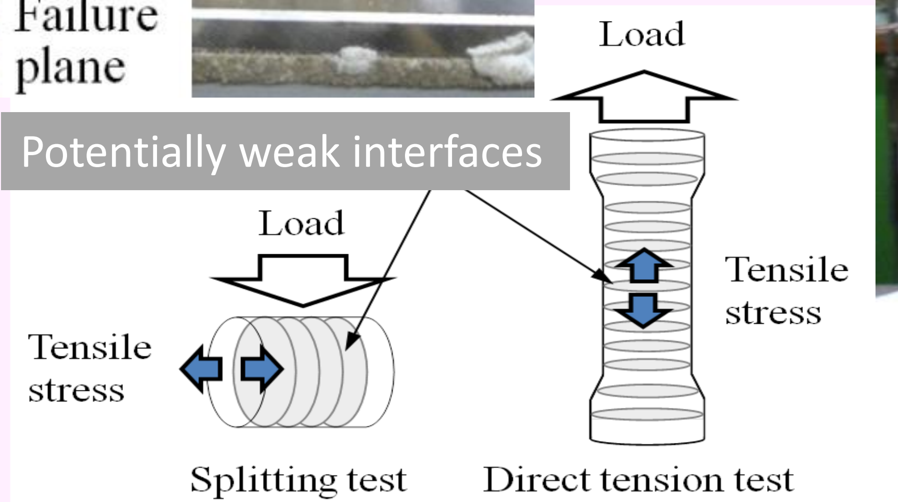

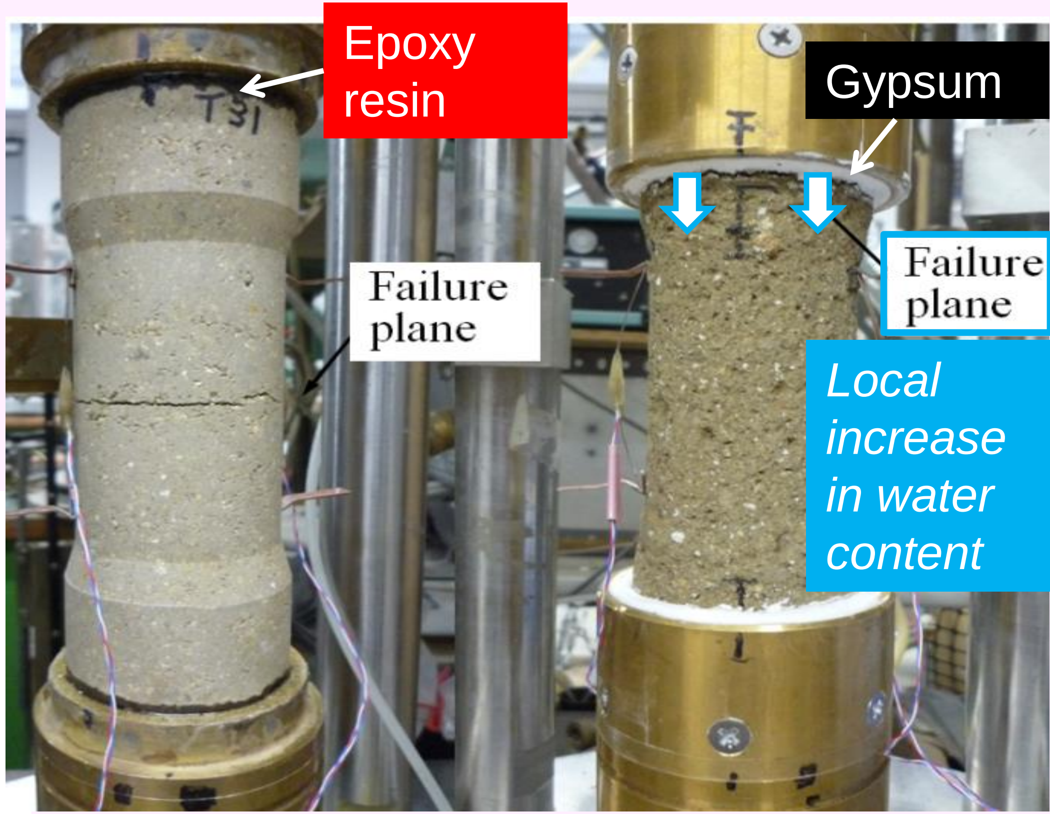

(Araki et al., 2016)

Unconfined torsional shear on hollow cylindrical specimen of cement-treated sand

Inner diameter: 3 cm (t= 2 cm) to 5 cm (t=1 cm)
t: thickness of specimen

Outer diameter: 7 cm

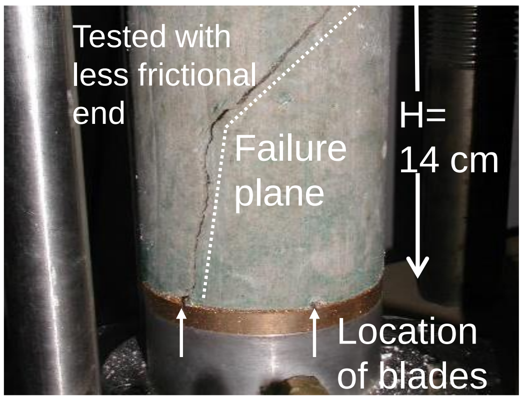

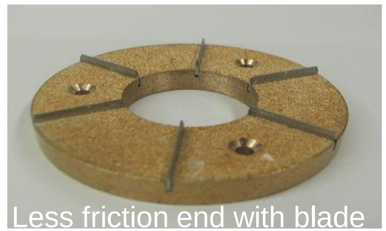

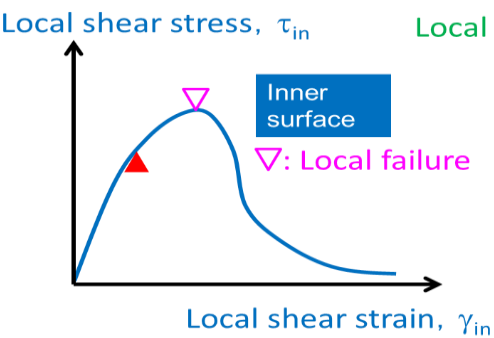

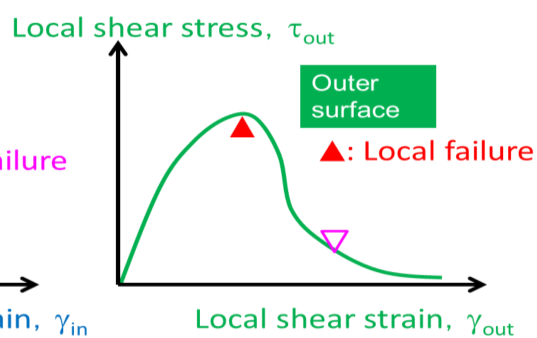

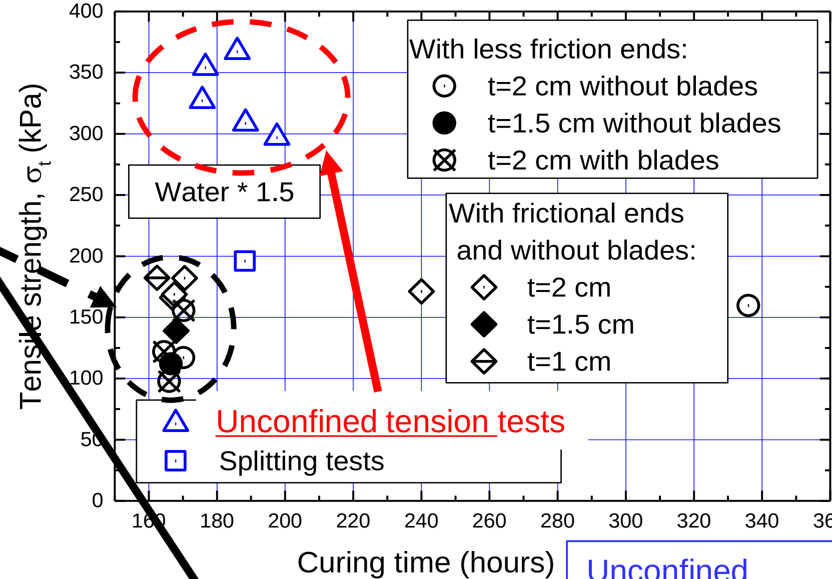

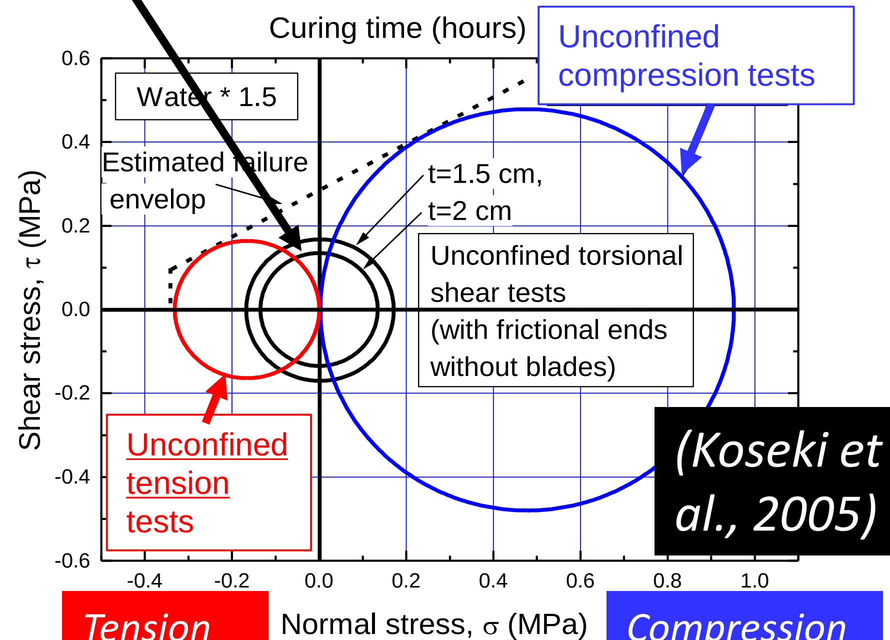

4.3 Long-term tests

Long-term creep loading tests using triaxial apparatus:

Hayano et al. (2001) on sedimentary soft rocks

AnhDan et al. (2006) on compacted gravels

Enomoto et al. (2015) on sands, and

Enomoto et al. (2016) on undisturbed natural gravelly soils

Stable performance of loading device, its control system and data acquisition system shall be ensured

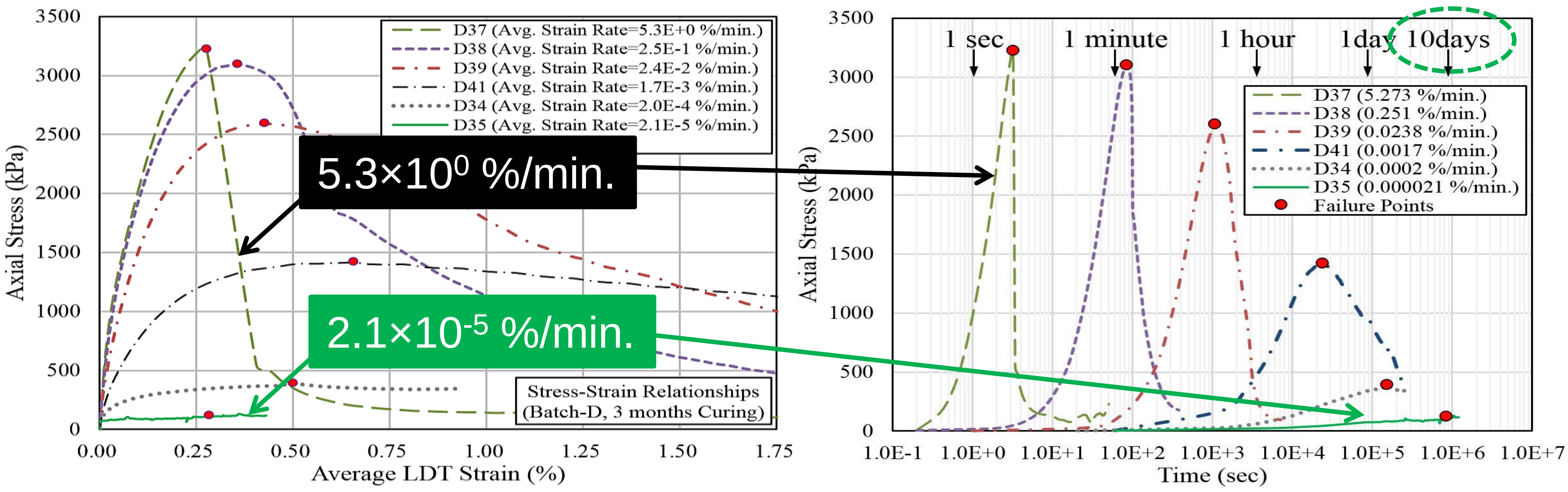

Unconfined monotonic compression tests under different strain rates on gypsum-mixed sand (*Maqsood et al., 2019, this symposium*)

Long-term stability of load cell, LDTs & external displacement transducer (converted into virtual specimen response)

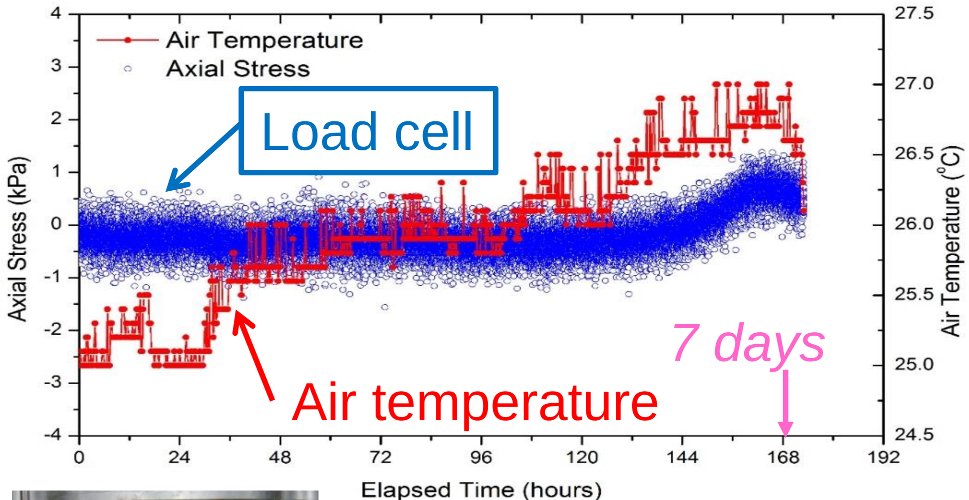

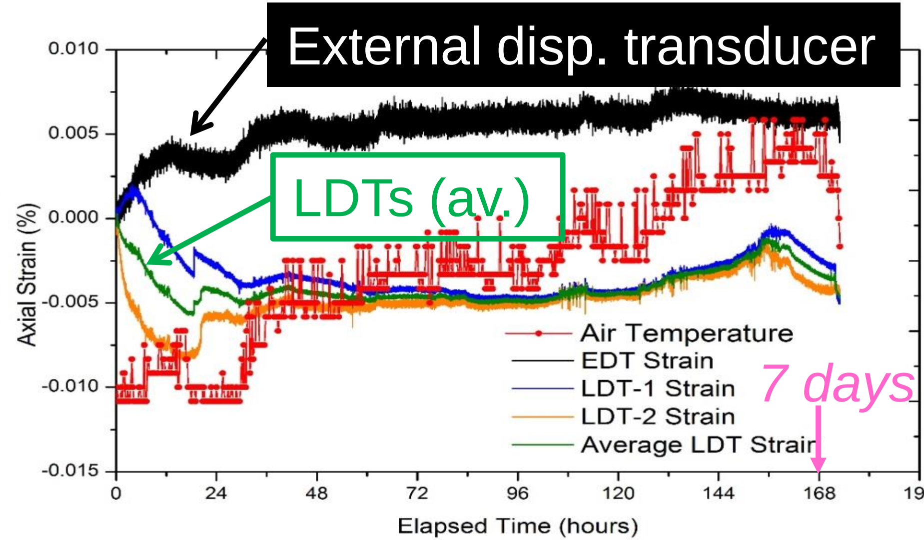

Latex rubber membranes start to allow penetration of cell water in about <u>100 hours</u> *(Tatsuoka et al., 1988)*

- ✓ *Inability to evaluate volume change of specimen*
- ✓ *Desaturation of initially saturated specimen*

Long-term air-permeability of micro-porous membrane filter

Advantage over ceramic disks in terms of equilibration time for measurement and control of pore water pressure in unsaturated soils *(Nishimura et al., 2012; Wang et al., 2016)*

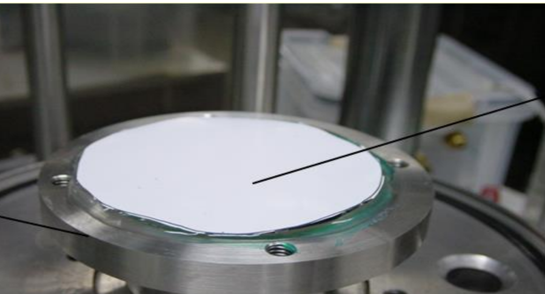

Membrane filter

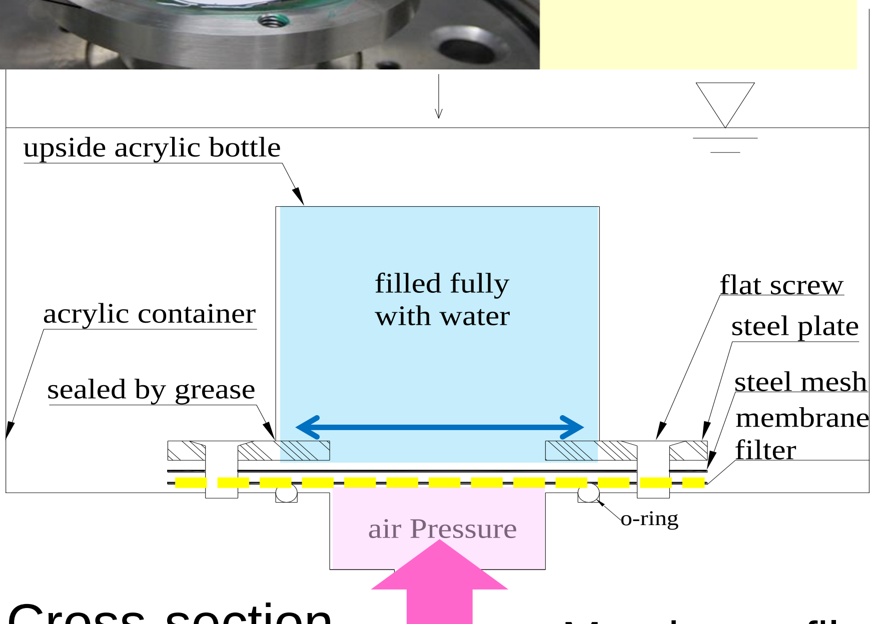

Cross-section
(Wang et al., 2017)

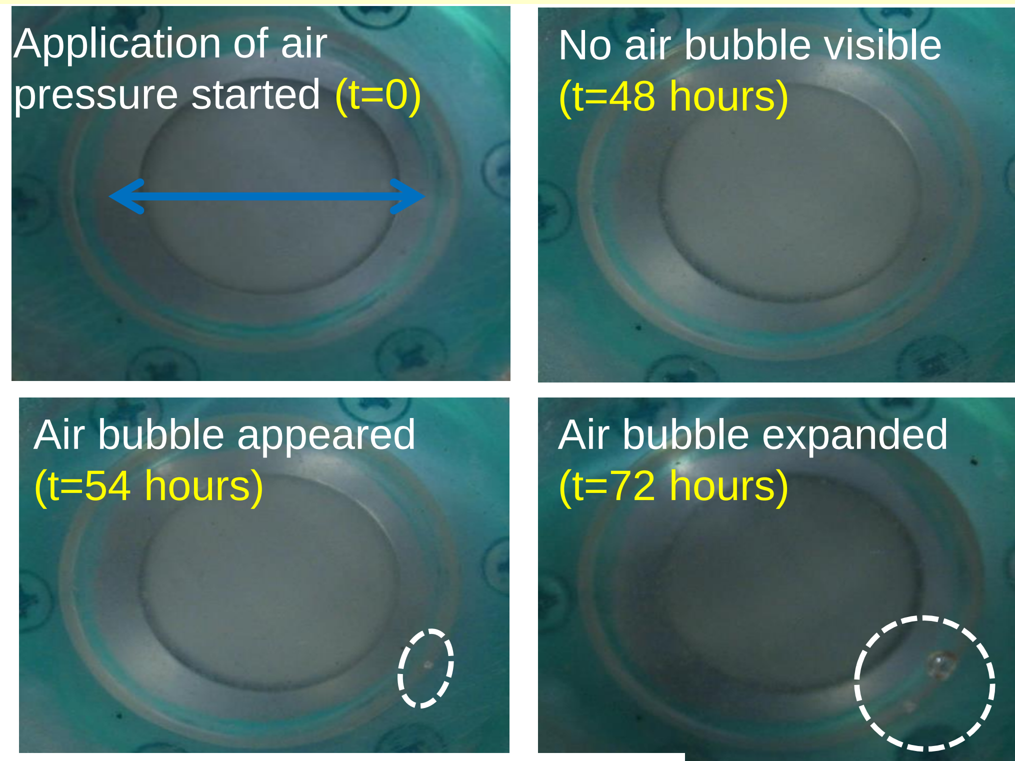

Membrane filter with nominal AEV of 250 kPa under sustained air pressure of 25 kPa

Summary of lessons learned from other special tests (1/2)

- Though rigid boundary is effective in keeping the specimen shape in large deformation tests, effects of interface friction shall be evaluated & considered properly.

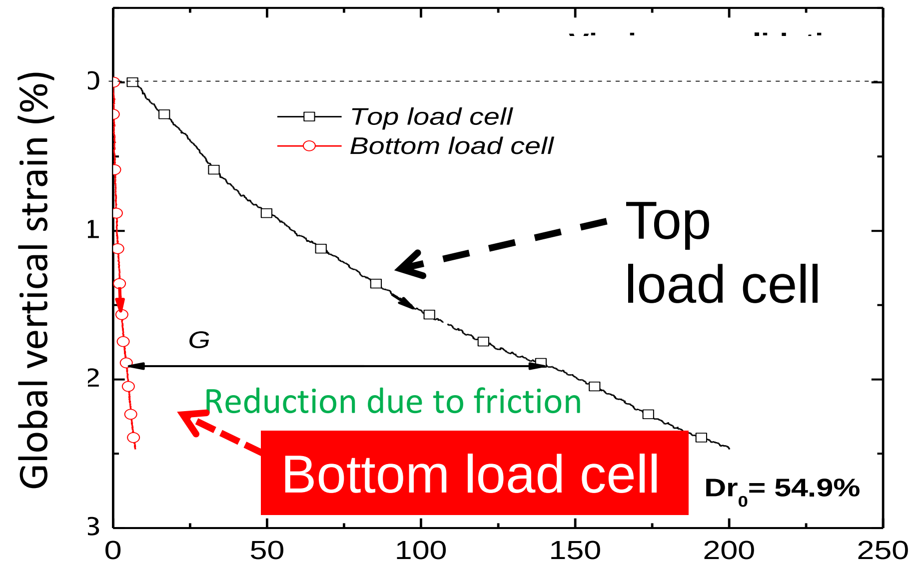

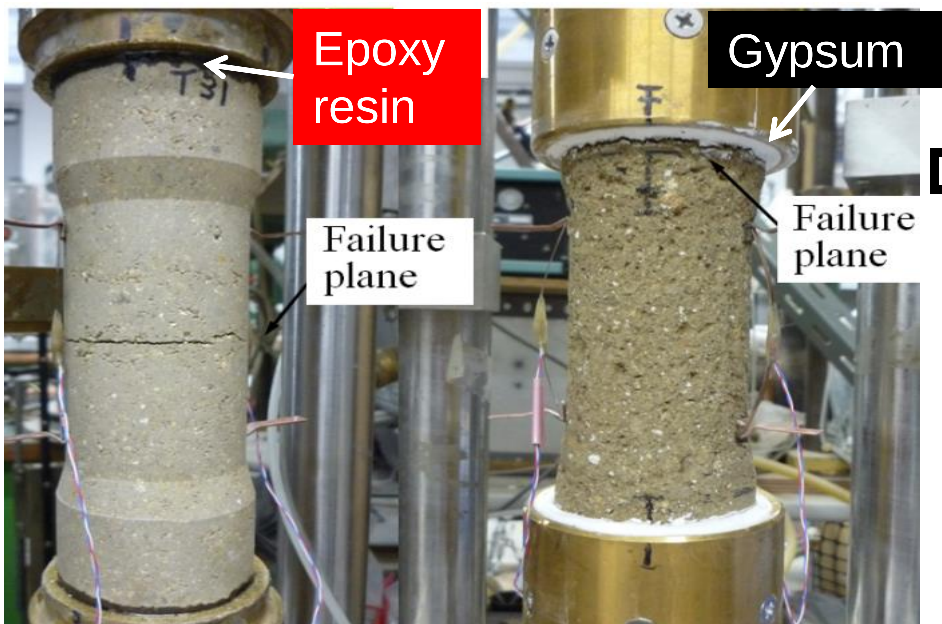

- In evaluating tensile behavior of bounded soil specimens, direct tension tests have advantages over splitting tests, while attentions are required on testing apparatus & procedures.

Summary of lessons learned from other special tests (2/2)

- ☐ In conducting long-term tests, stable performance of loading device, its control system and the data acquisition system shall be ensured.
- ✓ In long-term use of rubber and microporous membranes, possible penetration of water and air, respectively, shall be checked as well.

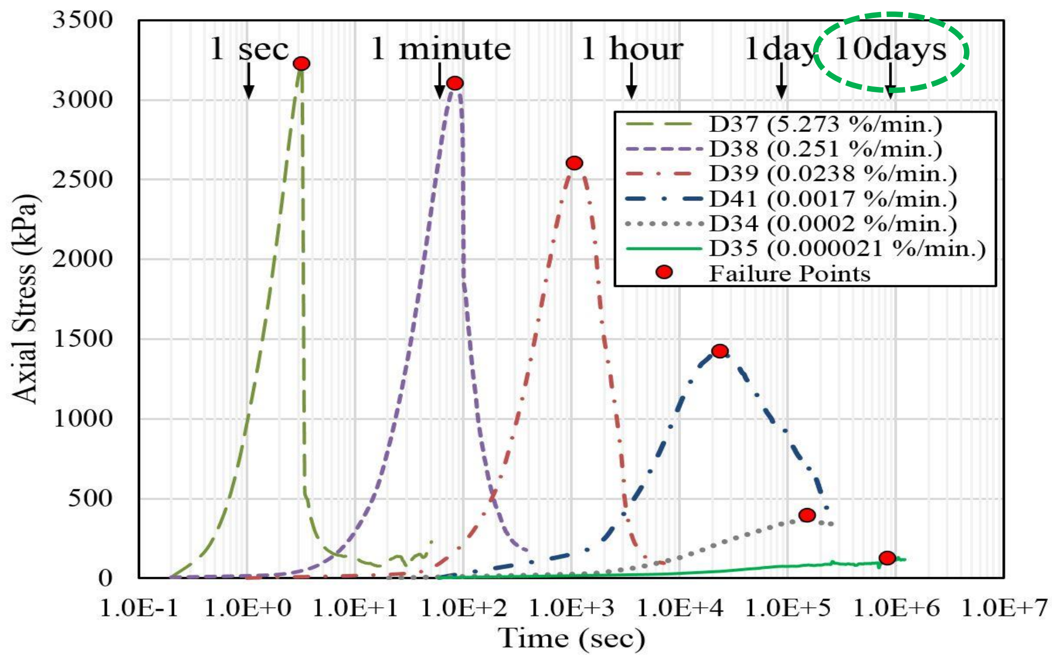

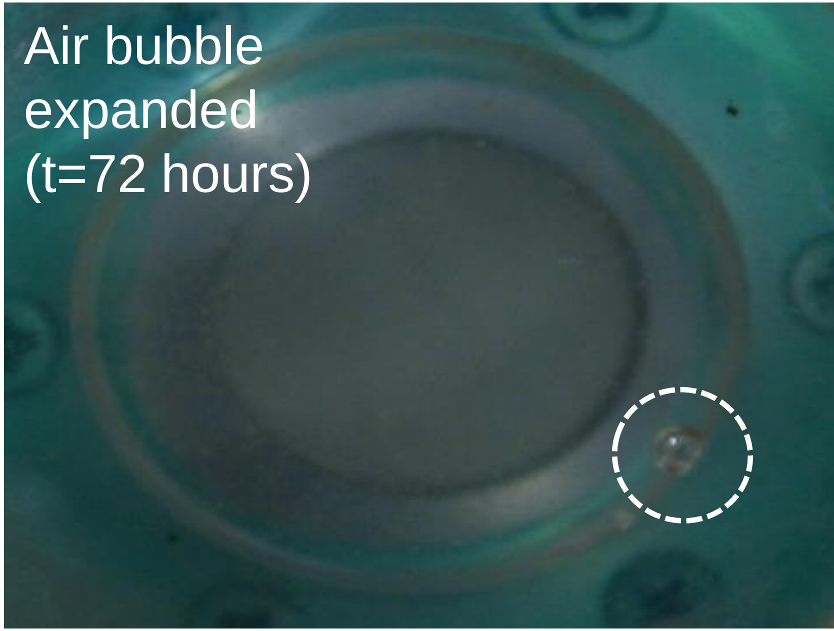

Outline

1. Introduction
2. Local measurements
    - 2.1 LDTs for cylindrical/prismatic specimens (triaxial)
    - 2.2 LDTs for hollow cylindrical specimen (torsional shear/triaxial)
    - 2.3 Local dynamic measurements
3. Unconventional liquefaction tests
    - 3.1 Liquefaction tests using motor-driven loading devices
    - 3.2 Cylindrical/prismatic specimens with thin sandy layer
    - 3.3 Segregated hollow cylindrical specimen
    - 3.4 Direct/indirect evaluation of local deformation during liquefaction
4. Other special tests
    - 4.1 Large deformation tests
    - 4.2 Direct tension tests
    - 4.3 Long-term tests
5. Concluding remarks

Concluding remarks

- ☐ Some of the “element” test results need to be analyzed and interpreted as boundary value problems in terms of the stress/strain non-uniformities and the specimen heterogeneity.
- ✓ *Possible effects of system compliance should be properly considered as well.*

- ☐ Each of the variety of laboratory stress-strain test methods has its specific advantages and limitations.
- ✓ *By developing an original way of application, the limitation may turn into an advantage.*